universität wien

MASTERARBEIT

Titel der Masterarbeit

„Influence of H_2S on the transcription factors HIF-1α and NF-κB in THP-1 macrophages“

verfasst von

Lilian Lohninger, BSc

angestrebter akademischer Grad

Master of Science (MSc)

Wien, 2013

Studienkennzahl lt. Studienblatt:	A 066 834
Studienrichtung lt. Studienblatt:	Masterstudium Molekulare Biologie
Betreut von:	ao. Univ.-Prof. Dipl.-Ing. Dr. Marcela Hermann

Acknowledgement

At this point, I want to use the opportunity to thank Prof. Hilde Laggner for supervising me in a very warm-hearted way during my master thesis and for giving me financial support. Moreover, I want to thank her for the welcoming atmosphere in the laboratory and the patience to explain everything unclear to me. She has accompanied me in an important part of my life, which I will always remember.

I Table of contents
II List of figures
III List of Tables
IV Table of abbreviations

II List of figures

III List of tables

IV Table of abbreviations

3-MST	3-mercaptopyruvate sulfurtransferase
3' UTR	3'-untranslated region
AA	ascorbic acid
ABCA1	ATP-binding cassette transporter A1
Ac	Acetylation
apoB	apolipoprotein B
ARD	ankryn repeat domain
ARD-1	acetyltranferase 1
ARE	adenlyate- and uridylate-rich element
ATM	ataxia telangiectasia mutated
BAFF	B-cell-activating factor of the TNF family
bHLH	basic helix-loop-helix
BSA	bovine serum albumin
bZIP	leucine-zipper-containing transcription factor
CAT	cysteine aminotransferase
CBS	cystathionine β-synthase
CK2	caseine kinase-II
CO	carbon monoxide
CPEB	cytoplasmatic polyadenylation-element-binding protein
CSE	cystathionine γ-lyase
DCs	dendritic cells
DHA	L-dehydroascorbic acid
DHLA	dihydrolipoic
ECM	extracellular matrix
eIF2α	eukaryotic initiation factor 2α
ERK	extracellular signal-regulated kinases
FIH	factor inhibiting HIF
GLUT1	glucose transporter 1
H	hypoxia
H_2S	hydrogen sulfide
H_2SO_3	persulfide
$H_2S_2O_3$	thiosulfate
HASMCs	human aortic smooth muscle cells
HB	hypotonic buffer
HBSS	Hank's balanced salt solution
HDL	high density lipoprotein
HIF-1α	hypoxia inducible factor 1α
HMG-1	high-mobility-group protein-I
hnRNP	heterogenous nuclear ribonucleoprotein
HRE	hypoxic response element

HSPG	heparan sulphate proteoglycan
HuR	human antigen R
IC_{50}	half maximal inhibitory concentration
IGF-2	insulin-like growth factor-2
IκB	inhibitor of NF-κB
IKK	IκB kinase
IFNγ	interferon γ
IL	interleukin
iNOS	inducible nitric oxide synthase
IRP	iron-response element-binding protein
LB	lysis buffer
LDH	lactate dehydrogenase
LDHA	lactate dehydrogenase A
LMP1	latent membrane protein-1
LPS	lipopolysaccharide
MAPK	mitogen-activated protein kinase
MEK-1	mitogen activated protein/extracellular signal-regulated kinase-1
MIP-1α	macrophage inflammatory protein-1α
N	normoxia
NF-κB	nuclear factor kappa-light chain-enhancer of activated B cells
NIK	NF-κB-inducing kinase
NO	nitric oxide
NOSH-aspirin	nitric oxide and hydrogen sulfide releasing aspirin
ODD	oxygen-dependent degradation domain
PARP	poly (ADP-ribose) polymerase
PDK-1	pyruvate dehydrogenase lipoamide isozyme 1
PI3K	phosphatidylinositol 3-kinase
PIC	protease inhibitor cocktail
PLGF	placenta growth factor
PMA	phorbol 12-myristate 13-acetate
Pro	prolyl
PTB	polypyrimidine tract-binding protein
pVHL	von Hippel-Lindau tumour suppressor
RANTES	regulated upon activation, normal protein-1α
RBP	RNA-binding protein
RHD	Rel homology domain
RPS3	ribosomal protein S3
ROS	reactive oxygen species
RT	room temperature
SD	standard deviation
SDS	sodium dodecyl sulfate
SMC	smooth muscle cells
SQR	sulfide:quionine oxido-reductase
SQR-SSH	SQR cysteines
TAD	transcriptional activation domain
TAD-N	N-terminal trans activation domain
TAD-C	C-terminal trans activation domain
TAMs	tumor-associated macrophages
TCR	T-cell receptors
TGF-α	transforming growth factor-α
T	threonine

TNF-α	tumour necrosis factor-α
TLRs	Toll-like receptors
TPP	tristetraprolin
Trx	thioredoxin
VSMC	vascular smooth muscle cell
VCAM-1	vascular cell adhesion protein 1
VEGF	vascular endothelial growth factor

1 Abstract

In mammalian cells, the transcription factor HIF-1 is essential for the regulation of oxygen supply. HIF-1 is a heterodimer composed of the O_2-dependent HIF-1α subunit and the constitutively expressed HIF-1β subunit. Hypoxia results in an excessive upregulation of HIF-1α protein expression, whereas it is abolished under normal oxygen supply due to proteosomal degradation. There are also several stimuli which stabilize HIF-1α under normoxic conditions, e.g. specific growth factors, ROS and nitrogen species. Throughout our investigations we could confirm the increasing effect of hypoxia on the HIF-1α expression.

Currently, little is known about the function of H_2S in the physiological system. Even, if H_2S has protective or damaging effects on living organisms is unclear to date. Thus, we aimed to get further insights into the meaning of hydrogen sulfides. Budde and Roth constituted that H_2S increases HIF-1α in *C. elegans*. Acting on this assumption, our aim was to investigate whether H_2S also enhances HIF-1α protein expression in THP-1 macrophages. Therefore we used a synthetic hydrogen sulfide donor, called GYY4137. In this analysis we could show that 1 mmol/l GYY4137 results in a significant enhancement of HIF-1α in THP-1 macrophages. The increasing effect of GYY4137, as H_2S-releaser, on HIF-1α was exhibited by us for the first time.

We also found that incubation of the cells with GYY4137 under hypoxic conditions results in an even more increased HIF-1α signal. HIF-1α migrates into the nucleus when it is activated. In this study we could demonstrate that GYY4137 was able to increase HIF-1a protein expression in the nucleus in H_2S treated macrophages. The pathway, by which H_2S initiates the activation of HIF-1α, is by now not investigated.

An important target protein of HIF-1α is the glucose transporter GLUT1, which mediates cellular glucose uptake. During our investigations we found that GYY4137 has a similar effect on GLUT1. Our evaluations showed that GLUT1 increases after H_2S incubation and is even more enhanced after incubation with H_2S under hypoxic conditions in THP-1 macrophages.

NF-κB is a transcription factor, whose target genes are involved in controlling apoptosis, cell adhesion, proliferation, innate- and adaptive immune response, inflammation, cellular stress response and tissue remodelling. HIF-1α and NF-κB share target genes and are in part activated by the same stimuli like ROS or cytokines. They are both important factors during inflammation and hypoxic episodes. This was the initial point to investigate whether HIF-1α accumulation can be mediated by the NF-κB pathway as it is known from the literature that the HIF-1α promoter has a functional NF-κB site. We found that the inhibitor of NF-κB, IκB, increases and that the NF-κB subunits p105, p50, p65 and pp65 decline in THP-1 cells after incubation with GYY4137. Upregulation of IκB results in a downregulation of NF-κB subunits. This downregulation of NF-κB subunits could be observed throughout our investigations. These findings lead us to the assumption that HIF-1α activation due to H_2S does not proceed via the NF-κB pathway because the opposite influences of GYY4137 on HIF-1α and NF-κB subunits exclude this possibility. If these findings are connected anyhow, is yet unknown. To investigate possible collective activators, onward investigations are necessary.

Fähling et al. showed that inhibition of p38 leads to a decrease of HIF-1α protein expression. The NF-κB and also the p38 MAPK kinase pathway can be induced by inflammatory and cell stress stimuli. This led us to another aim during our analysis, which was to investigate if HIF-1α or NF-κB activation can happen via the p38 MAPK pathway. Therefore we used a p38 MAPK inhibitor, called SB202190, which inhibits the signal transduction of the MAPK pathway by blocking the p38 activity. The attenuation of IκB as reaction on the inhibition of the p38 MAPK pathway is confusing, because an attenuated IκB activity results in an increase of NF-κB, which we could not observe. We found little effects on the NF-κB subunits or they were even declined after incubation with SB202190 under hypoxia. We found that HIF-1α accumulation due to GYY4137 decreases in THP-1 macrophages after incubation with SB202190, what leads us to the assumption that GYY4137 regulates HIF-1α at least in part by the p38 MAPK pathway. Further analysis is required to confirm our results.

2 Zusammenfassung

Für die Regulierung der Sauerstoffversorgung in Säugetierzellen ist der Transkriptionsfaktor HIF-1 essentiell. HIF-1 ist ein Heterodimer bestehend aus einer O_2-abhängigen Untereinheit, HIF-1α, und einer konstitutiv expremierten Untereinheit, HIF-1β. Hypoxische Verhältnisse in der Zelle führen zu einer Akkumulierung von HIF-1α, während normale Sauerstoffverhältnisse zu einem Abbau von HIF-1α durch das Proteosom führen. Es existieren jedoch auch Stimuli, die HIF-1α unter normoxischen Bedingungen stabilisieren, wie zum Beispiel spezifische Wachstumsfaktoren, ROS und NO. Den stabilisierenden Effekt von Hypoxie auf HIF-1α konnten wir während allen unseren Experimenten bestätigen.

Die Funktion von H_2S im physiologischen System ist bis dato erst wenig erforscht. Sogar die grundlegende Frage, ob H_2S die Zelle schützt oder schädigt, ist noch nicht vollkommen geklärt. Die vielen offenen Fragen bezüglich H_2S im physiologischen System führten uns dazu die Bedeutung von H_2S genauer zu erforschen. Budde und Roth stellten bereits die Vermutung auf, dass H_2S die HIF-1α Proteinexpression in *C. elegans* erhöhen kann. Basierend auf dieser Vermutung war unser Ziel zu untersuchen, ob H_2S auch die Proteinexpression von HIF-1α in THP-1 Makrophagen steigern kann. Dazu benutzten wir einen synthetischen H_2S-Donor namens GYY4137. Durch unsere Forschungsarbeit konnten wir zeigen, dass 1 mmol/l GYY4137 zu einem signifikanten Anstieg der HIF-1α Proteinexpression in THP-1 Zellen führt. Der beobachtete stimulierende Effekt von GYY4137, als H_2S-Donor, auf HIF-1α wurde von uns zum ersten Mal postuliert. Weiters konnten wir zeigen, dass die Inkubation von THP-1 Zellen mit GYY4137 unter hypoxischen Bedingungen zu einem zusätzlichen Anstieg von HIF-1α führt. Die Aktivierung von HIF-1α führt zur Migration des Proteins in den Kern. Unsere Untersuchungen konnten zeigen, dass GYY4137 zur Akkumulation von HIF-1α im Kern von THP-1 Makrophagen führt. Über welchen Signalweg H_2S die Aktivierung von HIF-1α bewirkt ist zur Zeit noch unklar.

Das Protein GLUT1 (Glukosetransporter 1) ist für die Glukoseaufnahme in die Zelle zuständig, wobei die Proteinexpression von GLUT1 durch HIF-1α eingeleitet wird. Während unseren Untersuchungen konnten wir feststellen, dass GYY4137 die Proteinex-

pression von GLUT1 erhöht, welche wiederum durch hypoxische Verhältnisse während der Inkubation mit dem H_2S-Donor in THP-1 Zellen zusätzlich verstärkt wurde.
NF-κB ist ein Transkriptionsfaktor dessen Zielproteine unter anderem eine Rolle in den folgenden Bereichen spielen: Kontrolle der Apoptose, Zelladhäsion, Zellproliferation, angeborene und erworbenen Immunantwort, Entzündung und zelluläre Reaktion auf Stress. Es existieren Proteine, die von beiden beschriebenen Transkriptionsfaktoren, HIF-1α und NF-κB, aktiviert werden können. Außerdem gibt es Reize, die HIF-1α und NF-κB aktivieren, wie zum Beispiel Cytokine und ROS. Auch während entzündlichen Prozessen und hypoxischen Episoden in der Zelle spielen beide Faktoren eine wichtige Rolle. Diese Übereinstimungen zwischen HIF-1α und NF-κB führten uns dazu, zu untersuchen, ob HIF-1α durch den NF-κB Signalweg aktiviert werden kann. Aus einschlägiger Literatur war uns bereits bekannt, dass der Promoter von HIF-1α eine funktionelle NF-κB Bindungsstelle besitzt. Wir konnten zeigen, dass GYY4137 in THP-1 Zellen zu einer Zunahme des Inhibitors von NF-κB, IκB, und zu einer Abnahme der NF-κB Untereinheiten p105, p50, p65 und pp65 führt. Die Schlussfolgerung, dass die Erhöhung von IκB konsequenterweise zu einer Abnahme von NF-κB führt, konnte während unseren Untersuchungen bestätig werden. Die erlangten Ergebnisse führten zu dem Fazit, dass die Akkumulation von HIF-1α durch H_22 nicht über den NF-κB Signalweg initiiert wird, da sich GYY4137 gegensätzlich auf die beiden Transkriptionsfaktoren auswirkt. Ob die Zunahme von HIF-1α und die Abnahme von NF-κB auf irgendeine andere Art miteinander verbunden sind, ist noch unklar. Weitere Untersuchungen sind notwendig, um mögliche gemeinsame Aktivatoren ausfindig zumachen.
Die Arbeitsgruppe um Fähling et al. konnte zeigen, dass die Blockierung von p38 zu einer Abnahme der HIF-1α Proteinexpression führt. Entzündungsreize und Reize, die Stress in der Zelle hervorrufen, können zur Aktivierung des NF-κB Signalweg als auch des p38 MAPK Signalweg führen. Dieses Wissen führt uns zu einer weiteren Frage, nämlich ob die Aktivierung von HIF-1α oder NF-κB durch den p38 MAPK Signalweg initiiert werden kann. Um dies zu untersuchen benutzen wir einen Inhibitor, namens SB202190. SB202190 blockiert p38 und dadurch den gesamten p38 MAPK Signalweg. Wir kamen zu der Erkenntnis, dass der p38 Inhibitor zu einer Abnahme von IκB führt. Diese Beobachtung war jedoch insofern unschlüssig, als verminderte IκB Konzentration

zu einem Anstieg von NF-κB führen sollte, was wir jedoch nicht beobachten konnten. Inkubation von THP-1 Zellen mit SB202190 resultierte sogar zu einer Abnahme mancher NF-κB Untereinheiten vor allem unter hypoxischen Bedingungen. Die beobachteten Effekte des p38-Inhibitor führten uns zu dem Schluss, dass der p38 Signalweg NF-κB beeinflussen kann. Weiters beobachteten wir, dass die durch GYY4137 induzierte Akkumulation von HIF-1α durch SB202190 in THP-1 Zellen reduziert wird. Das führte uns zu dem Fazit, dass die Aktivierung von HIF-1α durch GYY4137 zumindest zum Teil durch den p38 MAPK Signalweg reguliert wird. Um unsere Ergebnisse zu bestätigen sind jedoch weitere Untersuchungen notwendig.

3 Introduction

3.1 Hydrogen sulfide (H_2S)

3.1.1 Chemistry of H_2S

H_2S is a colourless, very volatile gas with a strong malodorous smell. It is a physiological signaling molecule with effects on almost every organ system, particular on the cardiovascular and gastrointestinal systems, immunology and cancer biology [reviewed in KASHFI and OLSON 2012]. Suggestion for the physiological concentration of H_2S ranges from 1 nmol to 150 μmol/l.

H_2S is well known as toxic gas and can occasionally be deadly. It can cause dizziness and loss of consciousness by suppressing the synaptic transmission in the central nerve system [ABE and KIMURA 1996]. The inability to breath is the major cause of death after H_2S intoxication [WANG 2002]. Excessive concentration can lead to apoptosis and inflammation. Values of H_2S under the normal physiological concentration are supposed to contribute to the development of hypertension, atherosclerosis, diabetes and myocardial infarction. Beside H_2S can act as a neuromodulator by binding the N-methyl-D-aspartate receptor in the brain [PERNA et al 2011].

H_2S is water-soluble up to a concentration of about 117 mmol/l. When dissolved in water, H_2S acts as a weak acid. In the chemical equation $H_2S \Leftrightarrow HS^- + H^+ \Leftrightarrow S^{2-} + H^+$, only the first reaction is physiological relevant, because the pK_{a1} is around 6.9, which is similar to the intracellular pH in many tissues and is not far below the pH of blood (pH 7.4). H_2S is unstable in solution and is rapidly oxidized in the presence of oxygen and metal catalyst, like ferric iron. The addition of iron chelators to the solutions can strongly delay the oxidation [reviewed in KASHFI and OLSON 2012].

The measurement of H_2S *in vitro*, but especially *in vivo* is very difficult. The two most commonly methods are the methylene blue spectrometric assay and S^{2-} ion selective electrodes [reviewed in KASHFI and OLSON 2012].

3.1.2 Biosynthesis of H_2S

There are 3 enzymes, which are mainly responsible for the biosynthesis of H_2S: cystathionine β-synthase (CBS), cystathionine γ-lyase (CSE) and the tandem enzymes cysteine aminotransferase (CAT) and 3-mercaptopyruvate sulfurtransferase (3-MST). CBS and CSE are cytosolic enzymes. In the first step of H_2S synthesis, CBS and CSE can act as catalysers. CBS catalyzes the β-replacement of homocysteine with serine, which leads to the formation of cystationine. The α,γ-elimination of cystathionine to form cysteine, α-ketobutyrate and NH_3 is catalyzed by CSE. Then, CBS and CSE can both form H_2S from cysteine via β-elimination. The next step is done by CAT, which transfers the amino group from cysteine to a keto acid, mostly α-ketoglutarate, and forms 3-mercaptopyruvate. Desulfuration of 3-mercaptopyruvate by 3-MST leads to the formation of the persulfide 3-MST-SSH. Thioredoxin (Trx) and dihydrolipoic (DHLA) serve as reductants in the cells and lead to the release of H_2S from 3-MST. The pathway described is the main pathway for the generation of H_2S, but others have also been identified [reviewed in KASHFI and OLSON 2012].

3.1.3 Metabolism of H_2S

Most of the formed H_2S is inactivated through mitochondrial oxidation. Thereby, two membrane-bound sulfide:quionine oxido-reductases (SQR) oxidize sulfide to sulfur and reduce their cysteine disulfides. This causes a persulfide group at each of the SQR cysteines (SQR-SSH). Afterwards, sulfur dioxygenase can oxidize one persulfide to sulfite (H_2SO_3). The sulfur transferase converts the other persulfide to sulfite and produces thiosulfate ($H_2S_2O_3$), which is afterwards also metabolized to sulfite. On this way, two H_2S are oxidized and the electrons are fed into the respiratory chain. The electrons are transferred to oxygen at complex VI, which is bound to the consumption of oxygen and water. In this metabolic cycle one mol oxygen is consumed for every mol H_2S, fed into the electron transport chain. This leads to the suggestion that low H_2S concentration favours oxygen consumption, most likely by feeding electrons to the electron transport chain, whereas high H_2S concentration leads to decreased oxygen consumption [reviewed in KASHFI and OLSON 2012].

The connection of H_2S to the mitochondrium is complex, because it can act as substrate and inhibitor of cytochrome oxidase, depending in part on its cellular integrity [LI et al. 2009].

Interaction of H_2S with other endogenous gases, like NO and carbon monoxide, are possible. The interaction with NO is multifunctional. One possibility is the formation of nitrosothiol, thereby inhibiting nitric oxide synthase and quenching ROS [LI et al. 2009].

3.1.4 Physiologic function of H_2S

The H_2S-producing enzyme CBS is highly expressed in the brain, more precisely in the hippocampus and the cerebellum. The H_2S, produced in the brain, functions as neuromodulator [ABE and KIMURA 1996]. H_2S can influence synapses and can protect the neuronal system from oxidative stress. It increases the reducing effort of neurons at which an involvement of the tyrosine kinase is assumed. This leads to the improvement of the survival of neurons in the brain [UMEMURA and KIMURA 2007]. There is an involvement of H_2S in associative learning supposed [ABE and KIMURA 1996].

H_2S has function on the brain by inducing long-term potentiation in the hippocampal and on the brain development. Furthermore it decreases the blood pressure by opening K_{ATP} channels. Thereby H_2S hyperpolarizes the cell membranes, leading to the relaxation of smooth muscle cells. Studies showed that H_2S relaxes the aorta *in vitro* and the portal vein of rats *in vivo* [WANG 2002].

H_2S mainly acts by sulfhydrating cysteines of target proteins, such as GAPDH and actin. So sulfhydration leads to an increase of the GAPDH activity and actin polymerisation. Important functions of H_2S are the vasodilatory effect and the participation in inflammatory processes [SEN et al. 2012].

Ancient bacteria and archea, such as the lungworm *Arenicola marina*, use H_2S as energy substrate. In mammalian cells H_2S can act as oxygen sensor and can regulate the energy production under stress conditions like hypoxia. The aroused demand on oxygen under hypoxic conditions can then be covered. The H_2S producing enzyme, CSE, uses cysteine as energy substrate in the cardiovascular system. Fu et al. showed that CSE translocate from the cytosol into the mitochondrium under hypoxic conditions, where it enhances the production of ATP by metabolizing cysteine to H_2S in vascular smooth muscle cells (SMCs). Thereby, the electrons from sulfide can be fed into the mitochondrial electron transport chain. Under resting conditions CSE is only found in the cytosol. They suggest that this way to generate energy is unique to cells whose metabolism is dependent on oxidative phosphorylation and oxygen supply. So H_2S is able to reduce the metabolic demand and can protect the mitochondria function and the respiratory system. Furthermore H_2S can act as antioxidant [FU et al. 2012].

The question, if H_2S acts anti- or pro-inflammatory, is highly discussed. One suggestion is, that high concentrations of H_2S enhance inflammation by dilating blood vessels, promoting oedema and triggering hyperalgesia, while low concentrations of H_2S act anti-inflammatory by interfering with the NF-κB and STAT pathway and thereby reduce the expression of pro-inflammatory molecules and upregulate the expression of anti-inflammatory molecules [LI et al. 2009].

3.1.5 Hydrogen sulfide releaser

H_2S releaser can be divided into sulfide salts, natural donors and synthetic donors. The most common sulfide salt is NaHS. Naturally occurring compounds are found mainly in food, for example in garlic, broccoli and rocket salad. Synthetic donors are, amongst others, GYY4137, cysteine analogues, S-prolyl cysteine, S-allyl cysteine, S-propargyl cysteine and N-acetyl cysteine [reviewed in KASHFI and OLSON 2012].

3.1.5.1 Sulfide salts

Sulfide salts are NaHS, Na_2S and CaS. They form HS^- out of H_2S immediately after solvation. Because their effect in tissue is extremely short, they probably cannot really be called H_2S-donating compounds, because they do not mimic the biological effect of naturally produced H_2S. This fact also limits their therapeutic application [reviewed in KASHFI and OLSON 2012].

3.1.5.2 Natural H_2S releaser

The best characterized naturally occurring H_2S releaser is found in garlic and is called allicin (diallyl thiiosulfinate) [BENAVIDES et al 2007]. Others are sulphoraphane, which is found in broccoli, and erucin, found in rocket salad. Allyl isothiocyanate, which is a compound in wasabi, mustard and horseradish belongs to this group too. All mentioned molecules belong to the group of isothiocyanates [reviewed in KASHFI and OLSON 2012].

3.1.5.3 GYY4137 and other synthetic H_2S releaser

GYY4137, with full chemical name morpholin-4-ium 4 methoxyphenyl (morpholino) phosphinodithioate, is, in contrast to NaHS, a slow releasing H_2S compound (Fig. 1). It is a water-soluble molecule and emits H_2S in aqueous solution *in vitro* and after intravenous or intraperitoneal injection in anesthetized rats *in vivo*. It is suggested that 1 mmol/l GYY4137 releases approximately 40 μmol H_2S in the first 10 minutes and then 40 μmol

per hour, but only for the next 80 minutes, when dissolved in acidic phosphate buffer. In aqueous solutions the release is pH and temperature dependent with less release at 4°C and greater release at pH 3.0, than at neutral or alkaline pH. When dissolved in buffer at pH 7.4 or 8.5 the release is less than 3 μmol/l H_2S. This is relatively little compared to the H_2S release when GYY4137 is dissolved in acidic buffer. Intraperitoneal or intravenous injection of 133 μmol/kg GYY4137 led to an increase of plasma H_2S from about 32 μmol/l H_2S to about 80 μmol/l in the time of 30 minutes, in rats. An elevated concentration of 50 μmol/l was observed for the next 3 hours [LI et al. 2008].

The molecular mechanism by which GYY4137 releases H_2S happens probably by protonation of the sulfide group, thereby forming a sulfhydryl moiety. This is followed by hydrolysis, which ends in the release of H_2S [LI et al. 2009].

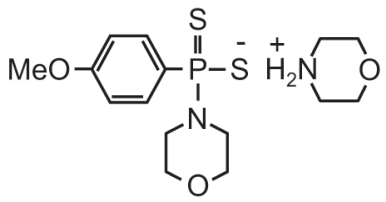

GYY4137

Figure 1: Chemical structure of GYY4137 [LI et al. 2008].

Further synthetic H_2S releasing substances are cysteine analogues. Cysteine is able to mimic the effects of H_2S through providing additional H_2S. Another class of synthetic donors are cysteine-activated H_2S releaser, which use the occurrence that in the presence of excess cysteine, N-(benzoylthio)benzamid slowly emits H_2S. A relatively new compound is nitric oxide and hydrogen sulfide releasing aspirin (NOSH-aspirin). Thereby NO is connected to a NSAID by an aromatic ring or aliphatic linker (NO-NSAIDs). This compound releases NO and H_2S and is suggested to be more effective than either one of them alone [reviewed in KASHFI and OLSON 2012].

3.1.5.4 Biology of GYY4137

The effects of GYY4137 in rat include slow developing but long lasting relaxation of the aorta, vasodilation of the pre-constricted kidney and antihypertensive effects. The vasodilatory effect of GYY4137 is due to the opening of smooth muscle K_{ATP} channels and was shown in rat and human blood vessels *in vivo*. It is suggested that GYY4137 can not only relax large blood vessels, but also small arterioles [LI et al. 2008].

Effects on the cardiac contractility or heart rate *in vitro* could not be observed. It was also shown that GYY4137 can exhibit an antihypertensive activity by developing a slow fall of the blood pressure, detectable after 30 minutes, which continued declining 120 minutes after injection in anesthetized rats. GYY4137 has a protective effect against ischemia and reperfusion injury, which also can be explained by the opening of K_{ATP} channels by H_2S. [LI et al. 2008]. Li et al. suggest an anti-inflammatory effect of GYY4137. In cultured RAW 264.7 cells, a decrease of LPS-induced inflammation markers (e.g. TNF-α, IL-1β, NF-κB and iNOS) was observed after GYY4137 treatment. This effect was also observed in rat blood. This group strengthens the possibility that GYY4137 has anti-inflammatory effects *in vivo* by decreasing activation of NF-κB transduction. Thereby it inhibits the expression of inducible nitric oxide synthase and cyclooxygenase-2 expression and consequently the biosynthesis of pro-inflammatory cytokines and mediators, like NO and prostanoids [LI et al. 2009]. Also an anti-cancer effect was observed *in vitro* and *in vivo* [LEE et al. 2011]. Experiments in cultured smooth rat muscle cells did not show cytotoxic effects, changes of the cell cycle distribution or enhanced p53 expression after GYY4137 treatment (up to 100 μmol/l) [LI et al. 2008].

The advantage of GYY4137 compared to NaHS is, that its effects are slower in onset and longer lasting [reviewed in KASHFI and OLSON 2012]. It exists the hypothesis that the effects observed for NaHS and GYY4137 are also caused by the simultaneously release of endogenous NO of both agents in cells [LI et al. 2008].

3.2 Hypoxia-inducible factor (HIF)-1α

HIF is a heterodimer, which consists of an α- and a β-subunit and belongs to the basic helix-loop-helix (bHLH) transcription factor family [WANG and SEMENZA]. HIF-1α is built out of 826 amino acids. Both, the α- and the β-subunit, contain two PAS domains (PAS-A and PAS-B), which are, together with the bHLH domain, necessary for dimerization and DNA-binding. HIF-1α also contains the domains TAD-N and TAD-C (N- and C-terminal TAD). TAD-N overlaps with the oxygen-dependent degradation domain (ODD), whereas TAD-C interacts with coactivators like p300/CBP (Fig. 2) [reviewed in LEE et al. 2004].

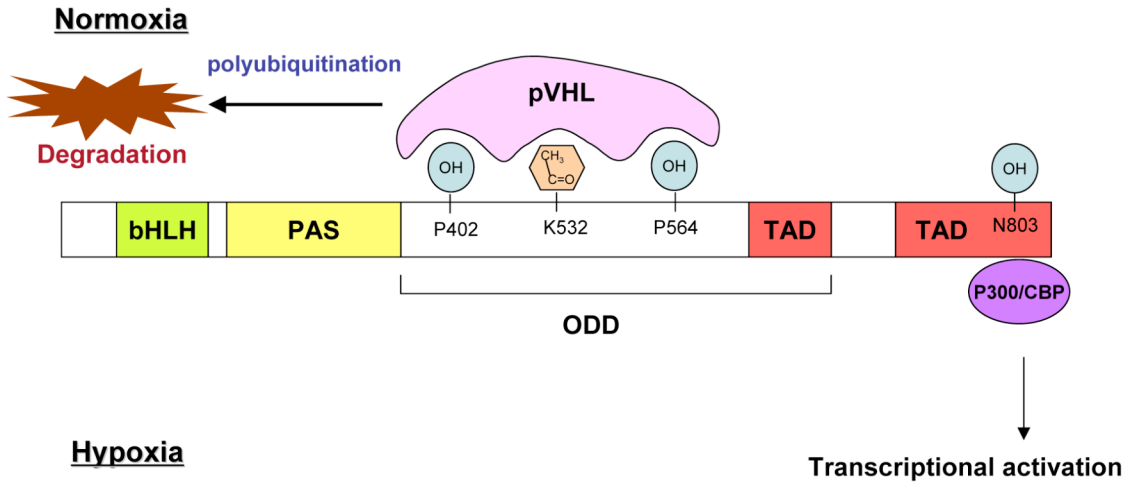

Figure 2: Structure of HIF-1α. The bHLH and the PAS domain are necessary for the dimerization with HIF-1β. The N-terminal TAD domain overlaps with the ODD domain and the C-terminal TAD domain is necessary for the interaction with cofactors [reviewed in LEE et al. 2004].

Beside HIF-1α, there are two other isoforms, namely HIF-2α and HIF-3α. HIF-1α is thought to be ubiquitously expressed, whereas HIF-1β is expressed cell specific [FÄHLING et al. 2012]. Studies indicate that HIF-2α shares high sequence homology and is similar regulated as HIF-1α and therefore is degraded under normal oxygen proportions. In contrast to the other two family members, HIF-3α lacks the transactivation domain and maybe acts as an antagonist in the HIF-system. The gene expression of HIF differs in different cell types [reviewed in LEE et al. 2004].

There are five splice variants of HIF-1α known [CHUN et al. 2003].

3.2.1 Stabilisation and regulation of HIF-1α

One regulator of HIF-1α is oxygen. Under normoxic conditions HIF-1α is rapidly degraded. The abundance of HIF-1α is prevalently regulated by a family of prolyl hydroxylases, called PHD1, PHD2 and PHD3. From these, PHD-2 is considered to be the most active [KAELIN and RATCLIFF 2008]. If oxygen is available, PHDs catalyze the hydroxylation of specific prolyl residues (Pro 402 and Pro 564), which are located in the ODD domain of HIF-1α [SCHOFIELD and RATCLIFFE 2005]. This hydroxylation is Fe(II)-dependent. Then, the hydroxylated HIF-1α is bound by the von Hippel-Lindau (pVHL) tumour suppressor protein, an E3 ubiquitin-protein ligase, which is a marker for ubiquitination, and subsequent proteasomal degraded of by the 26S proteosome. Beside PHDs, FIH (factor inhibiting HIF) is also able to limit HIF-1α protein level through similar mechanisms [reviewed in DEHNE et al. 2009]. Another critical step in the degradation of HIF-1α is the acetylation of Lys-532 by ARD-1 (acetyltranferase 1). A further mechanism to prevent HIF-1α activity is the hydroxylation of Asn^{803} in HIF-1α or Asn^{851} in HIF-2α. The hydroxylation blocks the interaction of the coactivator p300/CBP with HIF-1α [UDEN et al. 2008].

Hypoxia terms the condition, when oxygen supply to a tissue is reduced to a value below the physiological level. The oxygen concentration is considered to be below 5% during hypoxia. The blood perfusion of the tissue is thereby normal. Reasons can be reduction of the oxygen-carrying capacity of the blood, impaired use of oxygen by the tissue or that insufficient amount of oxygen reach the blood [DORLAND 2011].

Under hypoxic conditions the activity of PHDs decreases. This leads to the stabilization of HIF-1α. Then, HIF-1α is able to translocate into the nucleus, associate with p300/CBP, heterodimerize with HIF-1β and bind to hypoxic response elements (HREs) to induce the expression of target genes [reviewed in DEHNE et al. 2009]. These target genes participate in cell proliferation, cell survival, apoptosis, glucose metabolism, iron metabolism, pH regulation, erythropoiesis, extracellular matrix remodelling, inflammation and angiogenesis [FÄHLING et al. 2012] (Fig. 3).

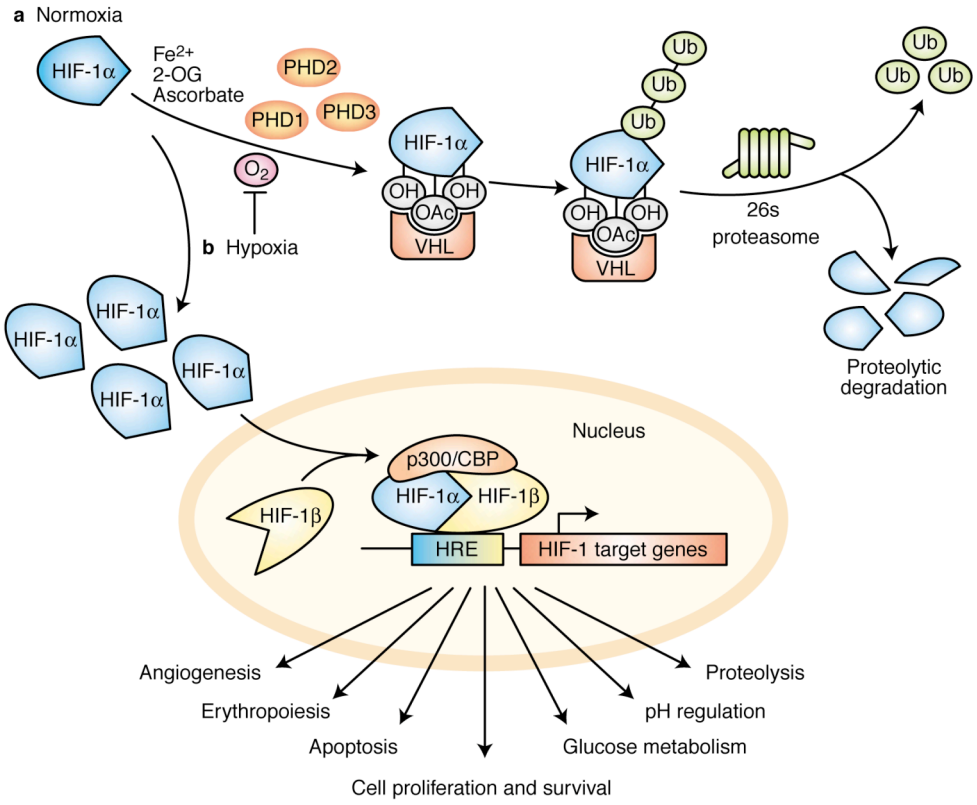

Figure 3: Regulation of HIF-1α by oxygen. (a) Under normoxic conditions HIF-1α is hydroxylated and bound by the pVHL. This leads to the recognition by the proteosome and further to the degradation of HIF-1α. (b) Under hypoxic conditions PHDs are inhibited, which leads to translocation of HIF-1α into the nucleus, where it dimerizes with HIF-1β. HIF-1 binds to the HREs within the promoters of target genes and activates coactivators such as p300/CBP. The activated genes have functions in multiple areas [CAROLL and ASHCROFT 2005].

Recent studies indicate that HIF-1α is also transcriptionally regulated, especially in the context of inflammation. A number of RNA-binding proteins (RBPs) were discovered which have been shown to influence the HIF-1α mRNA stability [FÄHLING et al. 2012]. Examples for RBPs are HuR (human antigen R), PTB (polypyrimidine tract-binding protein), heterogenous nuclear ribonucleoproteins (hnRNPs), tristetraprolin, nucleonlin, iron-response element-binding proteins (IRPs) and cytoplasmatic polyadenylation-element-binding proteins (CPEBs) [reviewed in GOROSPE et al. 2011]. The mRNA turnover is mainly controlled by the 3'-untranslated region (3' UTR) [FÄHLING et al. 2012]. It was shown that the 3' UTR of HIF-1α is highly conserved among vertebrate species. In

UTRs adenlyate- and uridylate-rich elements (AREs) are often found, which control the stability of the mRNA. One important ARE-interacting RBP of HIF-1α is tristetraprolin (TPP). Many target genes of TPP are involved in the inflammatory response. It interacts with its own 3' UTR leading to the destabilization of its own mRNA. Under hypoxia, TPP mediates HIF-1α destabilization. In contrast, under normoxic conditions, phosphorylation of TPP by the p38 MAPK pathway results in stabilization of HIF-1α mRNA following increased HIF-1α activity. Dependent on the phosphorylation state of TPP, it either acts as enhancer (phosphorylated) or inhibitor (unphosphorylated) of HIF-1α. By now, it is not clear if phosphorylated TPP does this by actively binding HIF-1α mRNA or if it competes with unphosphorylated TPP for the limited binding sites of HIF-1α mRNA or both [FÄHLING et al. 2012].

3.2.2 HIF-1α and inflammation

In inflamed tissues, the oxygen availability is often under the normal physiological value, what consequently leads to an increase of HIF-1α activity [reviewed in DEHNE et al. 2009]. HIF-1α can also be activated under normoxia during inflammation and can thereby prevent tissues from becoming hypoxic by initiating the inflammatory response [reviewed in ELTZSCHIG and CARMELIET 2011].

There are several effects, which can stabilize HIF-1α under normoxic conditions, because PHDs, which catalyze the hydroxylation of HIF-1α and marks them for degradation, are sensitive to alterations in the cellular redox balance, iron homeostasis and metabolite availability [reviewed in DEHNE et al. 2009]. Stabilization of HIF-1α can happen under normoxic conditions, for example through growth factors via the phosphatidylinositol 3-kinase (PI3K) and the MAPK pathway [FUKUDA et al. 2002].

As an early response to hypoxia the activation of the p38 MAP kinase pathway was observed. This pathway is induced during oxidative stress and plays a role in the regulation of cell differentiation, survival and apoptosis. Khandrika et al. found that reduced p38 MAPK activity led to a decreased HIF-1α expression in prostate cancer cells under hypoxic conditions. They suggest that activation of the p38 MAPK pathway results in the stabilization of HIF-1α [KHANDRIKA et al. 2009].

Nitric oxide (NO) has been reported to stabilize HIF-1α under normoxia, using in part the same pathway as hypoxia [PALMER et al. 2000]. Contrary, it was observed that NO decreases HIF-1α under hypoxic conditions. One explanation therefore is that NO competes with O_2 for the binding to mitochondrial cytochrome oxidases. These cytochrome oxidases consume a lot of oxygen within the cell. If there is less oxygen available in the cell, NO binds to cytochrome oxidase to reduce their O_2-consumption. The oxygen can then be consumed, for example by PHDs, which further leads to reduced accumulation of HIF-1α under hypoxic conditions in the presence of NO. iNOS (inducible nitric oxide synthases) produce NO as an immune defence mechanism and contain a HRE. HIF-1α is critically involved in the upregulation of iNOS during inflammation [reviewed in DEHNE et al. 2009].

Antioxidants, like ascorbate, are essential for PHDs to keep their iron reduced and thus to prevent their inactivation. Oxidative stress leads to the consumption of antioxidants. So, if cells suffer oxidative stress and consume higher amounts of antioxidants, the function of PHDs is limited [reviewed in DEHNE et al. 2009]. Ascorbate deficiency is one cause for HIF-1α accumulation in tumours [KAELIN and RATCLIFF 2008]. Consequently, this leads to the elevation of HIF-1α. In this context, reactive oxygen species, H_2O_2 and redox cycling agents increase HIF-1α activity. ROS oxidize the Fe(II) at the catalytic site of PHDs an lead to their inactivation. It also exists the suggestion that ROS inhibit HIF hydroxylases by oxidation of active site amino acids and thereby give rise to HIF-1α accumulation. In connection to inflammation, where ROS are present, increased HIF-1α levels can also be detected [reviewed in DEHNE et al. 2009].

Cytokines are part of the immune defence after pathogen invasion. Some of them, like TNF-α and IL-1β, cause the production of ROS and NO and the activation of PI3K and NF-κB pathway during defence. These mechanisms can cause accumulation of HIF-1α. A further factor responsible for inflammation are lipopolysaccharides (LPS), bacterial cell wall components, that have been shown to increase HIF-1α mRNA expression through the p42/44 MAPK pathway. Besides, LPS produce ROS, which, as already mentioned, also lead to the accumulation of HIF-1α in macrophages (Fig. 4) [reviewed in DEHNE et al. 2009].

The role of NF-κB in the mechanisms leading to an increase of HIF-1α is, by now, not fully understood. Because NF-κB is an important factor during inflammation and hypoxic episodes, as it is also the case in HIF-1α, a connection of both is possible [reviewed in DEHNE et al. 2009].

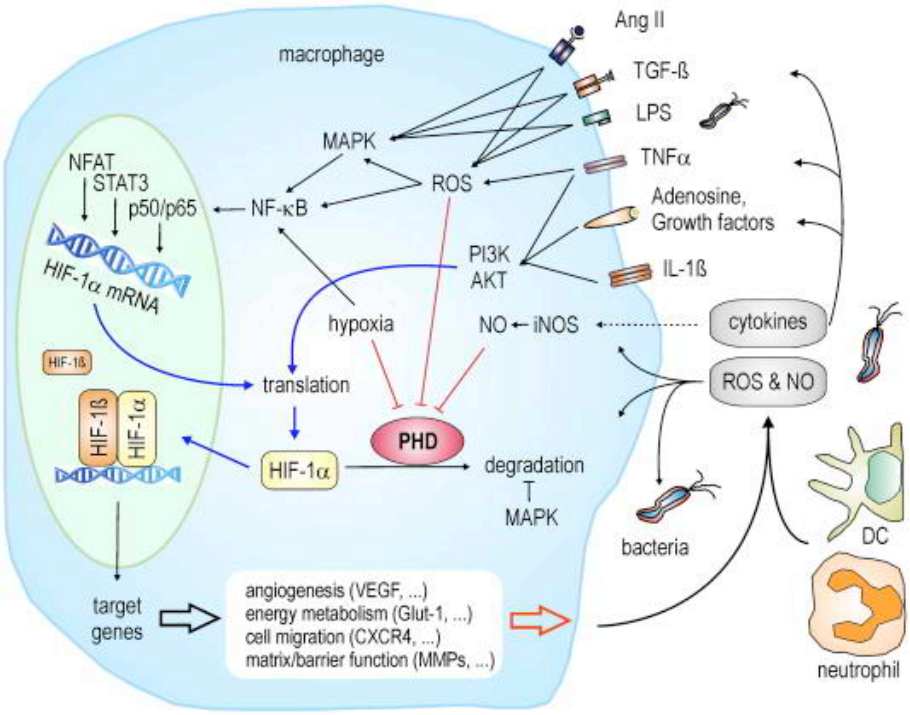

Figure 4: Regulation of HIF-1α in inflammatory microenvironment exemplified for macrophages. Multiple effects influence the protein amount and activity and subsequent the expression of target genes. Inhibiting effects are shown in red, stimulating in blue [reviewed in DEHNE et al. 2009].

3.2.3 Target genes of HIF-1α

HIF-1α induces the transcription of more than 70 genes, which have been found out through functional delineation of HRE [reviewed in DEHNE et al. 2009].

The vascular endothelial growth factor (VEGF) is a very important target gene of HIF-1α. As for HIF-1α protein, hypoxia induces the expression of VEGF mRNA and protein. VEGF is produced by cells to stimulate vasculogenesis and angiogenesis. In this case its function is to create new blood vessels during the embryonic development and after injury [KAJDANIUK et al. 2011]. In mammalians, 5 different isoforms were detected:

VEGF-A, VEGF-B, VEGF-C, VEGF-D and placenta growth factor (PLGF) [HOLMES et al. 2007]. VEGFs form cysteine cross-linked dimers. All VEGFs isoforms have different splicing variants with distinct properties and bind to specific subtypes of VEGF receptors. There are three types of VEGF receptors [CÉBE SUAREZ et al. 2006]. VEGF-A exists in 6 different splicing isoforms, formed out of one precursor mRNA in humans. Most of them are freely diffusible and have binding affinities to the extracellular matrix (ECM) and cell surface heparan sulphate proteoglycans (HSPGs). Two splice variants of VEGF-A remain bound to the ECM and are therefore not free diffusible [HOLMES et al. 2007].

Many proteins, activated by HIF-1α, play a role in the glucose metabolism, most notably the proteins belonging to the GLUT family [reviewed in LEE et al. 2004]. Glucose is the primary source for energy and carbon in all organisms and its transport highly conserved. The GLUT protein family is a multimembrane-spanning transporter family and consists of 14 members, which transport glucose across the cell membrane. GLUT1 is the main glucose transporter and composed out of 12 transmembrane domains with 6 extracellular loops. The highest expression of GLUT1 is found in human erythrocytes. GLUT1 also transports DHA (L-dehydroascorbic acid), an intermediate of ascorbic acid (AA), because the structure to that of glucose is very similar. Montel-Hagen et al. showed that GLUT1 is only expressed on erythrocytes by species which are unable to synthesize AA from glucose, namely humans, some higher primates, guinea pigs and fruit bats. Stomatin is a cholesterol-binding scaffolding protein. Interaction of GLUT1 with stomatin lead to the migration of GLUT1 into lipid rafts, resulting in reduced glucose uptake in the cell [MONTEL-HAGEN et al. 2008].

Some growth factors, for example the insulin-like growth factor-2 (IGF-2) and the transforming growth factor-α (TGF-α), are also target genes of HIF-1α, which, in turn, switch on HIF-1α expression and promote cell proliferation and survival [KAJDANIUK et al. 2011].

3.2.4 HIF-1α and disease

HIF-1α plays a role in many diseases, particularly in those, generating a hypoxic microenvironment, such as cancer, stroke and heart disease [reviewed in LEE et al. 2004]. Angiogenesis is an important tool of tumours to ensure sufficient energy and nutrient supply [reviewed in DEHNE et al. 2009]. HIF-1α, which promotes angiogenesis, was found to be overexpressed at high levels in human tumours as a result of hypoxic conditions and genetic alterations, which apply oncogenes and tumour suppressor genes. HIF-1α also plays a major role in tumour promotion and metastasis [CHUN et al. 2003]. When hypoxic conditions are present in tumours, HIF-1α is activated, which subsequent leads to the production of proangiogenetic factors like VEGF [reviewed in DEHNE et al. 2009]. But, HIF-1α can also be induced independently of oxygen supply in tumours. Phorbol esters, such as PMA, are well known tumour promoters. PMA is known to cause oxidative stress by activating the NADPH oxidase. Chun et al. showed that a particular human splice variant of HIF-1α, HIF-1α^{785}, is primarily regulated by PMA, heat shock and oxidative stress under normoxia. In tumours, increased energy metabolism leads to hyperthermia and oxidative stress. Furthermore, hydrogen peroxide can upregulate the expression of HIF-1α^{785}. The induction of HIF-1α^{785} by PMA was shown to happen via a redox-dependent mitogen activated protein/extracellular signal-regulated kinase-1 (MEK-1) pathway or by the redox-state. HIF-1α^{785} stabilization under normoxia can be explained by its loss of Lys^{532}, which prevents the acetylation of this splice form. Chun et al. showed that inhibition of the p38 mitogen-activated protein kinase pathway with the inhibitor SB203580 reduced the HIF-1α expression markedly. The role of oxidative stress in the stabilization of HIF-1α is controversial. An explanation for its dual role could be the different isoforms of HIF-1α, which are induced by different mechanisms. It is possible that during hypoxia HIF-1α is suppressed by oxidative stress, while under normoxia the splice variant HIF-1α^{785} is induced by oxidative stress [CHUN et al. 2003].

Because HIF-1α is overexpressed in many human cancer types, it maybe can be used as target for gene therapies. Blocking of HIF-1α possibly avoids oxygen and nutrient supply to tumours and prevents cancer progression. This could happen via a HIF-1α

antisense therapy, that inhibits the interaction between HIF-1α and CBP/p300 and particular small molecules [reviewed in LEE et al. 2004].

Atherosclerosis causes arterial stenosis, impaired perfusion of vessels and ischemia. When the systemic and cellular O_2 concentrations are disrupted it results in heart diseases, for example in a heart attack. The hypoxic conditions, which occur during these diseases lead to the induction of HIF-1α mRNA and protein expression and furthermore to the increased expression of VEGF during acute ischemia and infarction in human heart [reviewed in SEMENZA 2000]. HIF-1α is able to regulate cytokine production and T cell activation and thereby can attenuate inflammatory processes. It was shown that HIF-1α reduced the expression of the cytokine interferon γ (IFNγ) and atherosclerosis in mouse lymphocytes. Studies also showed that deletion of HIF-1α results in an increase of proinflammatory cytokines such as TNF-α, IL-2, IL-4 and IL-3. So an antiinflammatory quality of HIF-1α is suggested, which can cause a reduction of atherosclerosis [BEN-SHOSHAN et al. 2009].

3.2.5 HIF-1α and hydrogen sulfide (H_2S)

The regulation of HIF-1α transcription and protein expression by NO and CO have been reported earlier. A newer finding is the influence of the gasotransmitter H_2S on the HIF-1α transcription and expression. Wu et al. showed that hypoxia-induced accumulation of HIF-1α is reversed by NaHS and that this effect is independent of the proteosomal degradation of HIF-1α in HEK293T, Hep3B an EA.hy926 cells [WU et al 2012]. Kai et al. showed the same effect in Hep3B cells and additionally in neuronal SH-SY5Y cells, HeLa cells, primary cultured mouse hepatocytes and human aortic smooth muscle cells (HASMCs). The effect of H_2S was suggested to be caused by reducing the cellular oxygen consumption. The HIF-1α target genes GLUT1, VEGF, PDK-1 and LDHA were also shown to be decreased by H_2S. It was found that H_2S inhibits the hypoxia-induced HIF-1α accumulation by acting on the pVHL protein and the mitochondrium and not on the protein synthesis of HIF-1α [KAI et al 2012]. Wu et al. found that the suppression of HIF-1α by H_2S happens in part via enhanced eIF2α (eukaryotic translation initiation factor 2α) phosphorylation. Phosphorylation of eIF2α leads to the formation of the eIF2 ternary

complex, which then can inhibit HIF-1α translation. They also suggest that H_2S inhibits the mitochondrial O_2-consumption, leading to a higher oxygen availability in hypoxic cells and further to increased HIF-1α degradation [WU et al 2012].

Studies predict a protective effect of H_2S in respect to hypoxia, haemorrhage and reperfusion injury in mice. Budde and Roth found that H_2S leads to an increase of HIF-1α in *C. elegans*. *C. elegans* has one conserved homologue of the mammalian HIF-1α (*hif-1*). They also observed enhanced nuclear localization and transcription of HIF-1α target genes. These effects were independent of the VHL-1 protein, which is required for the regulation of HIF-1α under hypoxic conditions. This leads to the suggestion that there are multiple ways to activate HIF-1α. They also showed that HIF-1α is necessary for nematodes when they are exposed to H_2S. Besides, an increased HIF-1α level drastically enhanced the maximal tolerable H_2S level. They conclude that H_2S can activate HIF-1α maybe by two ways, stabilizing the protein and activate the transcription of HIF-1α. The observed protective effect of increased HIF-1α and H_2S during hypoxia presumes a connection between the activation mechanisms of these two [BUDDE and ROTH 2009].

Intraperitoneal injection of H_2S-donor NaHS to mice under 20% or 10% oxygen atmosphere, inhibited the expression of HIF-1α and target genes. This effect again was caused by the interaction of H_2S with the pVHL protein and the mitochondrium. In this *in vivo* study the alterations of HIF-1α were not due to changes in the circulatory or respiratory system in mice [KAI et al 2012].

3.3 Nuclear factor kappa-light chain-enhancer of activated B cells (NF-κB) family

NF-κB is the collective name of homodimeric or heterodimeric transcription factors. There are 15 possible homodimers and heterodimers, composed out of five gene products: NF-κB1 (p105/p50), NF-κB2 (p100/p52), RelA (p65), RelB and c-Rel. Some dimers are very common, whereas others are very rare. The subunit p50 is the processed product of p105, and p52 the processed product of p100. All polypeptides contain a Rel

homology domain (RHD), which is responsible for dimerization, nuclear localization and DNA binding. The proteins RelA, RelB and c-Rel contain a transcriptional activation domain, which is essential for transcriptional activation. Dimers, which contain one of these subunits act as transcriptional activators. As a consequence, dimers that are composed without RelA, RelB or c-Rel fail to activate the transcription of genes [reviewed in GHOSH et al. 2012]. Despite all NF-κB subunits have an obvious similar structure, they all have distinct and non-overlapping functions [reviewed in PERKINS 2007].

3.3.1 NF-κB pathway

NF-κB is one part in a signaling module comprising three components: IκB kinase (IKK), NF-κB and Inhibitor of NF-κB (IκB) [reviewed in GHOSH et al. 2012]. A stimulating signal, for example inflammation mediators, such as cytokines (e.g. TNFα) or bacterial LPS, oncogenes or UV light lead to the activation of IKK [UDEN et al. 2008]. Then, IKK becomes catalytically active and phosphorylates IκB, leading to its ubiquitination and subsequent to its degradation by the 26S proteosome. NF-κB, which was blocked by IκB, is now no longer blocked, can migrate into the nucleus and activate target genes. The activation of target genes happens via specific binding of NF-κB to the κB DNA binding site, which is 9-11 bp long and is located in the promoter or enhancer of more than 500 target genes [reviewed in GHOSH et al. 2012]. The transcription of target genes can both be activated and repressed by binding NF-κB on the κB-site of genes. Those target genes are involved in controlling apoptosis, cell adhesion, proliferation, innate- and adaptive immune response, inflammation, cellular stress response and tissue remodelling. Because of the fact that many other signaling pathways are also involved in regulating NF-κB target genes, the outcome of NF-κB activation depends on the cellular context of its induction [reviewed in PERKINS 2007].

In most cell types NF-κB is retained in the cytoplasm by a family of inhibitors, called IκB. There are eight family members in the IκB family: IκBα, IκBβ, IκBε, IκBγ (p105), IκBδ (p100) Bcl3, IκBζ and IκBNS [reviewed in GHOSH et al. 2012]. The three main inhibitors

of NF-κB in mammalian cells are IκBα, IκBβ and IκBε [reviewed in PERKINS 2007]. All of them contain an ankryn repeat domain (ARD), which enables an association of IκB with NF-κB. They inhibit NF-κB by binding it and leading to its degradation. IκBs prefer binding to dimers which contain a RelA or c-Rel subunit. The unprocessed subunits of NF-κB1 and NF-κB2, p105 and p100, respectively also act as inhibitors of NF-κB. The atypical IκB proteins Bcl3, IκBζ and IκBNS transcriptionally regulate the NF-κB activity [reviewed in GHOSH et al. 2012]. Bcl3 interacts with p50 and p52 and, unlike the others, is located in the nucleus and functions as coactivator. Another interesting fact is that homodimers out of the subunits p50 or p52 escape the regulation of IκB and therefore are often found in the nucleus [reviewed in PERKINS 2007].

The IKK family constitutes of four family members: IKKα (IKK1), IKKβ (IKK2), IKKγ (NEMO) and TBK1. IKKα and IKKβ can form heterodimers and homodimers and similarly do IKKγ and TBK1. IKKα and IKKβ can phosphorylate IκB leading to its degradation, but IKKβ is more active. IKKα regulates the processing of p100 to p52. IKKγ and TBK1 are indeed involved in the activation of NF-κB, but not in the phosphorylation of IκB [reviewed in GHOSH et al. 2012]. IKKβ stimulates especially anti-apoptotic, pro-inflammatory and pro-proliferative pathways. It can form an auto-feedback loop, by downregulating the signaling pathway that leads to its activation. Activation of IKKα can also have a pro-proliferative function by stimulating p53 activity [reviewed in PERKINS 2007].

There are distinct activation pathways for NF-κB: the canonical or classical pathway, the non-canonical or alternative pathway and the atypical pathway. The most frequently observed canonical pathway is induced by inflammatory stimuli, e.g. TNF-α and interleukin-1 (IL-1), T-cell receptors (TCR) or LPS. The rapid phosphorylation of IκB at Ser32 and Ser36 by the IKK complex and the subsequent degradation is typical for this pathway. In this pathway IKKα, IKKβ and NEMO form a complex. For the activation of the IKK complex the regulatory subunit NEMO is essential [reviewed PERKINS 2007].

In the atypical pathway, stimuli like ionizing radiation or chemotherapeutic drugs lead to the translocation of NEMO into the nucleus, where it is sumoylated and phosphorylated by the checkpoint kinase ataxia telangiectasia mutated (ATM). Then sumoylation is replaced by mono-ubiquitination, resulting in the export of NEMO once again in the cytoplasm and finally leading to activation of the IKK complex. Another atypical activation mechanism of NF-κB is the IKK-independent pathway, which is induced by hypoxia or hydrogen peroxide stimulation [reviewed PERKINS 2007].

The activation of CD40, lymphotoxin-β receptors, B-cell-activating factor of the TNF family (BAFF), LPS, and latent membrane protein 1 (LMP1) of Eppstein Barr virus lead to the initiation of the non-canonical pathway of NF-κB. In this pathway, IKKα activation by the NF-κB-inducing kinase (NIK) results in the processing of p100 to p52. The heterodimer p52-RelB is the most common form in this pathway (Fig. 5) [reviewed PERKINS 2007].

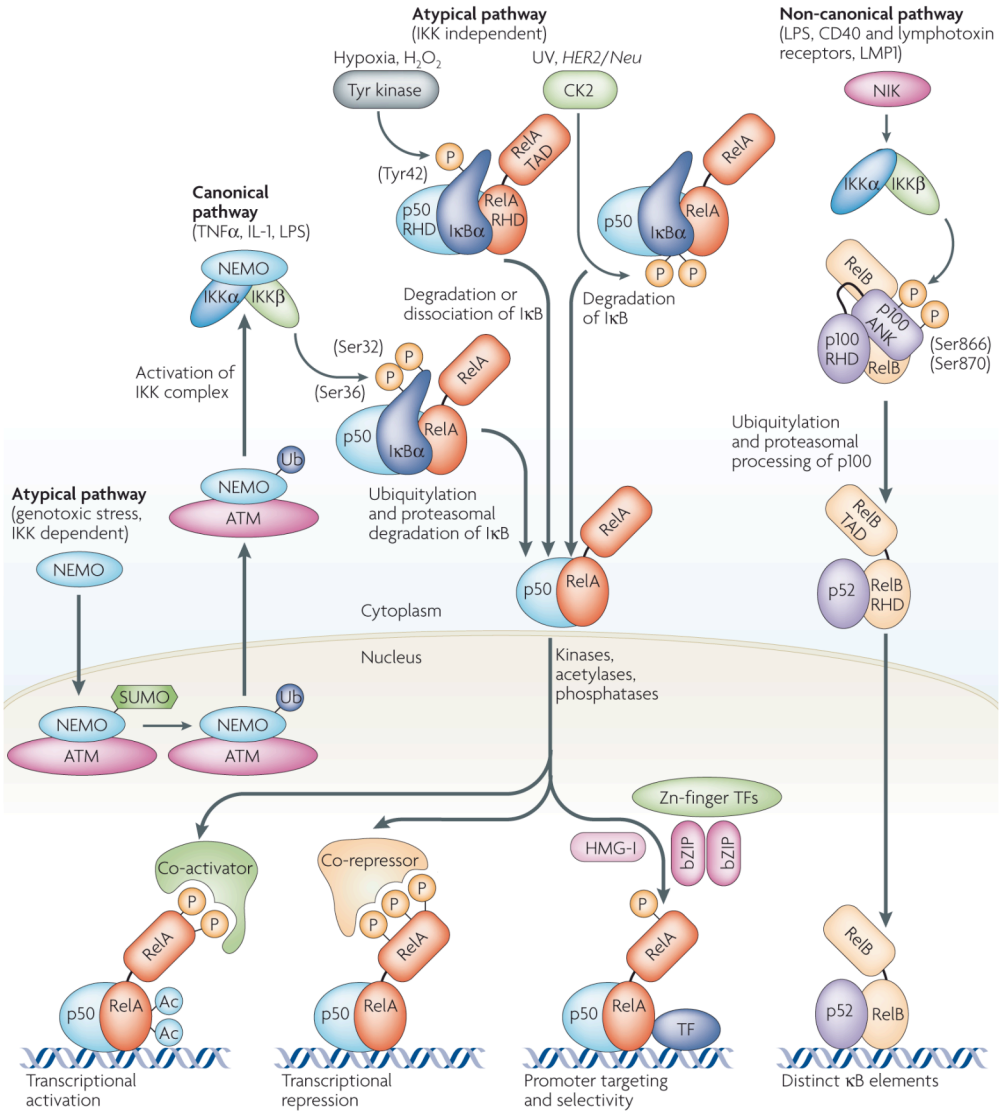

Figure 5: NF-κB pathways. The canonical pathway is IKKβ dependent. IKK2 induces the degradation of IκBα. This leads to the release of NF-κB, which then translocates into the nucleus. In the atypical IKK-dependent pathway, NEMO translocates into the nucleus. After association with ATM it relocates in the cytoplasm, where the activation of IKKβ occurs. In the IKK-independent atypical pathway the caseine kinase-II (CK2) and tyrosine-kinase are involved. The non-canonical pathway is initiated by NIK, whereby NEMO is not involved. The large subunit p100 is processed to the smaller subunit p52, which can then form a heterodimer with RelB. Ac (Acetylation), bZIP (leucine-zipper-containing transcription factor), HMG-1 (high-mobility-group protein-I), LMP1 (latent membrane protein-1), LPS (lipopolysaccharides) [reviewed in PERKINS 2007].

3.3.2 The physiologic roles of NF-κB

NF-κB is a master transcription factor and influences many cellular processes such as cell growth, cell survival, tissue and organ development, inflammation and stress response. It is involved in the development of the immune system and is essential for the innate and adoptive immune response. The outcome of NF-κB activation is highly dependent on the activation context [HAGEMANN et al. 2009].

Infection by pathogens lead to the activation of NF-κB by triggering TLRs (Toll-like receptors). These receptors are located on the cell surface of cells of the innate immune system like dendritic cells (DCs), macrophages and mucosal epithelial cells. Activation of NF-κB then leads to the induction of immune genes such as cytokines (TNF-α), interleukins (IL-1 and IL-6), chemokines (MIP-1α), RANTES (regulated upon activation, normal protein-1α) and adhesion molecules (E-selectin and VCAM-1). This subsequent results in the recruitment of immune cells to the site of infection [reviewed in BEINKE and LEY 2004].

Another function of NF-κB is the induction of molecules which have antibiotic activities (like defensins) and enzymes that produce reactive intermediates (e.g. iNOS).

T-cell activation of NF-κB happens by increasing the MHC proteins and CD80/86 on antigen-presenting cells [reviewed in BEINKE and LEY 2004].

NF-κB regulates the cell cycle by controlling the expression of cyclin D1. Cyclin D1 itself supports cell proliferation and survival [reviewed in BEINKE and LEY 2004].

NF-κB interacts with ROS to maintain the tolerable ROS level in the cell. The transcription factor can also induce the damage of the DNA when genotoxic agents cause cellular stress [SUN and LIU 2011].

Although the structure of the NF-κB subunits p105 (NF-κB1) and p100 (NF-κB2) are very similar, their function is distinct. The processed form of p100, p52, is important during organogenesis of the peripheral lymphoid system and for the differentiation of B-cells. The regulation of p100 is tightly regulated by specific stimuli. The processed form of p105, p50, plays an essential role in the immune and inflammatory response by controlling lymphocyte and macrophage function. Beside, p105 is constitutively expressed, in contrast to p100. Degradation of p105 results in the activation of MAPK pathway which

further can activate the ERK/MAP signaling cascade. Thus NF-κB1 also function as regulator of the MAPK pathway [reviewed in BEINKE and LEY 2004].
The MAPK kinase p38 can be induced by many inflammatory stimuli and cell stress stimuli, which also induce NF-κB. This leads to the suggestion that the p38 MAPK pathway can also influence the NF-κB pathway [SACCANI et al. 2002].

As consequence of the many functions of NF-κB, dysfunction of NF-κB can result in many different disease like autoimmune disease, chronic inflammation, cancer, neurodegenerative disease and metabolic disorders. In cancer the NF-κB pathway is constitutively active [SUN and LIU 2011]. Deregulated NF-κB can cause overproduction of cytokines and lead to chronic inflammatory disease like Crohn's disease and rheumatoid arthritis [reviewed in BEINKE and LEY 2004]. NF-κB regulates the functions of TAMs (tumor-associated macrophages). In this case the activation of NF-κB leads to the development of tumours. It induces the expression of cytokines like TNF-α and IL-6, which support the survival of the cell, cell growth and cell progression [HAGEMANN et al. 2009].

3.3.2.1 The anti-apoptotic effect of NF-κB

NF-κB can stimulate and repress programmed cell death (apoptosis) and proliferation. Activation of NF-κB by TNF-α leads to the prevention of apoptosis through the induction of anti-apoptotic genes and suppression of the JNK pathway [JAVELAUD and BESANCON 2001]. The anti-apoptotic effect of NF-κB can also be initiated by H_2S. H_2S stimulates NF-κB to bind the DNA to induce target gene expression. This happens by sulfhydrating the cysteine-38 of the p65 subunit of NF-κB. It further leads to the binding of the coactivator ribosomal protein S3 (RPS3), which regulates, among others, the nuclear function of NF-κB. TNF-α, in turn, can stimulate the transcription of CSE, which produces H_2S. The produced H_2S again sulfhydrates p65 and enhances its binding to RPS3. On this way, the binding of NF-κB to the promoter of anti-apoptotic genes is initiated. Sen et al. showed that treatment of $CSE^{-/-}$ mice with the H_2S donor GYY4137 prevents the induction of cell death by TNF-α [SEN et al. 2012].

In contrast, nitric oxide generated by iNOS leads to nitrosylation of p65 and has a contrary effect on the NF-κB activity compared to sulfhydration. So, NO reverses the anti-apoptotic effect of H_2S by inhibiting the activation of NF-κB through sulfhydration. This can happen subsequently to the activation by sulfhydration and decreases NF-κB activity [SEN et al. 2012].

3.3.3 NF-κB and H_2S

Although NF-κB activates most of the proinflammatory genes, the activation of proinflammatory genes by H_2S is NF-κB-independent. H_2S does not cause the degradation of IκB, which would then lead to the activation of NF-κB. Stuhlmeier et al. showed that H_2S can activate three MAPK pathways, which also can upregulate the expression of proinflammatory genes, but the accurate mechanism by which H_2S invoke an inflammatory response is unclear to date. It is suggested that H_2S blocks the binding of NF-κB to the DNA [STUHLMEIER et al. 2009].

Gao et al. found that H_2S inhibits the NF-κB signaling pathway and inflammatory cytokines in rats. They suggest a protective effect of H_2S on the cardiac system by downregulating NF-κB and thereby on the inflammatory system [GAO et al. 2012]. Ganster et al. previously also showed that H_2S inhibits the NF-κB signaling cascade in rats [GANSTER et al. 2010].

3.3.4 The connection of NF-κB to HIF-1α

NF-κB shares target genes with HIF-1α and there are stimuli which activate both. NF-κB is also one regulator of HIF-1α expression, because the promoter of HIF-1α reacts with NF-κB subunits. Thereby, p50 was observed to activate HIF-1α the most and p52 the fewest. Depletion of NF-κB results in a decreased HIF-1α mRNA level. NF-κB activation via TNFα further leads to an increase of HIF-1α mRNA and protein under normoxic conditions. Under hypoxic conditions, the situation is slightly different: changes of HIF-1α are only visible, when the NF-κB pathway is totally blocked. Nevertheless hypoxia-activated NF-κB regulates to some extend the HIF-1α level and activity. It was shown

that the activation of HIF-1α through H_2O_2 under normoxia is NF-κB-dependent [BONELLO et al. 2007].

3.4 Scavenger receptor-BI (SR-BI)

SR-BI plays an important role in the steroid and cholesterol metabolism. The highest protein expression of SR-BI is found in the adrenal gland, where it plays an important role in the selective uptake of HDL (high density lipoprotein)-cholesteryl esters for the synthesis of cholesterol-derived hormones, such as glucocorticoids (e.g. cortisol) and mineralocorticoids (e.g. aldosteron). SR-BI is also highly expressed in the liver, where it is the main receptor for HDL-cholesteryl ester uptake into the liver. In hepatocytes, SR-BI shows a high affinity to acLDL. It is involved in the selective uptake of cholesteryl esters from HDL and therefore can be characterized as functional HDL receptor. SR-BI binds native apolipoprotein B (apoB)-containing lipoproteins from the blood and transfers them into the hepatocytes. The receptor also plays an important role in macrophages. There, on the one hand, it takes up cholesterol associated with HDL- and apoB-containing lipoproteins and, on the other hand, it facilitates cholesterol efflux to HDL. Macrophages are dependent on the active cholesterol efflux by receptors, mainly by ATP-binding cassette transporter A1 (ABCA1), because they cannot limit their cholesterol intake by themselves. Thus, if an overload on cholesterol occurs, the formation of foam cells, large lipid filled macrophages, can happen [HOEKSTRA et al. 2010].

In the so-called reverse cholesterol transport, the first step to create HDL is the lipidation of apoA1. ApoA1 arranges the transport of cholesterol from peripheral cells, such as macrophages, back to the liver, where the excess cholesterol can be deposited via the bile. SR-BI is mainly responsible for mediating the uptake of HDL-cholesteryl ester into the liver, but can also be involved in the first step, creating HDL [HOEKSTRA et al. 2010].

Newer studies suggest an involvement of SR-BI in the control of cell physiology of endothelial cell, stem cells and progenitor cell physiology [HOEKSTRA et al. 2010].

4 Aim

In 2009, Budde and Roth found that H_2S increases HIF-1α in *C. elegans* [BUDDE and ROTH 2009]. Acting on this assumption, our first aim was to investigate whether H_2S affects HIF-1α protein expression in THP-1 macrophages. To explore the effects of H_2S on the cells, we used the synthetic H_2S donor GYY4137.

Another aim was to examine whether HIF-1α accumulation can be mediated by the NF-κB pathway. Because HIF-1α and NF-κB share target genes and are in part activated by the same stimuli, we suggested that this is a feasible consideration. Dehne et al. showed that the activation of the NF-κB pathway by ROS or NO can lead to an increase of HIF-1α [reviewed in DEHNE et al. 2009]. But, the accurate pathway, by which this can happen is by now not fully understood. So we wanted to investigate this mechanism, which leads to the stabilisation of HIF-1α via the NF-κB pathway, more precisely. As it is the case for HIF-1α, NF-κB is also an important factor during inflammation and hypoxic episodes. So, a connection of both is conceivable in this aspect [reviewed in DEHNE et al. 2009]. To answer this question, we aimed to determine the protein expression of NF-κB subunits during conditions in which protein HIF-1α expression was up-regulated in THP-1 macrophages.

Currently, little is known about the function of H_2S in the physiological system. Particularly the claim that H_2S has protective or damaging effects on living organisms is controversial. Thus, we aimed to get further insights into the physiologic role of hydrogen sulfides. Li et al. suggested that GYY4137 has an anti-inflammatory effect by decreasing NF-κB transduction [LI et al. 2008]. This was a further hint for us for the connection of HIF-1α and NF-κB in the context of hydrogen sulfide signaling.

Inflammatory stimuli and cell stress stimuli induce the NF-κB and also the p38 MAPK kinase pathway. This leads us to the suggestion that the p38 MAPK pathway may also influence the NF-κB pathway. By inhibiting the p38 MAPK pathway with the inhibitor SB202190 in our cell model, we aimed to examine if the HIF-1α, the NF-κB pathway or both can be blocked through this component. We did so to further investigate the question if H_2S affected HIF-1α or NF-κB activation can happen via the p38 MAPK pathway.

5 Materials and Methods

If not noted otherwise, the used chemicals were products of Sigma-Aldrich, Merck, and Roth.

5.1 Cell culture

5.1.1 THP-1 cells

For the following experiments THP-1 cells were used. The THP-1 cell line is a human monocyte cell line, which was isolated in 1980 from the blood of an one-year old boy, who suffered from acute monocytic leukaemia [TSUCHIYA et al. 1980]. The cells were cultured in cell culture medium (see 5.1.2) in cell culture flasks (Greiner bio-one, 250 ml, 75 cm^2) and kept in an incubator (HERAcell 240 CO_2 incubator, Thermo Scientific), adjusted at 37°C and 5% CO_2. New, preheated medium was given to the cells every 2 to 3 days. The density of the cells was adjusted to 0.5 millions/ml. The supply of the cells with fresh medium, the adjusting of the right density, the exposure and the incubation of the cells were done under sterile conditions in a Lamina air flow (MSC-Advantage, Thermo Scientific). The lamina air flow was sterilised every day by ultraviolet light. Also the instruments used for handling with the cells were kept sterile.

5.1.2 Preparation of cell culture medium

The THP-1 cells were cultured in liquid medium (RPMI-1640), supplemented with 10% fetal bovine serum (GIBCO), 2 mmol/l L-glutamine, 0.1 mg/ml streptomycin and 100 U/ml penicillin. The storage life of the medium depends on glutamine, which is stable for about one month. The medium was stored at 6°C and was tempered at 37°C in a water bath (JB Aqua 18Plus, Grant) before use.

5.1.3 Determination of cell number and viability

For the determination of cell number and cell viability the Casy® Cell Counter and Analyser (Innovatis) was used. Therefore, 50 µl cell suspension were dissolved in 10 ml Casy ton (Roche). For THP-1 cells particular settings were programmed, which were chosen before the measurement.

5.1.4 Differentiation of THP-1 cells to macrophages

Treatment of THP-1 monocytes with phorbolester for three days leads to differentiation of the THP-1 cells to macrophages. The initially swimming cells adhere to the surface and develop macrophage-like characteristics. The morphology of the cells changes from round cells to cells with dendrites which form cell clusters (Fig. 6) [TSUCHIYA et al. 1982; AUWERX 1991].

A **B**

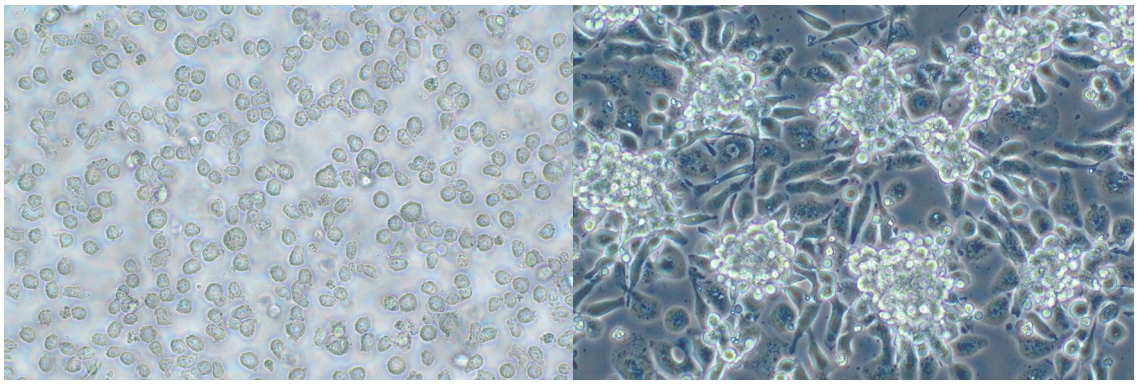

Figure 6: THP-1 cells. THP-1 monocytes (A) were differentiated towards macrophages (B) with 160 nmol/l PMA for 72 hours. The cells on the pictures are boosted on the 100-fold.

For all experiments 3 ml or 18 ml of cell suspension with a density of 0.5 millions/ml were seeded in 6-well plates (9,6 cm^2 growth area; TPP or SPL Life Sciences) or single plates with 58 cm^2 growth area (Nunclon) respectively, and incubated with 160 nmol/l PMA (phorbol 12-myristate 13-acetate) for 72 hours at 37°C. After this time the THP-1 monocytes were differentiated to macrophages.

5.1.5 Incubation of differentiated THP-1 cells

After differentiation the medium supernatant was removed and the cells were washed two times with preheated HBSS (Hank's balanced salt solution) to remove nutrients of the old medium. The cells were incubated without or with 125, 250, 500 or 1000 μmol/l GYY4137. To achieve the specific concentrations, GYY4137 stock solution were diluted with HBSS. The final volume was 1 ml per well in 6-well plates, and 6 ml in plates with 58 cm^2 growth area. The incubation time was either 6 or 24 hours.

For some experiments the p38-inhibitor SB202190 (Sigma-Aldrich) was used. To create the specific concentration of SB202190, the stock solution (10 mmol/l in DMSO) was diluted in 37°C preheated HBSS. Afterwards, the appropriate amount of diluted SB202190 was used to receive concentrations of 1, 5 and 10 μmol/l in a total volume of 6 ml in 58 cm^2 culture dishes. For the additional incubation with GYY4137, cells were first incubated for 30 minutes with SB202190, diluted only in 5 ml HBSS. Afterwards, 1 ml HBSS or 1 ml GYY4137 with a concentration of 6 mmol/l were added. The final concentration of GYY4137 was 1 mmol/l. The incubation time was either 6 or 24 hours.

5.2 Cell culture experiments under hypoxic conditions

For some experiments, hypoxic conditions were chosen. Therefore, cells were placed into a hypoxic chamber (Billups-Rothenberg) through which a specific gas (1% O_2, 5% CO_2, 94% N_2) was piped at a flow rate of 15 to 20 litres per minute. This was done for 5 minutes for 6-well plates and 10 minutes for single plates. Afterwards, the sealed chamber was placed into an incubator with 37°C during the incubation.

5.3 Preparation of whole cell lysates

Used solutions:

• Lysis buffer: 125 mmol/l Tris-HCl, pH 6.5, 2% SDS, 10% glycerol, 100 mmol/l DTT, 1% protease inhibitor cocktail (PIC) added immediately before the use

• 5x PBS: 40 g NaCl, 1 g KCl, 1 g KH_2PO_4, 15 g Na_2HPO_4*12 H_2O for 1 litre filled up with distilled H_2O; pH 7,4 adjusted with HCl; diluted 1:5 before the use

The following steps were done on ice. The supernatants were transferred into Eppendorf tubes (1.5 ml volume) for further use (LDH measurement) and the remains aspirated. The adherent cells in 6-well plates were washed twice with 1.5 ml ice-cold PBS per well. 100 µl lysis buffer per well were applied on the cells for at least 5 minutes. Afterwards, the cells were detached from the surface with cell scrapers, one scraper for each different incubation. The cell suspensions were pipetted into Eppendorf tubes and lysed for one hour one ice. As next step, the suspensions were sonified for about 2 seconds and then centrifuged (Eppendorf Centrifuge 5417R) at 14 000 x g for 10 minutes at 4°C. The supernatants were again transferred into new Eppendorf tubes and stored at -20°C.

5.4 Preparation of nuclear extracts

The chemicals used for the preparation of cytoplasmic and nuclear extracts were from Active Motif (Nuclear Extract Kit version C4) and were used according to manufacturer instruction.

Used solutions:
• PBS/phosphatase inhibitors (PBS/PI): 6.6 ml 10x PBS, 56.1 ml distilled water, 3.3 ml Phosphatase Inhibitors for 8 dishes (∅ 10 cm); should be used on the same day

• Hypotonic Buffer (HB): 0.85 ml 10x hypotonic buffer, 7.65 ml distilled water for 16 dishes (∅ 10 cm); can be stored at 4°C for 1 week

• Complete Lysis Buffer (LB): 45 µl 10 mmol/l DTT, 400.5 µl lysis buffer AM1, 4.5 µl PIC for 8 dishes (∅ 10 cm); should be used on the same day

The following steps were done on ice. Buffers and all tubes needed were placed on ice before beginning the assay. 500 µl of cell supernatant per dish were transferred into Eppendorf tubes for further use (LDH and VEGF measurement) and the remains aspirated. The adherent cells were washed with 5 ml PBS/PI per dish. Then 3 ml ice-cold PBS/PI per dish were applied on the cells. The presence of phosphatase inhibitors limits further protein modifications. The cells were removed from the dishes by gently scraping with cell lifters and transferred into 15 ml Falcon tubes on ice. The cell suspensions were centrifuged for 5 minutes at 500 rpm in a centrifuge pre-cooled at 4°C (Eppendorf Centrifuge 5403). The supernatants were discarded. The pellets were resuspended in 500 µl HB per tube, transferred into Eppendorf tubes and incubated for 15 minutes on ice. The hypotonic buffer swells the cell membrane and makes it fragile. Then, 25 µl detergent per tube were added. The detergent causes leakage of the cytoplasmatic proteins into the supernatant. They were vortexed for 10 seconds at highest setting followed by centrifugation for 30 seconds at 14 000 x g in a centrifuge pre-cooled at 4°C (Eppendorf Centrifuge 5417R). The supernatants (the finished cytoplasmic lysates) were transferred into new tubes on ice, aliquoted and stored at -80°C. The remaining pellets were used for the collection of the nuclear fraction by detaching it with 50 µl LB per tube. The tubes were vortexed for 30 seconds at highest setting and incubated for 30 minutes on ice on the belly dancer with maximum speed (Stovall). Afterwards the tubes were vortexed for 30 seconds at highest setting and centrifuged for 10 minutes at 14 000 x g in a centrifuge, pre-cooled at 4°C. The supernatants (the ready-made nuclear fractions) were transferred into new tubes on ice, aliquoted and stored at -80°C.

5.5 Determination of protein concentration

The protein concentration of the cytoplasmatic cell lysates was determined with a NanoDrop® Spectrophotometer (ND-1000, Thermo Scientific). This instrument uses the absorption peak of proteins, more precisely, that of aromatic amino acids, at a wavelength of 280 nm to determine the protein concentration. After the console was calibrated with water and 1x hypotonic buffer, 3 µl per cell lysate were applied on the measuring point.

5.6 Western Blot

The first step of Western blot analysis is the separation of proteins within a cell lysate according to their sizes by gel electrophoresis. This happens via a SDS-polyacrylamide gel. SDS (sodium dodecyl sulfate) is an anionic detergent, which loads all proteins negatively and thereby enables them to move towards a positive pole when voltage is applied. Small proteins move faster than bigger ones. In the second step, the separated proteins from the gel are blotted onto a nitrocellulose membrane on which proteins of choice can be immunologically detected by using specific antibodies.

5.6.1 Sample preparation for gel electrophoresis

Used solutions:

• Lysis buffer: see 5.3 preparation of whole cell lysates

• sample buffer for whole cell lysates: lysis buffer (see 5.3), 10% 2-mercaptoethanol (Bio-Rad), bromphenol blue

• 4x sample buffer for cytoplasmatic and nuclear cell lysate (1 ml): 500 µl glycerol, 450 µl sample buffer (240 µl 0.5 mol/l Tris-HCl, pH 6.8, 210 µl distilled water, 8% SDS), 50 µl 2-mercaptoethanol, bromphenol blue

• PBS: see 5.3 preparation of whole cell lysates

First the thawed lysates were vortexed and diluted to equal protein amounts with PBS. One part of sample buffer was mixed with 3 parts of cell lysates. According to the antibody description, the probes were heated at 90°C for 5 minutes or lysed for 30 minutes at room temperature to denature the proteins. Afterwards, the probes were shortly centrifuged and then applied to the gel.

5.6.2 SDS-polyacrylamide gel electrophoresis

Used solutions:

• Tris-HCl buffer for gel preparation: 3M Tris-HCl, 0.3% SDS, pH 8,45

• 10x Tris/glycine buffer: 250 mM Tris, 2M glycine, 10% SDS

• Electrophoresis buffer: 1x Tris/glycine buffer

For electrophoresis, the Mini-PROTEAN®3 cell-system (Bio-Rad) was used. Glass plates with a spacer thickness of 0.75 mm for gel preparation were washed with distilled water and ethanol (70%) and then assembled into the gel cassettes according to the instruction manual. The gels were mixed (table 1) and poured between the plates. The resolving gels were made with 8% or 10% polyacrylamide and were overlaid with isopropanol (30%) during the polymerisation process to prevent the gel from drying-out. After about 15 minutes, when polymerisation was complete, the isopropanol was removed. The stacking gels made with 4% polyacrylamide were poured on the top of the resolving gels. Gel combs (10 or 15 lanes) were inserted into the stacking gels to form wells. The polymerisation of the stacking gels lasted approximately 15 minutes, after which the gels were ready for use.

	10% resolving gel (2 gels)	8% resolving gel (2 gels)	4% stacking gel (2 gels)
Distilled water	2.7 ml	3.2 ml	2.2 ml
Acrylamide/bis-Acrylamide 30% solution	2.7 ml	2.2 ml	0.6 ml
3 mol/l Tris-HCl buffer	2.7 ml	2.6 ml	1.4 ml
10% Ammonium persulfate	60 µl	60 µl	30 µl
N,N,N',N'-Tetramethylethylendiamine (Fluka)	6 µl	6 µl	3 µl

Table 1: Instruction for the production of SDS-polyacrylamide gels.

The gel cassettes were built into the electrophoresis chamber according to the instruction manual. Then, the chamber was filled up with electrophoresis buffer and the combs removed. Before filling the gel slots, they were flushed with electrophoresis buffer with the help of a syringe. Wells of gels with 15 lanes were filled with 10 µl, those with 10 lanes with 20 µl probe. Also a protein ladder (Page Ruler™ Prestained Protein Ladder or Spectra™ Multicolor Broad Range Protein Ladder, Thermo Scientific) was filled in one slot per gel. Slots, which were not used for samples, were filled up with sample buffer. A voltage of 180 V was applied and the electrophoresis done for 90 to 110 minutes in a fridge. After the run, the gels were carefully dismounted out of the gel cassettes and used for western blotting.

5.6.3 Western blotting

Used solutions:

• Transfer buffer: 100 ml 10x Tris/glycine buffer (see 5.5.2), 200 ml methanol for 1 litre, stored at 4°C

The gels were pulled out of the gel cassette and built into a transfer cassette (Mini-Trans-Blot® Cell, Bio-Rad) according to the instruction manual. The transfer cassettes were composed in following order: white side of the transfer cassette (positive electrode), sponge, filter paper, nitrocellulose membrane (0.45 µm, Bio-Rad), gel, filter paper, sponge, black side of the transfer cassette (negative electrode). The sponges, filter papers and nitrocellulose membranes were soaked in transfer buffer prior to use. Air bubbles between the membrane and the gels were prevented. For cooling, an ice cassette was put into the transfer chamber, which was then filled up with transfer buffer. The transfer was done with an amperage of 0.4 A for 2 cassettes and 0.8 A for 4 cassettes for 1 hour.

Afterwards, the membranes were stained with Ponceau red S (Biolab) to make the protein lines visible and the cutting of the membrane possible.

The membranes were cut according to the protein sizes of proteins of interest, so that different segments could be incubated with different antibodies.

5.6.4 Immunodetection

Used solutions:

• 10x TBS: 200 mM Tris-HCl, 1.45 M NaCl, pH 7.4

• Washing buffer (TBS-T): 1x TBS, 0.1% Tween®20

• Blocking buffer: Washing buffer, 5% non-fat dried milk (Fixmilch instant, Maresi)

• Primary antibodies:

The primary antibodies were diluted at the recommended dilution in TBS-T with bovine serum albumin (BSA) or dry milk according to instruction manual.

Antibody	Host	Isotype	Mol. Wt.	Dilution	Producer
β-Actin	mouse	IgG2a	42 kDa	1:3000, 3% BSA	Sigma-Aldrich
Calnexin	rabbit	Polyclonal	75 kDa	1:10000, 3% BSA	Abcam
Caspase 3	rabbit	IgG	17, 19, 25 kDa	1:1000, 5% milk	Cell signaling
Caspase 9	rabbit	IgG	17, 35, 37, 47 kDa	1.1000, 5% milk	Cell signaling
GLUT1	rabbit	polyclonal	55 kDa	1:1000, 5% BSA	Abcam
HIF-1α	mouse	IgG1	120 kDa	1:300, 3% BSA	BD bio-sciences
IκB-α	mouse	IgG1	39 kDa	1:1000, 5% milk	Cell signaling
Phospho-IκB-α	mouse	IgG1	40 kDa	1:1000, 5% milk	Cell signaling
p38	rabbit	IgG	40 kDa	1:1000, 5% BSA	Cell signaling

Phospho-p38	rabbit	IgG	43 kDa	1:1000, 5% BSA	Cell signaling
p50	rabbit	polyclonal	50 kDa	1:1000, 5% BSA	Cell signaling
p65	rabbit	IgG	65 kDa	1:1000, 5% BSA	Cell signaling
Phospho-p65	rabbit	IgG	65 kDa	1:1000, 5% BSA	Cell signaling
p105	rabbit	polyclonal	120 kDa	1:1000, 5% BSA	Cell signaling
PARP	rabbit	IgG	24, 89, 116 kDa	1:1000, 5% BSA	Cell signaling
SR-BI	rabbit	polyclonal	82 kDa	1:3000, 3% BSA	Novus
VEGF	mouse	IgG1	25-52 kDa	1:1000, 5% milk	Abcam

• Secondary antibodies: goat-anti-mouse IgG-HRP conjugate (Biorad), goat-anti rabbit-HRP conjugate (Cell Signaling)

All incubation and washing steps were done on the belly dancer. Membrane segments were incubated with blocking buffer, approximately 12.5 ml per segment, for 1 hour at RT (room temperature) to prevent unspecific binding of the primary antibody. Afterwards, the blots were washed two times for 5 minutes with washing buffer. Incubation with the specific primary antibodies was done over night at 4°C. The next day, the blots were washed 3 times for 10 minutes with washing buffer, before incubating with the secondary antibodies for 1 hour at room temperature. Afterwards, the blots were washed again 3 times for 10 minutes with washing buffer.

Proteins were detected by chemiluminescence using a Chemi Imager (Fusion Fx7). The blots were incubated with ChemiGlow West Chemilumineszenz Substrat Kit (protein

simple), enhancer and peroxide solution mixed 1:1, for 5 minutes,. The blots were positioned under a CCD camera in the detection chamber for measuring the chemiluminescence intensity.

5.7 LDH-assay

LDH release was measured with the LDH-assay (LDH Cytotoxicity Assay Kit) from Cayman Chemical Company.

To survey the putative cytotoxicity of the incubations a lactate dehydrogenase (LDH) measurement was done. LDH is a soluble enzyme in the cytosol that is released into the surrounding culture medium when cells are damaged or lysed.
For the measurement of LDH, a LDH cytotoxicity assay kit was used which is based on two reactions. First, LDH catalyzes the reduction of NAD^+ in the LDH reaction solution to NADH and H^+. In the second step, diaphorase uses the new built NADH and H^+ to reduce tetrazolium (INT) salt to a coloured formazan. Formazan can be measured at a wavelength between 490 and 520 nm and is proportional to the LDH amount in the cell supernatant.

For every measurement a LDH standard was made. Therefore, 6 Eppendorf tubes, for 6 measuring points, were prepared. In the first tube, with highest dilution, 475 µl reacting solution and 25 µl LDH-standard were pipetted. This point accords to 10 mU per ml. In tubes 2 to 6, 250 µl reacting solution were pipetted. The serial dilution was done with 250 µl from tube 1 to 5. In tube number 6, no LDH-standard was added, because this was used as blank value.

For measuring the LDH in the cell supernatants, they were thawed and vortexed.
100 µl cell supernatant and 100 µl reaction solution were pipetted per well in a 96 well-plate. 100 µl of HBSS, mixed with 100 µl of reaction solution, was used as blank value, which was afterwards subtracted from the values of the cell supernatants. Also, 100 µl LDH-standard were mixed with 100 µl reaction solution per well for establishing a stan-

dard line. The plate was incubated for 30 minutes, protected from light at the belly dancer at room temperature. Afterwards the absorption was measured with a photometer for microtiter plates (iMark™, Bio-Rad) at a wavelength of 490 nm. The absorption of the dilution series was used to create a linear regression.

The LDH activity in the samples was determined according to the following equation:
LDH activity (μU) = ($A_{490\ nm}$ – blank value of HBSS) / slope

5.8 VEGF-assay

For the quantitative determination of vascular endothelial growth factor (VEGF) in the cell supernatants, the Quantikine® VEGF immunoassay (R&D systems) was used. The VEGF immunoassay was done according to the instructions of the producer. A VEGF stock solution was used to produce a dilution series. 50 μl of assay diluent RD1W were added in each well. Afterwards, 200 μl of standards, controls and samples, brought at room temperature, were pipetted into the wells so that immobilized antibodies could bind present VEGF. The plate was covered with the adhesive strip provided and incubated for 2 hours at room temperature. Then, each well was aspirated and washed with 200 μl wash buffer for three times, so unbound substances were washed away. After the last wash step, the plate was blotted against clean paper towels. Afterwards 200 μl of an enzyme-linked polyclonal antibody, specific for VEGF, was added to the wells and covered with a new adhesive strip. Incubation was done for 2 hours at room temperature. Any unbound antibody-enzyme reagent was removed by doing three wash steps with 200 μl wash buffer per well. Then 200 μl of substrate solutions was added to each well and incubated for 20 minutes. Afterwards, 50 μl stop solution was added to each well. The substrate solution led to the development of colour, which was measured at a wavelength of 450 nm within 30 minutes after adding the stop solution by using a microplate reader (iMark™, Bio-Rad). The intensity of the colour was proportional to the amount of VEGF bound in the initial step.
To calculate the results, the average zero standard optical density was subtracted from each standard, control and sample to create a standard curve.

5.9 Statistical evaluation

For the statistical evaluation, the computer program GraphPad Prism (Version 3.02) was used. The results are presented as single value when experiment was done once or twice or as mean values of 3 to 6 independent experiments ± standard deviation. For specific effects the statistical significance was calculated by one-way analysis of variance (ANOVA) with *post hoc* testing by Newman-Keuls test. Values with $p<0.05$ (*), $p<0.01$ (**) and $p<0.001$(***) were regarded as statistically significant.
For the calculation of chemiluminescence intensities of protein bands after western blotting, the computer program Alpha EaseFC (ChemiImager 4400) was utilized.

6 Results and discussion

6.1 Cytotoxicity of GYY4137

THP-1 cells were differentiated toward macrophages with 160 nmol/ PMA for 72 hours. The differentiated cells were incubated without or with 62.5, 125, 250, 500 or 1000 μmol/l GYY4137, as described above in the method chapter (5.1.5). To achieve the specific concentrations, GYY4137 was dissolved in HBSS. The final volume was 1 ml per well in 6-well plates, and 6 ml in plates with 58 cm^2 growth area. The incubation time was either 6 or 24 hours and was done under normoxic (21% O_2, 0.96% Ar, 0.04% CO_2, 78% N_2) and hypoxic conditions (1% O_2, 5% CO_2, 94% N_2).

To monitor cytotoxic effects of GYY4137, LDH was measured in the cell supernatant spectrophotometrically at a wavelength of 490 nm.

After incubation of THP-1 macrophages without or with 62.5 - 1000 μmol/l GYY4137 no changes in the LDH-activity could be observed. Also, no differences between normoxic and hypoxic conditions on the cell viability could be found. This led us to the suggestion, that the cells can handle hypoxic condition up to 24 hours very well (Fig. 7).

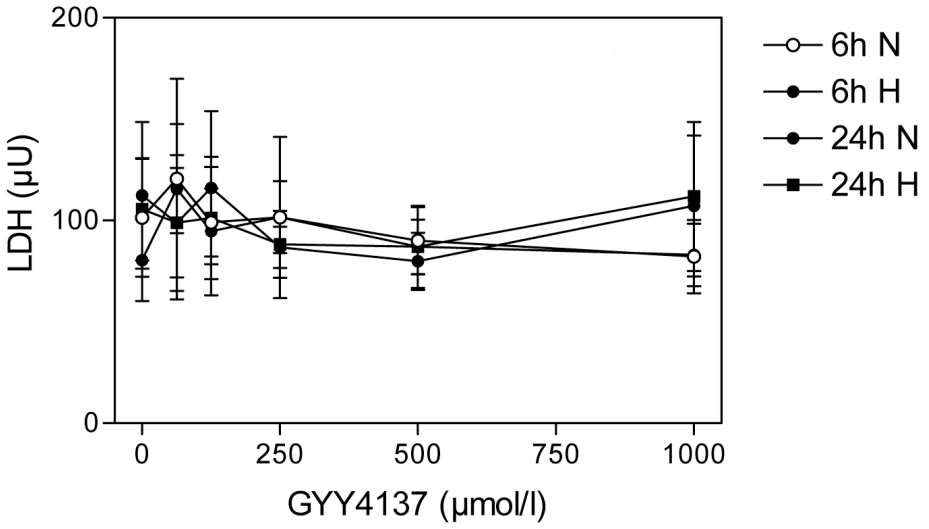

Figure 7: Determination of the LDH-activity after incubation of THP-1 macrophages without or with 62.5 - 1000 µmol/l GYY4137. THP-1 cells were differentiated towards macrophages with 160 nmol/l PMA for 72 hours. Afterwards the cells were incubated with increasing concentrations of GYY4137 for 6 or 24 hours under normoxic and hypoxic conditions. The amount of LDH was measured spectrophotometrically. The values are the mean values +/- SD of 3-6 independent experiments. N (normoxia), H (hypoxia).

The next thing we monitored was, if the cells undergo apoptosis due to the chosen experimental conditions. To test this, the cells were incubated with different concentrations of GYY4137. Afterwards they were screened for caspase 3, caspase 9 and PARP (poly (ADP-ribose) polymerase) cleavage products. When cells initiate programmed cell death, the inactive forms of caspases were cleaved to become active and to start a cascade, which further lead to the cleavage of other proteins (e.g. PARP) that trigger the apoptotic process. So if cleavage products of caspases or target proteins can be detected, this points out, that the cells initiate apoptosis.

As there were no cleavage products of caspase 3, caspase 9 and PARP detected, showing that the cells did not undergo apoptosis during the experiments, this led us to the assumption that incubation with GYY4137 up to a concentration of 1 mmol/l does not chase the cells into programmed cell death after 6 and 24 hours. Also hypoxic conditions did not harm the cells in a way that would initiate apoptosis. Only after 24 hours incubation cleaved products of caspase 9 could be detected under both hypoxic and

normoxic conditions. This could be explained by the longer incubation time in which more cleaved products can accumulate in the cells. Since the effect was independent of GYY4137 and reduced oxygen-conditions, the cleaved products of caspase 9 were considered to be irrelevant.

Although H_2S was expected for a long time to exclusively have toxicological effects [REIFFENSTEIN et al. 1992], we could not find harmful impacts of GYY4137 on our cell model up to a concentration of 1 mmol/l. This finding is concordant to those of LI et al., who also found no cytotoxic effect of GYY4137 in cultured smooth rat muscle cells [LI et al. 2008] and RAW 264.7 cells [LI et al. 2009]. It is to mention that the concentration of GYY4137 in their experiments was lower, namely 100 μmol/l. They also confirmed these finding in a mouse model, in which they also found no cytotoxic effects of 133 μmol/kg daily injection of GYY4137. In our experiments we tested the cytotoxicity of GYY4137 by measuring the LDH release and monitoring caspase cleavage products. We could not observe elevated LDH values or signs of promoted cell death, indicating that the slow and sustained release of H_2S by GYY4137 is not toxic. LI et al. additionally showed that GYY4137 did not change the cell cycle distribution or enhances the p53 protein expression, which is a prominent tumour suppressor protein [LI et al. 2008]. This also points out that the releaser is not poisonous to cells. Moreover, LI et al. suggest a positive effect of the releaser, explained by the anti-inflammatory properties of GYY4137 [LI et al. 2009].

6.2 Concentration-dependent increase of HIF-1α with GYY4137

To evaluate the effect of increasing concentrations of GYY4137 on the HIF-1α protein expression, THP-1 cells were differentiated toward macrophages with 160 nmol/l PMA for 72 hours. The differentiated cells were incubated without or with 62.5,125, 250, 500 or 1000 μmol/l GYY4137 in HBSS, as described above in the method chapter (5.1.5). The cells were incubated for either 6 or 24 hours under normoxic (21% O_2, 0.96% Ar, 0.04% CO_2, 78% N_2) or hypoxic conditions (1% O_2, 5% CO_2, 94% N_2) at 37°C.

Figure 8 shows that GYY4137 led to a concentration-dependent increase of HIF-1α in THP-1 macrophages after 6 and 24 hours under normoxic and hypoxic conditions. The effect of a continuous increase of the HIF-1α protein expression was stronger and better visible after 24 hours than after 6 hours. Incubation of THP-1 macrophages with 1 mmol/l GYY4137 showed the highest effect. Hypoxic conditions additionally enhanced the signal in contrast to normoxic conditions (Fig. 8).

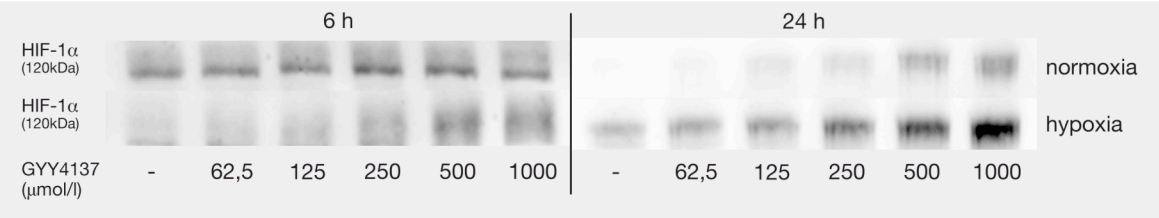

Figure 8: Effect of GYY4137 on the protein expression of HIF-1α. THP-1 cells were differentiated towards macrophages with 160 nmol/l PMA for 72 hours. The whole cell lysates were used to perform Western blot analyses. Protein expression of HIF-1α without or with GYY4137 treatment was detected after 6 and 24 hours under normoxic and hypoxic conditions. One representative Western blot of 2-5 independent experiments is shown.

To show the effect of H_2S on the basal HIF-1α protein expression, the amount of HIF-1α protein after incubation of the cells without GYY4137 was set 1 and seen as initial value. After 6 hours, HIF-1α increased slowly with increasing concentrations of GYY4137 and was strongly enhanced after incubation with 1000 μmol/l GYY4137. HIF-1α protein expression was more than 3 times higher compared to the initial value (Fig. 9).
First shown by Wang and Semenza in 1993 [SEMENZA and WANG 1993], several studies confirmed that HIF-1α is stabilized under hypoxic conditions, what we also clearly could observe. An increase of about 10-fold was determined due to hypoxic conditions for 6 hours. After 6 hours hypoxia, 1000 μmol/l GYY4137 enhanced the expression of HIF-1α at the 1.5-fold. It is to mention that under hypoxic conditions 125.5 μmol/l GYY4137 already led to an 1.4 fold increase of HIF-1α. So the further elevation with higher concentrations of GYY4137 only enhanced the HIF-1α signal minimally. One explanation therefore could be that 6 hours hypoxic incubation is not enough time to

clearly show the continuous enhancement of HIF-1α with increasing concentrations of GYY4137 (Fig. 9).

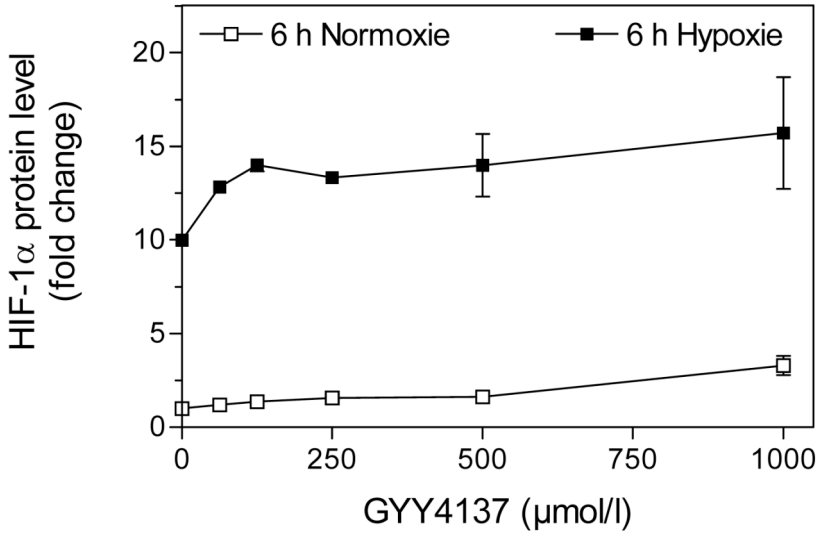

Figure 9: Effect of increasing concentrations of GYY4137 on HIF-1α protein expression after 6 hours normoxia or hypoxia. THP-1 cells were differentiated towards macrophages with 160 nmol/l PMA for 72 hours. Protein expression of HIF-1α after incubation without or with 62.4, 125, 250, 500 or 1000 µmol/l GYY4137 was detected after 6 hours under normoxic and hypoxic conditions. The signals of HIF-1α were adjusted with calnexin or β-actin. The values are the mean values +/- SD of 3 independent experiments.

A continuous increase of HIF-1α with growing concentration of GYY4137 could also be observed after 24 hours normoxia. GYY4137 under 24 hours normoxia led to the biggest multiplication of HIF-1α protein expression compared to 24 hours hypoxia or only 6 hours incubation. Again the amount of HIF-1α protein in THP-1 macrophages after 24 hours incubation without GYY4137 was used as control and set 1. 1000 µmol/l GYY4137 resulted in a 5 times higher signal of HIF-1α compared to the control (Fig. 10). Hypoxia for 24 hours also showed the concentration dependent increase of HIF-1α due to GYY4137. Hypoxia for 24 hours led to a 4-fold increase of basal HIF-1α. Again, the highest value of HIF-1α was measured after incubation with 1000 µmol/l GYY4137. There, HIF-1α protein expression was 2.5 times higher after incubation with 1000 µmol/l GYY4137, when compared to the HIF-1α protein level after incubation without GYY4137 (Fig. 10).

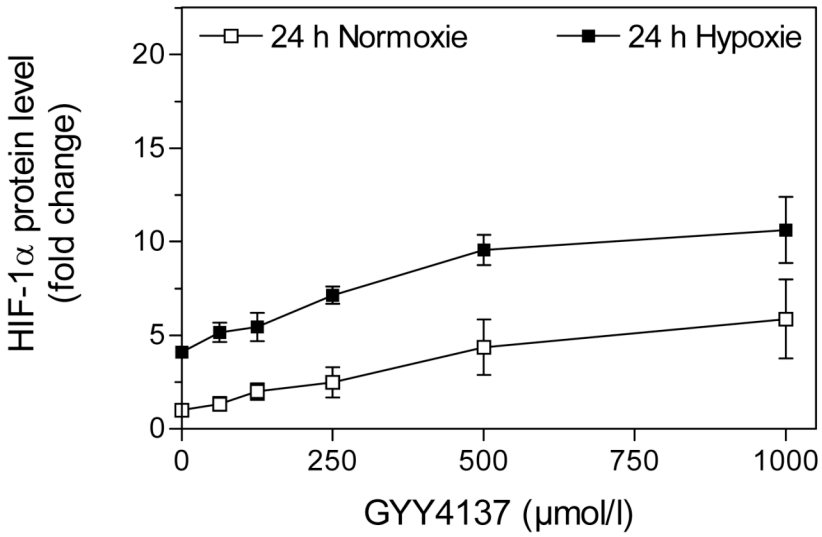

Figure 10: Effect of increasing concentrations of GYY4137 on HIF-1α protein expression after 24 hours normoxia or hypoxia. THP-1 cells were differentiated towards macrophages with 160 nmol/l PMA for 72 hours. Protein expression of HIF-1α after incubation without or with 62.4, 125, 250, 500 or 1000 µmol/l GYY4137 was detected after 24 hours under normoxic and hypoxic conditions. The signals of HIF-1α were adjusted with calnexin or β-actin. The values are the mean values +/- SD of 3-5 independent experiments.

For the Western blot in figure 8 and the evaluations of the effect of GYY4137 after 6 and 24 hours, and under normoxic and hypoxic conditions (Fig. 9 and 10), different exposure times were used to point out the different effects of GYY4137 under distinct conditions. To point out the different effects of GYY4137 under distinct conditions (6 hours normoxia, 6 hours hypoxia, 24 hours normoxia and 24 hours hypoxia), one exposure time was chosen for the Western blot below (Fig. 11) and the HIF-1α signals are depicted with their respective loading control. So, the enormous increase of HIF-1α after 6 hours hypoxia is especially evident. To show that GYY4137 also affects the HIF-1α protein expression under normoxic conditions and after 24 hours hypoxia, the signals of HIF-1α after 6 hours hypoxia had to be overexposed.

Interestingly, an incubation time of 6 hours hypoxia led to a higher signal of HIF-1α compared to an incubation time of 24 hours hypoxia. The highest signal was found when cells were incubated with 1 mmol/l GYY4137 for 6 hours under hypoxic conditions and led to a about 16–fold increase of HIF-1α compared to basal HIF-1α under normoxia. When cells were incubated for 24 hours hypoxia, a 11–fold increase of HIF-1α

was observable (Fig 9 and 10) in the presence of 1 mmol/l GYY4137 compared to basal HIF-1α under normoxic conditions. The much stronger protein intensity of HIF-1α after 6 hours hypoxia compared to 24 hours could be explained by the existence of a negative feedback loop. Berra et al. suppose that there is a till now unidentified proteosomal targeting factor, which is distinct from pVHL and induced by HIF-1α. This factor may lead to the degradation of HIF-1α over time [BERRA et al. 2001]. A negative feedback loop in which p53 is involved and causes the degradation of HIF-1α is also supposable [HOFER et al. 2001].

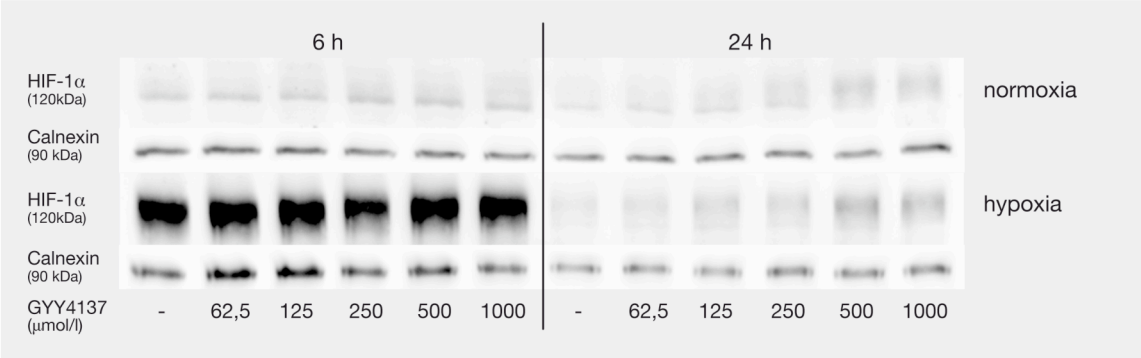

Figure 11: Effect of GYY4137 on the protein expression of HIF-1α. THP-1 cells were differentiated towards macrophages with 160 nmol/l PMA for 72 hours. The whole cell lysates were used to perform Western blot analyses. Protein expression of HIF-1α without or with GYY4137 treatment was detected after 6 and 24 hours under normoxic and hypoxic conditions. One representative Western blot of 2-5 independent experiments is shown. Calnexin was used as loading control.

Our findings result in the conclusion that GYY4137 increases HIF-1α concentration-dependently. This is not concordant to the insight of Wu et al. and Kai et al., who observed the contrary effect. Both found that H_2S decreases HIF-1α under hypoxia in several cell lines in a dose-dependent manner. Wu et al. explained their finding with the enhanced phosphorylation of eIF2α (eukaryotic initiation factor 2α), which is associated with increased suppression of HIF-1α [WU et al. 2012]. Kai et al. found that H_2S inhibited hypoxia induced accumulation of HIF-1α by inducing the degradation of HIF-1α and not by affecting the synthesis of HIF-1α under normoxia and hypoxia. Their explanation therefore was that H_2S decreases the mitochondrial O_2-consumption, leading to an increase of oxygen in hypoxic cells, resulting in HIF-1α degradation [KAI et al. 2012]. In an

in vivo study with mice, Kai et al. could not confirm this [KAI et al. 2012]. Thereby it is important to point out that Wu et al. and Kai et al. used NaHS as H_2S-releaser, in concentrations ranging from 100 to 1000 μmol/l. As NaHS is known to release H_2S very fast and only for a short time and GYY4137 releases small amounts for longer times, the contrary results can be explained in part by this differences. The distinct findings could also be explained by the different experimental setups, including the used H_2S-releaser, application amounts and formulas of H_2S, used organisms (different cell types and animal models) and duration of hypoxia.

Compatibly to our results, Budde and Roth found that H_2S upregulates HIF-1α protein expression in *C. elegans* in a manner independent of the VHL protein [BUDDE and ROTH et al. 2009].

To evaluate the amount of newly synthesised HIF-1α, the concentration of HIF-1α mRNA has to be detected by PCR. At this point it is to mention that we observed the protein amount of HIF-1α by western blotting and not the transcription of HIF-1α DNA to mRNA. So the next steps to investigate the effect of H_2S on HIF-1α and to confirm our findings would be to detect the mRNA level after GYY4137 incubation.

Another gasotransmitter which upregulates HIF-1α is CO [CHOI et al. 2010]. In this context it would be interesting to investigate if there are interferences in the activation mechanisms of these two.

The pathway, by which GYY4137 induces stabilisation of HIF-1α, is by now not investigated and requires further investigations.

Throughout our experiments, we used PMA to differentiate human monocytes to macrophages. Fähling et al. found that PMA in THP-1 cells generally leads to an increase of TPP, but especially to an enhancement of the phosphorylation state of TPP, which resulted in an increase of HIF-1α. They also found that the inhibition of p38 MAPK by the SB 220025 inhibitor lead to suppression of TPP phosphorylation and subsequent to a decrease of HIF-1α. However, TPP phosphorylation was not abolished by the inhibitor, leading to the suggestion that there are alternative routes to phosphorylate TPP [FÄHLING et al. 2012]. This indicates that the basal HIF-1α level in our cell model maybe was enhanced in all incubation types even in the control. Fähling et al. also

found that knockdown of HIF-1α or TPP in THP-1 macrophages lead to the loss of their ability to migrate [FÄHLING et al. 2012]. This leads us to the hypothesis that TPP and/or HIF-1α are required to complete the differentiation of THP-1 monocytes to macrophages.
The role of TPP in the activation mechanism of HIF-1α also supports the hypothesis that there is a connection between HIF-1α and inflammation [FÄHLING et al. 2012].

6.3 Influence of GYY4137 on the HIF-1α target genes GLUT1 and VEGF

After we could clearly observe an effect of GYY4137 on HIF-1α, we wanted to check if the target proteins of HIF-1α, GLUT1 and VEGF, are also influenced by the H_2S-releaser. Therefore, we differentiated THP-1 cells toward macrophages with 160 nmol/ PMA for 72 hours. The differentiated cells were incubated without or with 125, 250, 500 or 1000 µmol/l GYY4137 in HBSS, as described above in the method chapter (5.1.5) and were incubated for either 6 or 24 hours under normoxic (21% O_2, 0.96% Ar, 0.04% CO_2, 78% N_2) or hypoxic conditions (1% O_2, 5% CO_2, 94% N_2).

GLUT1 increased due to GYY4137 under normoxic and hypoxic conditions after 6 and 24 hours. The highest signal of GLUT1 was found after incubation with 1 mmol/l GYY4137 under hypoxic conditions for 24 hours. We suppose that the upregulation of GLUT1 happens via HIF-1α. The specific signaling pathway in the cell, leading to the activation of HIF-1α through H_2S and subsequent presumably GLUT1, is not known to date (Fig. 12).

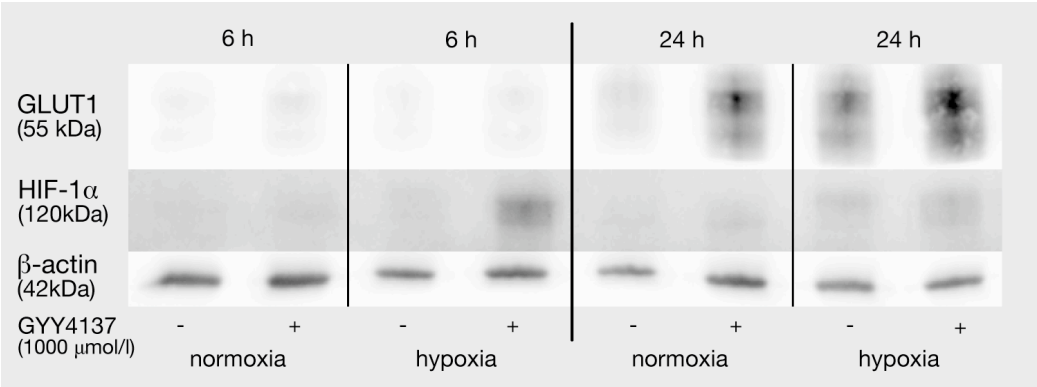

Figure 12: Effect of 1000 μmol/l GYY4137 on the protein expression of GLUT1 and HIF-1α. THP-1 cells were differentiated towards macrophages with 160 nmol/l PMA for 72 hours. The whole cell lysates were used to perform Western blot analyses. Protein expression of GLUT1 and HIF-1α were detected after incubation with or without 1000 μmol/l GYY4137 after 6 and 24 hours under normoxic and hypoxic conditions. One representative Western blot of 2-5 independent experiments is shown. β-actin was used as loading control.

The vascular endothelial growth factor, VEGF, is another target protein of HIF-1α, on which the effect of GYY4137 was investigated. The expression of VEGF mRNA and protein can also, like HIF-1α, be induced by hypoxia [reviewed in LEE et al. 2004].

In the Western blot below (Fig. 13), the effects of different concentrations of GYY4137 on the VEGF protein expression after incubation under normoxic and hypoxic conditions for 6 hours and 24 hours are shown. For this Western blot, one exposure time was chosen, so the different signal intensities for distinct incubation types can be compared with each other. The highest signal was found after incubation under hypoxic conditions for 6 hours. This result is concordant to that of HIF-1α, for which the greatest signal was also found after 6 hours hypoxic treatment. Nevertheless, a conclusion cannot be drawn out of these observations, because an effect of GYY4137 is not noticeable. It is to mention, that the VEGF protein is very hard to detect by Western blotting and therefore many researchers switch to the measurement of VEGF in the cell supernatant.

Figure 13: Effect of GYY4137 on the protein expression of VEGF. THP-1 cells were differentiated towards macrophages with 160 nmol/l PMA for 72 hours. The whole cell lysates were used to perform Western blot analyses. Protein expression of VEGF after treatment without or with GYY4137 treatment was detected after 6 and 24 hours under normoxic and hypoxic conditions. One representative Western blot of 2-5 independent experiments is shown.

To detect VEGF in the cell supernatants a sandwich ELISA was used. An increase of VEGF due to GYY4137 was also not detected with this technique. Although studies indicate that hypoxia influences VEGF, no difference between normoxic and hypoxic conditions on the VEGF level could be found. An explanation therefore is by now not available. An elevation of VEGF was observed after 24 hours incubation, compared to 6 hours (Fig. 14). Thus can be explained by the fact that freely diffusible splice variants of VEGF are secreted by the cell continuously and therefore after 24 hours more VEGF can accumulate in the cell supernatants than after 6 hours.

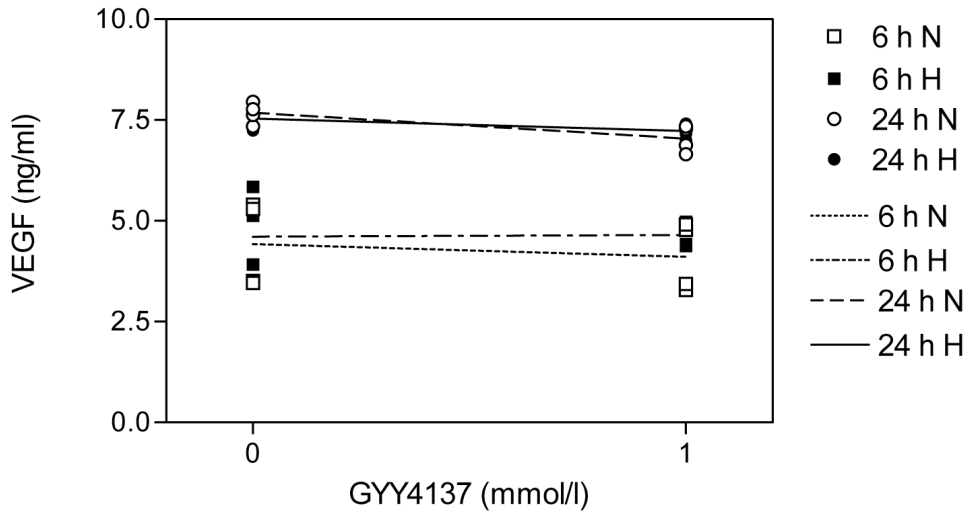

Figure 14: Effect of 1 mmol/l GYY4137 on VEGF protein expression. THP-1 cells were differentiated towards macrophages with 160 nmol/l PMA for 72 hours. Afterwards cells were incubated with or without 1 mmol/l GYY4137 for 6 or 24 hours under normoxic or hypoxic conditions. The amount of VEGF in the cell supernatants was measured via sandwich ELISA spectrophotometrically. The values show duplicates of 2 independent experiments.

The detection of VEGF with a sandwich ELISA did not show any effect of H_2S on the protein level. Nevertheless, we detected a slight increase of VEGF due to GYY4137 under hypoxic conditions by western blotting. An increase of VEGF due to H_2S was previously also shown by Liu et al.. They demonstrated for the first time the proangiogenic effect of H_2S under hypoxia in VSMCs (vascular smooth muscle cells), by showing that H_2S increased HIF-1α and subsequent VEGF. Since HIF-1α directly regulates VEGF it is obviously that HIF-1α is critically involved in the angiogenic response of cells. Liu et al. speculate that H_2S initiate the Akt pathway, which activates HIF-1α and then mobilises VEGF [LIU et al. 2010].
To date, a more detailed interpretation of these results is not possible. Further investigations are necessary to understand the effect of GYY4137 on VEGF more precisely and to draw conclusions.

6.4 Influence of GYY4137 on the SR-BI protein expression

The scavenger receptor class B type 1 is a member of the scavenger receptor family, a family of integral membrane glycoproteins. This receptor family recognizes polyanionic structures of endogenous, (e.g. oxidized low density lipoproteins) or exogenous (e.g. LPS) origin. There are 8 different classes (A-H), classified according to their multidomain structure, whereas SR-BI belongs to the class B, as the name already says.

Because of our interest in SR-BI from experiments done in the past we also monitored the influence of GYY4137 on the SR-BI protein.
Our first result of inquiry was that SR-BI is expressed in THP-1 macrophages. An effect of GYY4137 on SR-BI was also observed under hypoxia.

The Western blot below (Fig. 15) shows the relative decrease of SR-BI due to rising concentrations of GYY4137, with the weakest signal found after treatment with 1000 μmol/l GYY4137 and after 6 hours hypoxia. In contrast, HIF-1α increased with rising

GYY4137 concentrations. After 24 hours, the effect of GYY4137 on SR-BI is not longer visible. Generally, the relative intensity of SR-BI found after 6 hours hypoxia is stronger than after 24 hours hypoxia. To draw conclusions out of these observations, a more detailed screening of this effect is necessary.

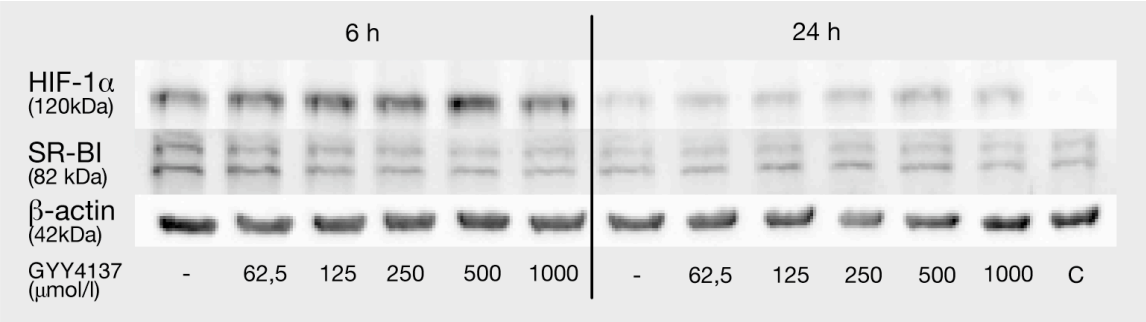

Figure 15: Effect of GYY4137 on the protein expression of SR-BI under hypoxic conditions. THP-1 cells were differentiated towards macrophages with 160 nmol/l PMA for 72 hours. The whole cell lysates were used to perform Western blot analyses. Protein expressions of SR-BI and HIF-1α after treatment without or with rising concentrations of GYY4137 were detected after 6 and 24 hours under hypoxic conditions. The control (C) is the relative protein concentration measured without GYY4137 under normoxic conditions for 24 hours. One representative Western blot of 2-3 independent experiments is shown. β-actin was used as loading control.

6.5 Influence of GYY4137 on HIF-1α and NF-κB subunits and distribution of these proteins between the cytoplasm and the nucleus

To evaluate the effect of GYY4137 on the protein expression of HIF-1α, its target protein GLUT1, NF-κB subunits (p105, p65, pp65 and p50) and IκB, THP-1 cells were differentiated toward macrophages with 160 nmol/ PMA for 72 hours. The differentiated cells were incubated with or without 1000 μmol/l GYY4137 for either 6 or 24 hours under normoxic (21% O_2, 0.96% Ar, 0.04% CO_2, 78% N_2) or hypoxic conditions (1% O_2, 5% CO_2, 94% N_2). Afterwards cell lysates were prepared with a nuclear extraction kit (Active Motif).

Budde and Roth already observed an enhanced nuclear localization of HIF-1α and increased transcription of HIF-1α target genes due to H_2S in *C. elegans* [BUDDE and ROTH 2009]. For us, the initial point for the following experiments was the suggestion

that HIF-1α migrates into the nucleus when it is activated. Hence, if HIF-1α is induced, a higher concentration in the nucleus was expected. This suggestion was confirmed by Western blot analysis.

As seen in the representative Western blot below (Fig. 16), the signals of both HIF-1α, and GLUT1, is much higher in the nucleus than in the cytosol after incubation with GYY4137 and hypoxia. This indicates that both migrate into the nucleus upon activation. HIF-1α and GLUT1 were induced by 1 mmol/l GYY4137 and 6 hours hypoxia, whereas hypoxia led to a stronger effect. The combination of both led to the highest signal.

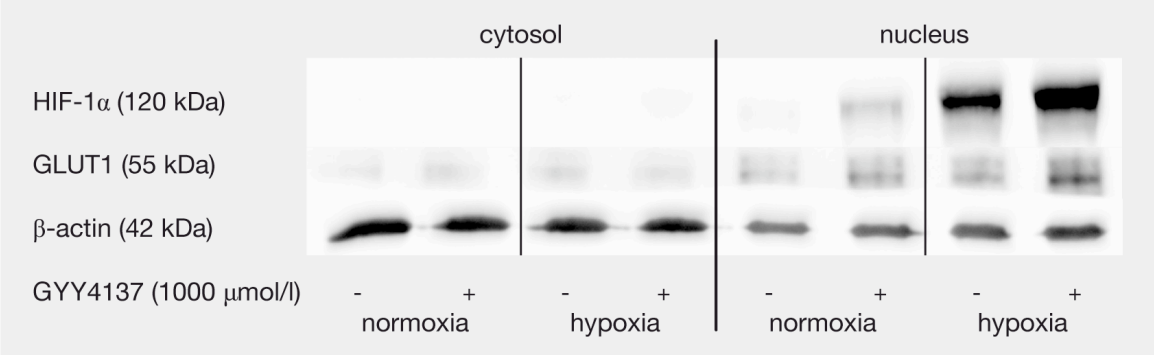

Figure 16: Effect of GYY4137 and 6 hours hypoxia on the protein expression of HIF-1α and GLUT1 in the cytosol and in the nucleus. THP-1 cells were differentiated towards macrophages with 160 nmol/l PMA for 72 hours. The cytosolic and the nuclear cell lysates were used to perform Western blot analyses. Protein expression of HIF-1α and GLUT1 after treatment with or without 1000 μmol/l GYY4137 were detected after 6 hours normoxia or hypoxia. One representative Western blot of 3 independent experiments is shown. β-actin was used as loading control.

The evaluation of 3 independent experiments showed even more clearly the enormous difference between the HIF-1α protein concentration in the cytoplasm and the nucleus. The value measured without GYY4137 after 6 hours normoxia in the nucleus was set 1 (control) and all other values were referred on this value. An increase due to GYY4137 under normoxia is visible in the nucleus. It is evident that hypoxia led to a much higher enhancement of HIF-1α than GYY4137. The increase of HIF-1α due to 6 hours hypoxia in combination with 1 mmol/l GYY4137 is significant compared to its control without GYY4137. The concentration of HIF-1α in the nucleus after GYY4137 treatment under hypoxic conditions is 21-times higher than the control under normoxia (Fig. 17).

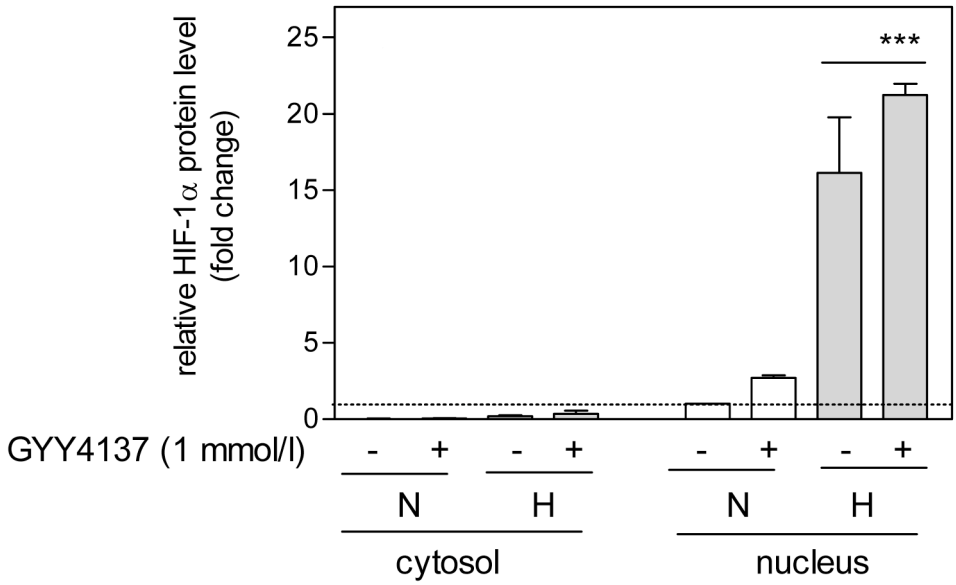

Figure 17: Effect of GYY4137 and 6 hours hypoxia on the protein expression of HIF-1α in the cytosol and in the nucleus. THP-1 cells were differentiated towards macrophages with 160 nmol/l PMA for 72 hours. The cytosolic and the nuclear cell lysates were used to perform Western blot analyses. Protein expression of HIF-1α after treatment with or withour 1 mmol/l GYY4137 was detected after 6 hours normoxia or hypoxia. The values are the mean values +/- SD of 3 independent experiments (*** $p<0.001$ vs. control (without GYY4137)).

For the evaluation of the concentrations of GLUT1 after GYY4137 and hypoxic treatment for 6 hours, the concentration of GLUT1 without GYY4137 under normoxic conditions in the nucleus served as reference point and was set 1. As observed for HIF-1α, GLUT1 was also found in higher concentrations in the nucleus than in the cytosol. GYY4137 and hypoxia respectively led to an increase of GLUT1 in the nucleus. 1 mmol/l GYY4137 in combination with hypoxic conditions enhanced the GLUT1 protein expression the most and led to a significant increase of GLUT1 after 6 hours. The concentration of GLUT1 after GYY4137 and 6 hours hypoxic treatment was duplicated. As GLUT1 is a target protein of HIF-1α, this seems to be a logical consequence. Even though in a smaller extend, the effect of hypoxia on GLUT1 was observed in the cytosol (Fig. 18).

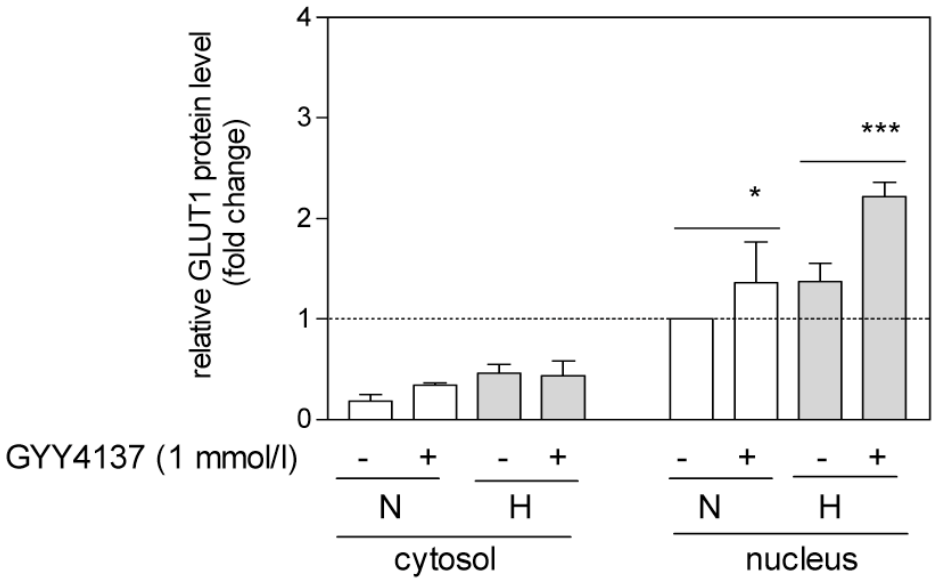

Figure 18: Effect of GYY4137 and 6 hours hypoxia on the protein expression of GLUT1 in the cytosol and in the nucleus. THP-1 cells were differentiated towards macrophages with 160 nmol/l PMA for 72 hours. The cytosolic and the nuclear cell lysates were used to perform Western blot analyses. Protein expression of HIF-1α after treatment with or without 1 mmol/l GYY4137 was detected after 6 hours normoxia or hypoxia. The values are the mean values +/- SD of 3 independent experiments (* $p<0.05$, *** $p<0.001$ vs. control (without GYY4137)).

24 hours of hypoxia led to a similar effect as 6 hours on the protein expression of HIF-1α and GLUT1. Again, the signals found were much higher in the nucleus than in the cytosol. HIF-1α and GLUT1 were activated by 1 mmol/l GYY4137 and 24 hours hypoxia. Combination of both caused the highest signal (Fig. 19).

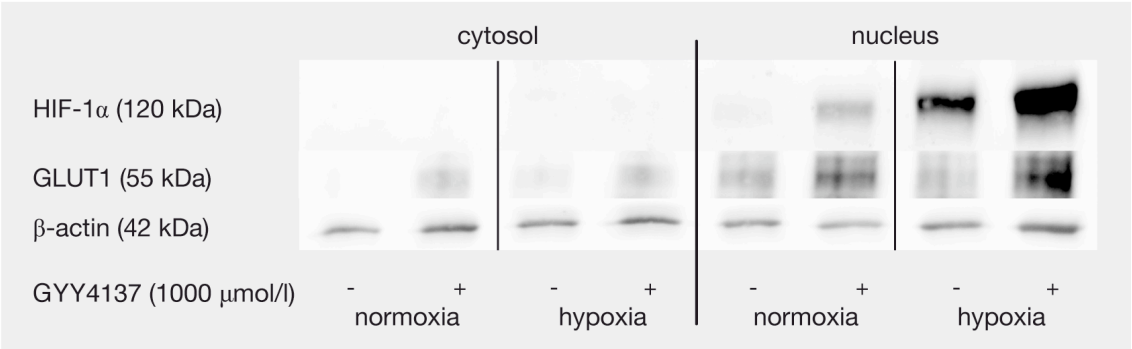

Figure 19: Effect of GYY4137 and 24 hours hypoxia on the protein expression of HIF-1α and GLUT1 in the cytosol and in the nucleus. THP-1 cells were differentiated towards macro-

phages with 160 nmol/l PMA for 72 hours. The cytosolic and the nuclear cell lysates were used to perform Western blot analyses. Protein expression of HIF-1α and GLUT1 after treatment without or with 1 mmol/l GYY4137 were detected after 24 hours normoxia or hypoxia. One representative Western blot of 3 independent experiments is shown. β-actin was used as loading control.

For the evaluation of the concentrations of HIF-1α and GLUT1 after treatment with GYY4137 and hypoxia for 24 hours, the concentrations of HIF-1α and GLUT1 without GYY4137 under normoxic conditions in the nucleus served as reference points. After 24 hours incubation time, 1 mmol/l GYY4137 resulted in a significant increase of HIF-1α in the nucleus. Hypoxic treatment amplified HIF-1α again. Both, GYY4137 and 24 hours hypoxia, led to a more than 6 times higher signal than the initial value. 24 hours incubation time made these effects, even if in much smaller extend, also visible in the cytosol. As discussed above for whole cell lysates (chapter 4.3), we could again observe that 6 hours incubation time led to a higher increase of HIF-1α than 24 hours. After 6 hours hypoxia, HIF-1α was increased by GYY4137 at the 21-fold compared to its normoxic control in the nuclear fraction, whereas 24 hours hypoxia and GYY4137 enhanced HIF-1α only at the 6-fold (Fig. 20).

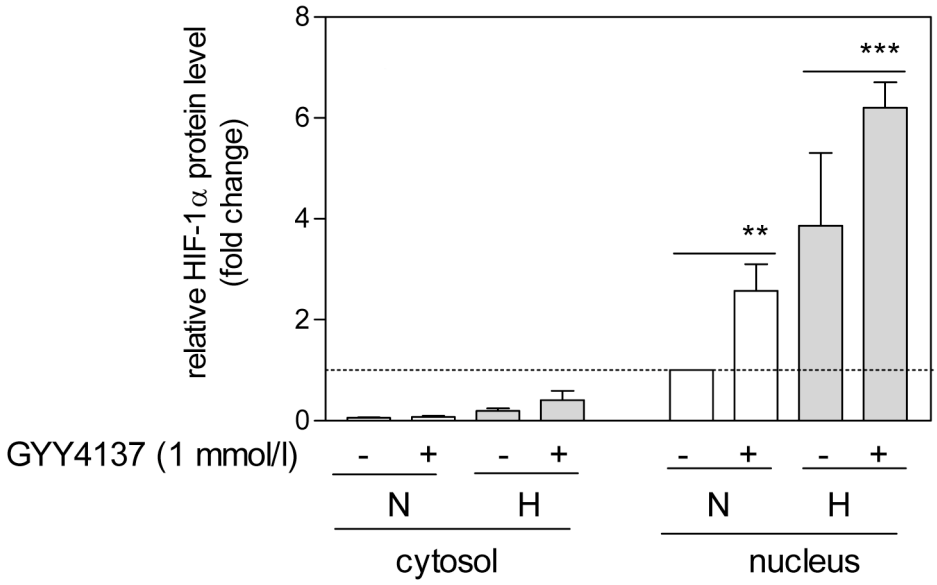

Figure 20: Effect of GYY4137 and 24 hours hypoxia on the protein expression of HIF-1α in the cytosol and in the nucleus. THP-1 cells were differentiated towards macrophages with 160 nmol/l PMA for 72 hours. The cytosolic and the nuclear cell lysates were used to perform Western blot analyses. Protein expression of HIF-1α after treatment with or without 1 mmol/l

GYY4137 was detected after 24 hours normoxia or hypoxia. The values are the mean values +/- SD of 3 independent experiments (** $p<0.01$, *** $p<0.001$ vs. control (without GYY4137)).

The same effects were observed for GLUT1 in the nucleus. Both, 1 mmol/l GYY4137 and 24 hours hypoxia led to a significant increase of the protein. But, incubation of THP-1 cells with 1 mmol/l GYY4137 had a stronger effect on the protein expression than 24 hours hypoxia. After 6 hours the effects were opposite, hypoxia had a higher effect on the GLUT1 protein expression than the H_2S-releaser. Similar effects, but with lower signals, could be observed in the cytosol. In the cytosol the stronger enhancement through hypoxic treatment compared to GYY4137 was conserved (Fig. 21).

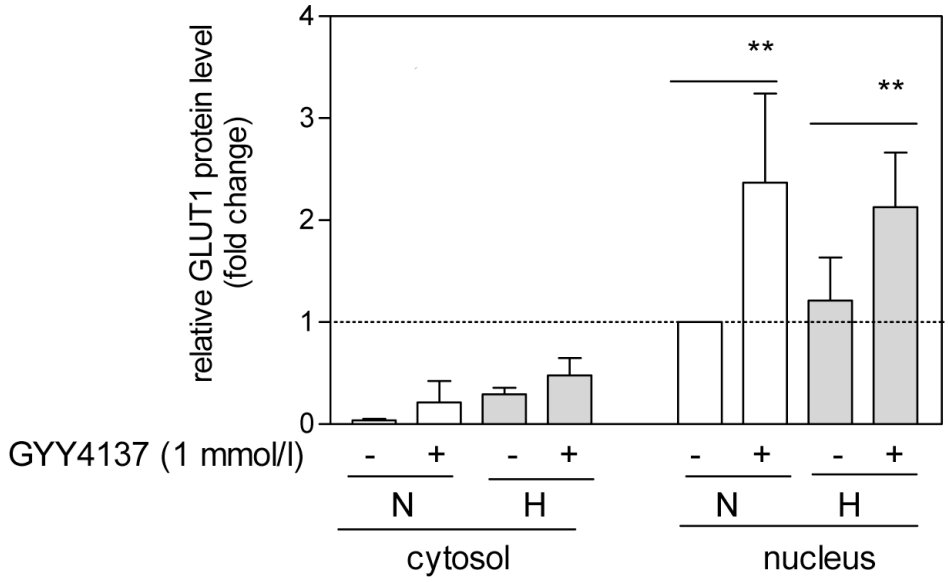

Figure 21: Effect of GYY4137 and 24 hours hypoxia on the protein expression of GLUT1 in the cytosol and in the nucleus. THP-1 cells were differentiated towards macrophages with 160 nmol/l PMA for 72 hours. The cytosolic and the nuclear cell lysates were used to perform Western blot analyses. Protein expression of GLUT1 after treatment with or without 1 mmol/l GYY4137 was detected after 24 hours normoxia or hypoxia. The values are the mean values +/- SD of 3 independent experiments (** $p<0.01$ vs. control (without GYY4137)).

As already discussed above (6.2 Concentration-dependent increase of HIF-1α), HIF-1α increased due to GYY4137 and hypoxia. As GLUT1 is a prominent target gene of HIF-1α, it was not astonishing to find these effects also for GLUT1 protein.

Hypoxia leads to the stabilization of HIF-1α and enables it to translocate into the nucleus. There, HIF-1α heterodimerizes with HIF-1β to induce the expression of target genes, for example GLUT1 [reviewed in DEHNE et al. 2009]. Budde and Roth showed that hypoxia and H_2S resulted in an increase of HIF-1α and an enhanced nuclear localization of HIF-1α in *C. elegans* [BUDDE and ROTH 2009]. We also approved these findings, to my knowledge for the first time in a human cell line. HIF-1α protein was much higher in the nucleus after GYY4137 or hypoxic treatment compared to the cytosol. This accumulation was also found for the HIF-1α target protein GLUT1.
The pVHL protein marks HIF-1α for proteosomal degradation [reviewed in DEHNE et al. 2009]. The H_2S-dependent increase of HIF-1α in *C. elegans* was found to be autonomous of the VHL protein, leading to the suggestion that there are more than one activation mechanisms [BUDDE and ROTH 2009]. A pVHL-independent activation mechanism for HIF-1α has also been described in mammalian cells (OZER et al. 2005; TO and HUANG 2005). In our experiments we could show an enhanced HIF-1α protein. If the elevated HIF-1α protein signal, found in our experiments, occurred because of enhanced protein stability, decreased protein degradation, increased mRNA transcription or upregulated protein translation is unclear to date.
An increase of HIF-1α caused by hypoxia has been shown numerous times. Hypoxia consequently results in a change of the redox balance in cells and so does H_2S [BUDDE and ROTH 2009]. This concordance between hypoxia and H_2S could be the initial point for an explanation for the accumulation of HIF-1α due to H_2S. Exogenous applied H_2S possibly disrupts the respiratory system by inhibiting the cytochrome oxidase of the cell [COOPER and BROWN 2008]. Although we could not show any cytotoxic effect of GYY4137, it could be that the cell counters a respiratory disturbance by upregulating HIF-1α protein.

To investigate if HIF-1α accumulation proceeds via the NF-κB pathway, we checked the concentrations of IκB and NF-κB subunits after treatment with 1 mmol/l GYY4137 under normoxic or hypoxic conditions for 6 or 24 hours. Our reference points for the analysis of IκB and the NF-κB subunits p105, p50, p65 and pp65, were the values measured

without GYY4137 under normal oxygen conditions after 6 or 24 hours respectively. Per experiment two reference points were used, one for the cytosolic fraction and one for the nuclear fraction. So these two points were set 1 and all other values from the respective fraction referred on them. We chose this kind of presentation to focus on the effects of GYY4137 and hypoxia and to a lesser extent on the distribution within the cell. However the later effects will be mentioned in the text if necessary.

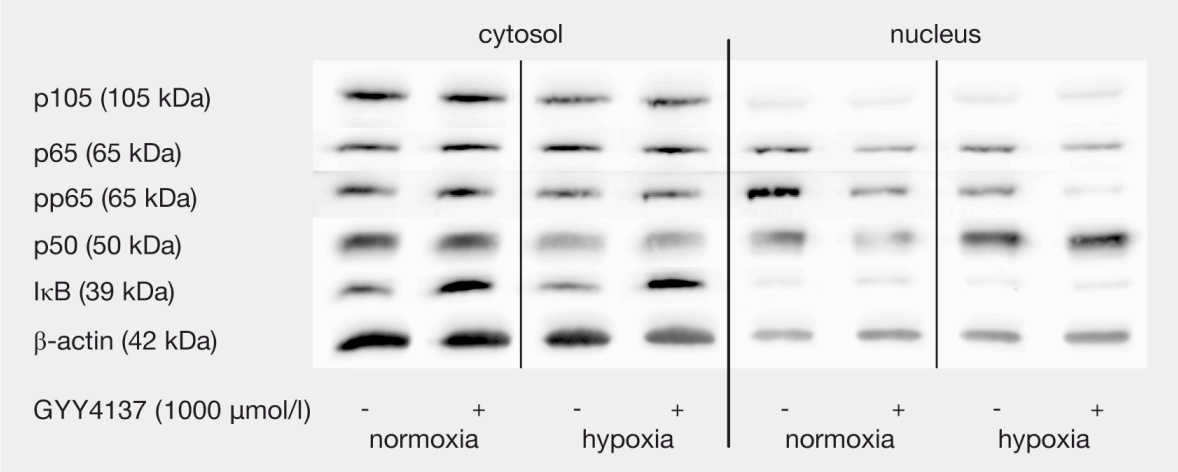

Figure 22: Effect of GYY4137 and 6 hours hypoxia on the protein expression of IκB and NF-κB subunits in the cytosol and in the nucleus. THP-1 cells were differentiated towards macrophages with 160 nmol/l PMA for 72 hours. The cytosolic and the nuclear cell lysates were used to perform Western blot analyses. Protein expression of IκB and NF-κB subunits after treatment with or without 1 mmol/l GYY4137 were detected after 6 hours normoxia or hypoxia. One representative Western blot of 3 independent experiments is shown. β-actin was used as loading control.

In the representative Western blot above (Fig. 22), the signals of IκB had a higher intensity (about 3-fold) in the cytosol than in the nucleus after 6 hours. We found that IκB, like HIF-1α, increased with 1 mmol/l GYY4137 under normoxic and hypoxic condition for 6 hours. An effect on IκB through hypoxia could not be detected (Fig. 23).

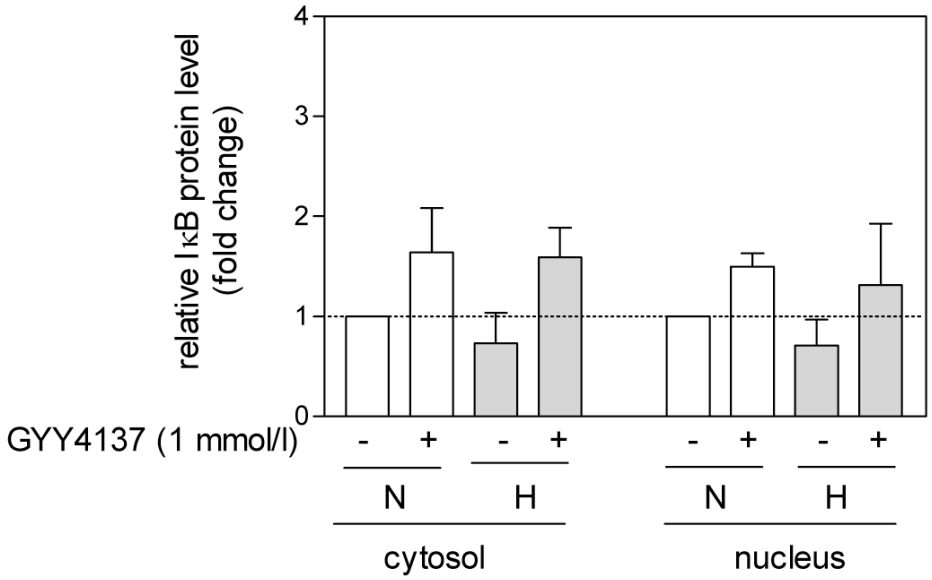

Figure 23: Effect of GYY4137 and 6 hours hypoxia on the protein expression of IκB in the cytosol and in the nucleus. THP-1 cells were differentiated towards macrophages with 160 nmol/l PMA for 72 hours. The cytosolic and the nuclear cell lysates were used to perform Western blot analyses. Protein expression of IκB after treatment with or without 1 mmol/l GYY4137 was detected after 6 hours normoxia or hypoxia. The values are the mean values of 3 independent experiments.

Also the concentrations of the NF-κB subunit p105 show a higher intensity in the cytosol than in the nucleus after 6 hours. Although the effect of 1 mmol/l GYY4137 is seen in the Western blot not very intensively, evaluations of 3 independent experiments showed a slight decrease of p105 due to the H_2S-releaser after 6 hours. This decline was observed both under normoxic and hypoxic conditions in the cytosol and in the nucleus. However, the effects are rather small. The concentration of the processed form of the NF-κB subunit p105, p50, was much higher in the nucleus than in the cytosol after 6 hours. So the apportionment was different to that of p105. It should be mentioned here, that the protein bands depicted on figure 22 result from different exposure times for cytosolic compared to nuclear fractions. Statistic evaluations showed us that the amounts of p50 in the nucleus were 3 to 5-fold higher, compared to those in the cytosol (data not shown). This fits to the assumption that predominantly the active processed form of p105, p50, migrates into the nucleus to activate target genes. As shown for p105, p50 was also slightly decreased in the cytosol under hypoxia. We could not ob-

serve an effect due to hypoxic treatment In the nucleus. An impact of 1 mmol/l GYY4137 could not clearly be extinguished (Fig. 24).

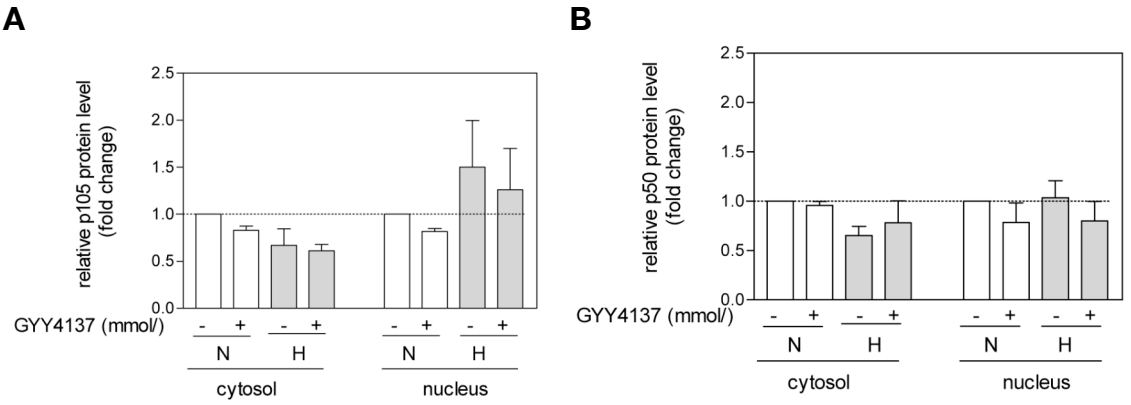

Figure 24: Effect of GYY4137 and 6 hours hypoxia on the protein expression of the NF-κB subunit p105 (A) and p50 (B) in the cytosol and in the nucleus. THP-1 cells were differentiated towards macrophages with 160 nmol/l PMA for 72 hours. The cytosolic and the nuclear cell lysates were used to perform Western blot analyses. Protein expression of p105 (A) and p50 (B) after treatment with or without 1 mmol/l GYY4137 was detected after 6 hours normoxia or hypoxia. The values are the mean values +/- SD of 3 independent experiments.

The concentrations of p65 were higher in the nucleus than in the cytosol (data not shown) after 6 hours incubation. Although the effects are not very intense, an attenuation of p65 through 1 mmol/l GYY4137 in the cytosol and the nucleus could be detected. Hypoxia had no effect on the protein expression of p65, neither in the cytosol, nor in the nucleus (Fig. 25). On the activated phosphorylated form of p65, pp65, hypoxia showed an effect. It led to a decrease of pp65 in the cytosol and in the nucleus after 6 hours. GYY4137 again showed a reducing effect on pp65 under all conditions. Combination of GYY4137 and hypoxic treatment attenuated pp65 the most. In the cytosol the initial value was decreased to about the half and in the nucleus the initial value was decreased to about a fifth from the appropriate reference points (Fig. 25).

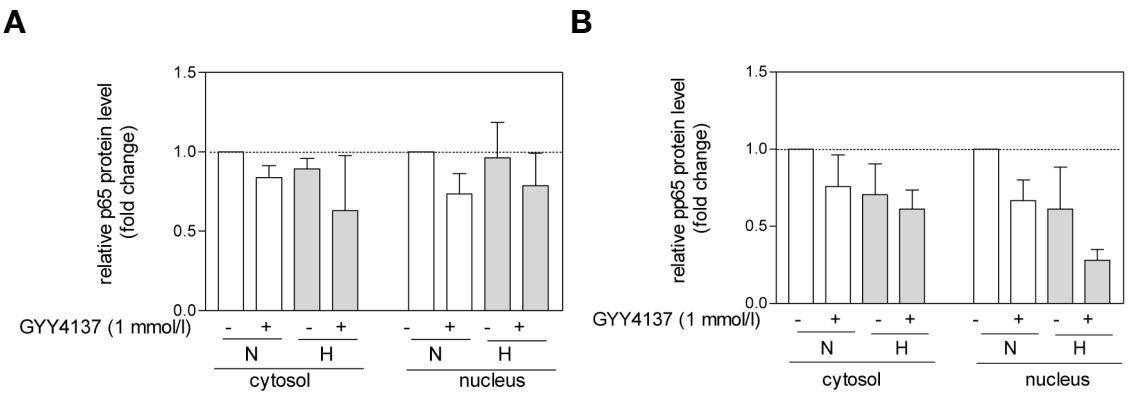

Figure 25: Effect of GYY4137 and 6 hours hypoxia on the protein expression of the NF-κB subunit p65 (A) and pp65 (B) in the cytosol and in the nucleus. THP-1 cells were differentiated towards macrophages with 160 nmol/l PMA for 72 hours. The cytosolic and the nuclear cell lysates were used to perform Western blot analyses. Protein expression of p65 (A) and pp65 (B) after treatment with or without 1 mmol/l GYY4137 was detected after 6 hours normoxia or hypoxia. The values are the mean values +/- SD of 3 independent experiments.

The same experiments, which are discussed above, were also done for 24 hours (Fig. 26).

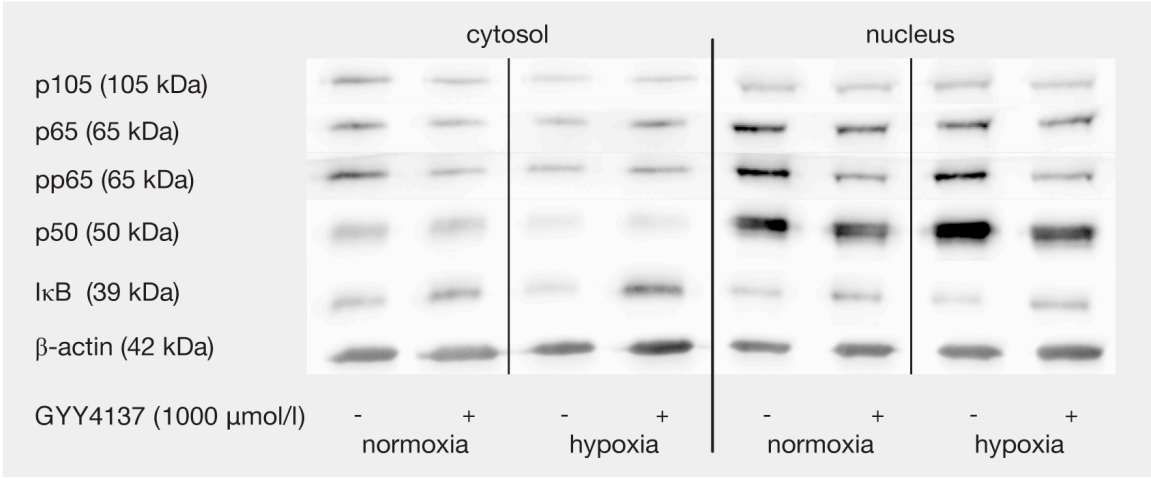

Figure 26: Effect of GYY4137 and 24 hours hypoxia on the protein expression of IκB and NF-κB subunits in the cytosol and in the nucleus. THP-1 cells were differentiated towards macrophages with 160 nmol/l PMA for 72 hours. The cytosolic and the nuclear cell lysates were used to perform Western blot analyses. Protein expression of IκB and NF-κB subunits after treatment with or without 1 mmol/l GYY4137 were detected after 24 hours normoxia or hypoxia. One representative Western blot of 3 independent experiments is shown. β-actin was used as loading control.

After 24 hours, the stimulating effect of 1 mmol/l GYY4137 on IκB was preserved. GYY4137 led to a significant increase of IκB up to more than the double, both in the cytosol and in the nucleus, although the effect was better visible in the nucleus. Even though the signals of IκB were more intense in the cytosol after 6 and 24 hours (about 3-fold), it is astonishing to find relatively high signals of IκB in the nucleus too, particularly after 24 hours, because IκB was thought to be only active in the cytosol. Again, hypoxia showed no consequence on the IκB protein expression after 24 hours.

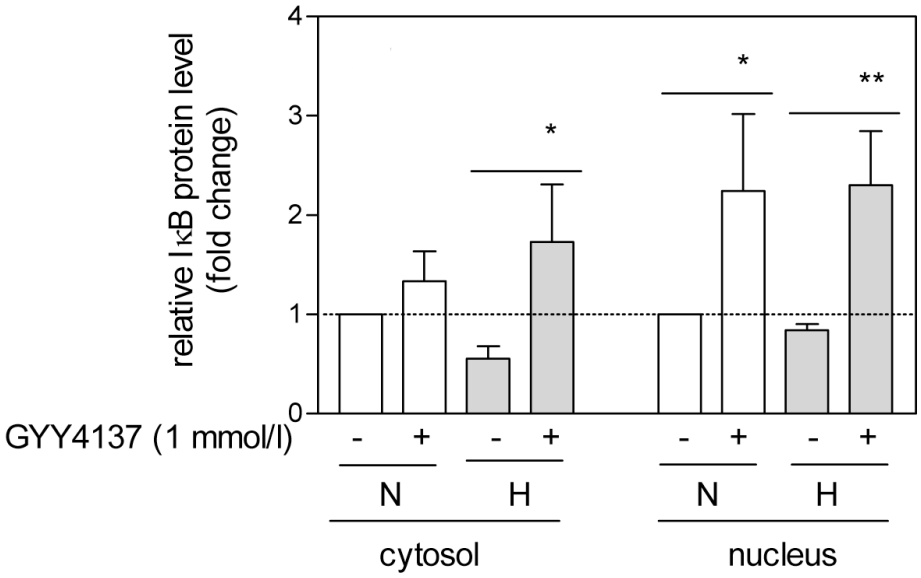

Figure 27: Effect of GYY4137 and 24 hours hypoxia on the protein expression of IκB in the cytosol and in the nucleus. THP-1 cells were differentiated towards macrophages with 160 nmol/l PMA for 72 hours. The cytosolic and the nuclear cell lysates were used to perform Western blot analyses. Protein expression of IκB after treatment with or without 1 mmol/l GYY4137 was detected after 24 hours normoxia or hypoxia. The values are the mean values +/- SD of 3 independent experiments (* $p<0.05$, ** $p<0.01$ vs. control (without GYY4137)).

After 24 hours incubation time, the data achieved for the NF-κB subunit p105 and its processed form p50, were difficult to interpret. Both forms tended to decrease due to 1 mmol/l GYY4137 and due to hypoxic conditions (Fig. 28). As observed after 6 hours, the concentration of p50 is higher in the nucleus than in the cytosol. This is also observable in the Western blot above (Fig. 26). After 6 hours the values of p50 are approximately 5 times higher in the nucleus than in the cytosol. After 24 hours, the difference of the con-

centration of p50 between the cytosol and the nucleus was even greater, it was about 7 times higher (Fig. 28).

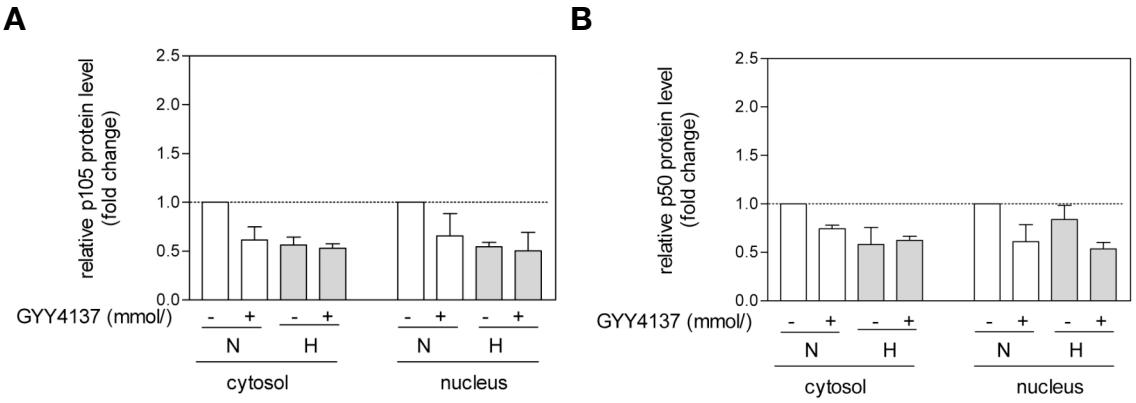

Figure 28: Effect of GYY4137 and 24 hours hypoxia on the protein expression of the NF-κB subunit p105 (A) and p50 (B) in the cytosol and in the nucleus. THP-1 cells were differentiated towards macrophages with 160 nmol/l PMA for 72 hours. The cytosolic and the nuclear cell lysates were used to perform Western blot analyses. Protein expression of p105 (A) and p50 (B) after treatment with or without 1 mmol/l GYY4137 was detected after 24 hours normoxia or hypoxia. The values are the mean values +/- SD of 3 independent experiments.

As seen in the Western blot above (Fig. 26), the signals of p65 and pp65 were more intense in the nucleus, about 2-fold, than in the cytosol after 24 hours. Except the concentration of p65 in the cytosol under hypoxia, the concentration of p65 and phosphorylated p65 declined after incubation with 1 mmol/l GYY4137 for 24 hours. The same effect was observed after 6 hours. 24 hours hypoxia led to a decrease of these two subunits, but only in the nucleus. GYY4137 and hypoxia attenuated the p65 protein expression in the nucleus the most. It dropped on the half of the corresponding reference value under normoxic conditions. This combination also had the highest effect on the activated phosphorylated form of p65, pp65. Under these circumstances, the concentration of pp65 was reduced to a fifth of the corresponding reference value. It is to underline that, independent of low oxygen conditions, 1 mmol/l GYY4137 led to a significant decrease of pp65 (Fig. 29).

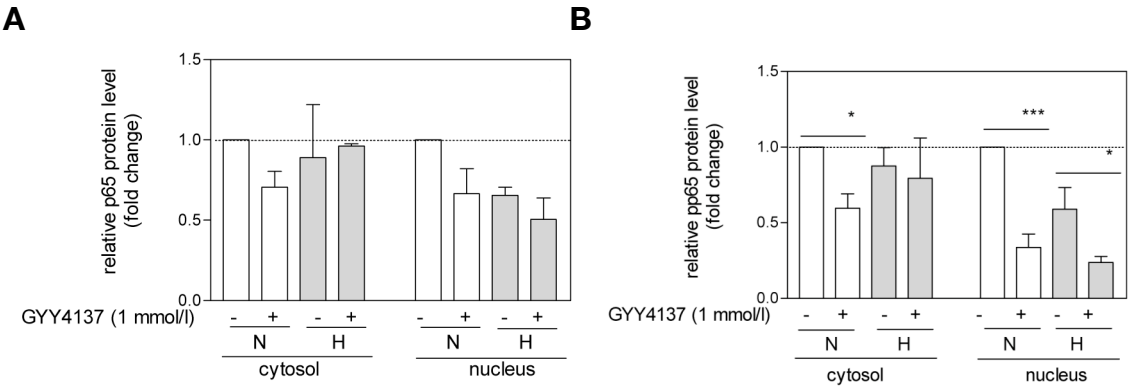

Figure 29: Effect of GYY4137 and 24 hours hypoxia on the protein expression of the NF-κB subunit p65 (A) and pp65 (B) in the cytosol and in the nucleus. THP-1 cells were differentiated towards macrophages with 160 nmol/l PMA for 72 hours. The cytosolic and the nuclear cell lysates were used to perform Western blot analyses. Protein expression of p65 (A) and pp65 (B) after treatment with or without 1 mmol/l GYY4137 was detected after 24 hours normoxia or hypoxia. The values are the mean values +/- SD of 3 independent experiments (* $p<0.05$, *** $p<0.001$ vs. control (without GYY4137)).

In the following 2 tables the effects of GYY4137 and hypoxic treatments on the respective protein levels compared to those detected in untreated cells are summarized:

6 hours

	cytosol			nucleus		
	GYY4137	hypoxia	hypoxia + GYY4137	GYY4137	hypoxia	hypoxia + GYY4137
HIF-1α	↑	↑	↑↑	↑	↑	↑↑
GLUT1	↑	↑	↑	↑	↑	↑↑
IκB	↑	-	↑	↑	-	↑
p105	↓	↓	↓↓	↓	↑	↑
p50	-	↓	↓	↓	-	↓
p65	↓	↓	↓	↓	-	↓
pp65	↓	↓	↓↓	↓	↓	↓↓

	24 hours					
	cytosol			nucleus		
	GYY4137	hypoxia	hypoxia + GYY4137	GYY4137	hypoxia	hypoxia + GYY4137
HIF-1α	↑	↑	↑↑	↑	↑	↑↑
GLUT1	↑	↑	↑↑	↑	-	↑
IκB	↑	-	↑	↑	-	↑
p105	↓	↓	↓↓	↓	↓	↓↓
p50	↓	↓	↓	↓	↓	↓↓
p65	↓	-	-	↓	↓	↓↓
pp65	↓	-	-	↓	↓	↓↓

Table 2: Summary of the effects of 1 mmol/l GYY4137 and hypoxia on the protein expression of HIF-1α, GLUT1, IκB, p105, p50, p65 and pp65 after 6 and 24 hours. ↑ (increase), ↓ (decrease), - (no effect).

To summarize, 1 mmol/l GYY4137 and hypoxia significantly enhanced the HIF-1α protein expression. The increase of IκB with GYY4137 after 6 hours as well as after 24 hours was the first hint against our assumption that the HIF-1α accumulation due to GYY4137 happens via the NF-κB signaling pathway. If IκB is increased, NF-κB subunits will be decreased because of the inhibition by the inhibitor IκB, which consequently, if activated through the NF-κB pathway, should lead to a depleted HIF-1α signal. A downregulation of NF-κB subunits was observed. We act on the assumption that this happened because of the increase of the inhibitor of NF-κB. 1 mmol/l GYY4137 and hypoxia tended to result in a decline of the NF-κB subunits p105, p50, p65 and pp65. This is another argument against the hypothesis that HIF-1α accumulation could proceed via the NF-κB pathway. The opposite influences of GYY4137 and hypoxia on HIF-1α and NF-κB subunits exclude the possibility of HIF-1α activation through the NF-κB pathway. The increase of HIF-1α and GLUT1 could be explained by the inhibiting effect of GYY4137 on the proteosome. Blocking of the proteosome results in increased protein amounts. In our case, we detected enhanced HIF-1α and GLUT1 protein. IKK phosphorylates IκB, leading to its ubiquitination and subsequent to its degradation by the proteosome. NF-κB, which was blocked by IκB, is then no longer blocked and can activate target genes [reviewed in GHOSH et al. 2012]. Because IκB is also degraded by

the proteosome, inhibition of the proteosome by GYY4137 would lead to a decrease in IκB degradation, what we could observe, as we detected an increase of IκB due to GYY4137. The increase of the inhibitor of NF-κB probably caused the decrease of NF-κB subunits. Summerized, the hypothesis that GYY4137 blocks the proteosomal degradation is implausible.

NF-κB and HIF-1α share target genes and there are stimuli that activate both [BONELLO et al. 2007]. Therefore it seemed likely that H_2S activates both. Bonello et al. pointed out that NF-κB is one regulator of HIF-1α protein expression, by showing that the promoter of HIF-1α reacts with NF-κB subunits. Depletion of NF-κB results in a decreased HIF-1α mRNA level, and activation of NF-κB via TNFα, lead to an increase of HIF-1α mRNA and protein under normoxic conditions. They indicated that hypoxia-activated NF-κB regulates, at least to some extend, HIF-1α level [BONELLO et al. 2007]. Because we did not detect the mRNA level of HIF-1α, we could not survey these findings to confirm this hypothesis.

Inflammation mediators, such as cytokines or bacterial LPS, lead to the activation of IKK und subsequent to the increase of NF-κB [UDEN et al. 2008]. In inflamed tissues, the oxygen availability is often under the normal physiological value, what consequently leads to an increase of HIF-1α activity [reviewed in DEHNE et al. 2009]. But HIF-1α can also be activated during inflammation under normoxia [reviewed in ELTZSCHIG and CARMELIET 2011]. Cytokines cause the production of ROS and NO and further lead to the activation of the PI3K and the NF-κB pathway. ROS and NO can also cause the accumulation of HIF-1α [reviewed in DEHNE et al. 2009]. Because both, NF-κB and HIF-1α, are important factors during inflammation and hypoxic episodes, a connection of both seems likely. Although there are some hints for a combined activation mechanism in the connection to inflammation, we could not underline this hypothesis, because HIF-1α increased, while NF-κB tended to decrease due to H_2S throughout our investigations. Because we could not find an upregulation of NF-κB due to H_2S, we assume that H_2S does not cause an immunologically relevant reaction.

Our results fit to those of Stuhlmeier et al., who found that, although NF-κB activates most of the proinflammatory genes, the activation of proinflammatory genes by H_2S is

NF-κB-independent. They conclude that H_2S does not cause the degradation of IκB, which would then lead to the activation of NF-κB subunits [STUHLMEIER et al. 2009].
Gao et al. found that H_2S inhibits the NF-κB signaling pathway. Further, they suggest a protective effect of H_2S on the cardiac system by downregulating NF-κB and thereby the inflammatory response [GAO et al. 2012]. Decreased NF-κB subunits due to H_2S were also observed by us.
So, it is most likely that HIF-1α and NF-κB activation is not coupled in our case. If there is an activation mechanism which activates both, is unclear to date. To investigate possible collective activators, further investigations are necessary.

6.6 Influence of the p38-inhibitor SB202190 on HIF-1α and NF-κB subunits

As an early response to hypoxia the activation of the p38 MAP kinase pathway was observed. Khandrika et al. suggested that activation of the p38 MAPK pathway results in the stabilization of HIF-1α [KHANDRIKA et al. 2009]. The MAPK kinase p38 can also be induced by inflammatory stimuli and cell stress stimuli, which also induce NF-κB [SACCANI et al. 2002]. These findings lead us to the suggestion that the p38 MAPK pathway may also influence the NF-κB pathway. Chun et al. showed that the inhibition of the p38 mitogen activated protein kinase pathway with the inhibitor SB203580 reduced the HIF-1α expression markedly under hypoxia in different cell models [CHUN et al. 2003]. By inhibiting the p38 MAPK pathway with the inhibitor SB202190 in our cell model, we aimed to examine if the HIF-1α, the NF-κB pathway or both can be blocked through this component. We did so to further investigate the question if H_2S can affect HIF-1α or NF-κB activation via the p38 MAPK pathway.

At first we checked if SB202190 is cytotoxic for THP-1 macrophages. Therefore a LDH measurement was done after 6 and 24 hours incubation under normoxic and hypoxic conditions. Neither after 6 nor after 24 hours 5 μmol/l SB202190 caused a notable increase of LDH, leading to the assumption that SB202190 is not toxic to the cells (Fig. 30).

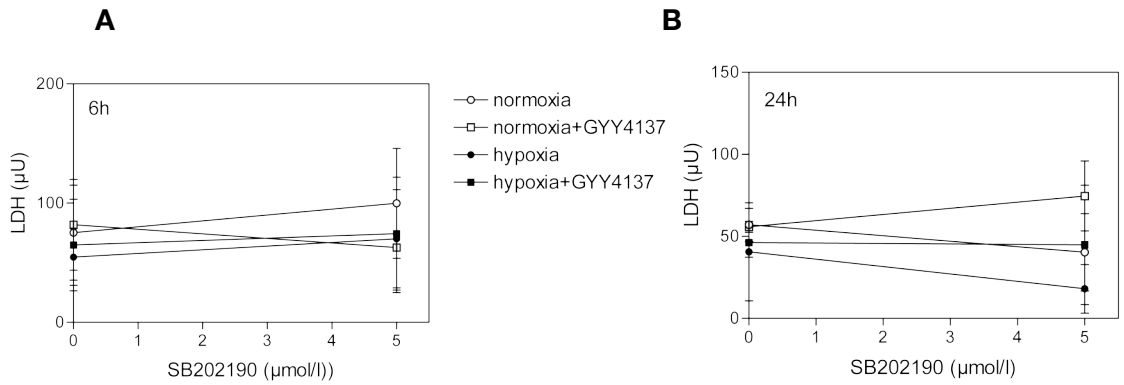

Figure 30: Determination of the LDH-activity after incubation of THP-1 macrophages with 5 µmol/l SB202190 after 6 (A) and 24 (B) hours. THP-1 cells were differentiated towards macrophages with 160 nmol/l PMA for 72 hours. Afterwards the cells were incubated with or without 5 µmol/l SB202190 and additional 0 or 1 mmol/l GYY4137 for 6 (A) or 24 (B) hours under normoxic and hypoxic conditions. The amount of LDH was measured spectrophotometrically. The values are the mean values +/- SD of 3 independent experiments.

The next step was to evaluate the appropriate concentration of SB202190 for our further experiments. Therefore, THP-1 macrophages were incubated without or with 1, 5 or 10 µmol/l SB202190 for 24 hours under normoxic conditions. Our interest was, in which concentration the inhibitor attenuates the HIF-1α protein expression the most. We found that this was the case at a concentration of 5 µmol/l SB202190. The p38-inhibitor decreased the HIF-1α accumulation due to GYY4137 at about 55% from the control value without SB202190. Without additional incubation of cells with GYY4137, SB202190 resulted in a decline of the HIF-1α protein amount at about 47% compared to the value measured without SB202190 (Fig 31).

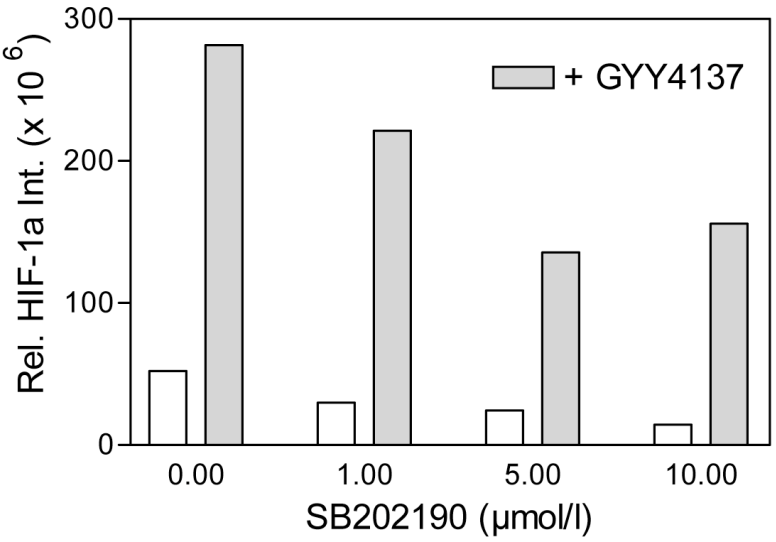

Figure 31: Effect of increasing concentrations of SB202190 on HIF-1α protein expression after 24 hours normoxia. THP-1 cells were differentiated towards macrophages with 160 nmol/l PMA for 72 hours. Protein expression of HIF-1α after incubation without or with 1, 5, or 10 µmol/l SB202190 in combination without (blank bars) or 1 mmol/l GYY4137 (grey bars) was detected after 24 hours normoxia in the nucleus. Values result from one experiment.

TPP can act as enhancer (phosphorylated) or inhibitor (unphosphorylated) of HIF-1α, whereas the phosphorylation of TPP happens via the p38 MAPK pathway. Under normoxic conditions TPP is phosphorylated resulting in the stabilization of HIF-1α mRNA [FÄHLING et al. 2012]. Fähling et al. could also show that inhibition of p38 with the inhibitor SB 220025 led to a decrease of HIF-1α protein expression [FÄHLING et al. 2012].

Because HIF-1α was expressed least when using the p38 inhibitor at a concentration of 5 µmol/l SB202190, this concentration was used for all further experiments (Fig. 31).

The influence of 5 µmol/l SB202190 alone or together with 1 mmol/l GYY4137 on protein expression of p38, HIF-1α, GLUT1, p105, p50, p65 and IκB was monitored under normoxic and hypoxic conditions for 6 or 24 hours.

Inhibition of p38 by the inhibitor SB202190 showed no significant effect on the protein expression of p38 after 6 hours, neither in the cytosol nor in the nucleus. On the acti-

vated, phosphorylated form of p38, pp38, treatment of the cells with SB202190 for 6 hours caused an increase on the protein expression during normoxia or hypoxia. After 24 hours SB202190 led to a slight increase of p38 under normoxic conditions in the cytosol, which was possibly enhanced by additional incubation with GYY4137. Under hypoxic conditions, no effects of SB202190 were detectable in the cytosol after 24 hours. In the nucleus, SB202190 and GYY4137 led to a slight decrease of p38 protein expression during hypoxia, but not so under normoxic conditions. For the phosphorylated p38, the effects observed were similar. After 24 hours, the p38-inhibitor caused an elevation of the pp38 protein expression under normoxic conditions, but not under hypoxic conditions. In the nucleus, SB202190 showed no effect on pp38 after 24 hours. But GYY4137 led to a decrease of pp38 independent of oxygen conditions (Fig. 32).

A (6h cytosol)

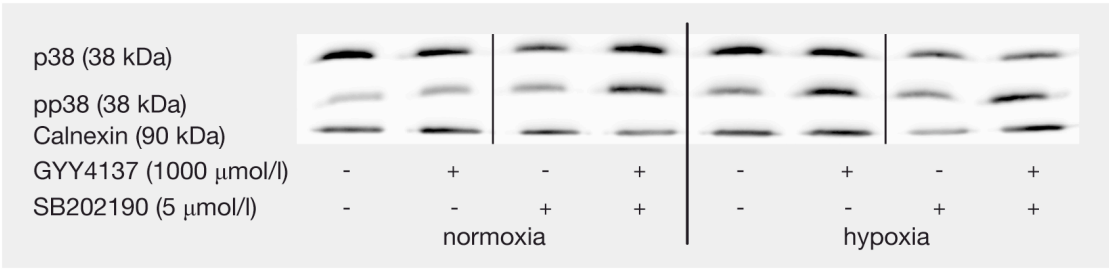

B (6h nucleus)

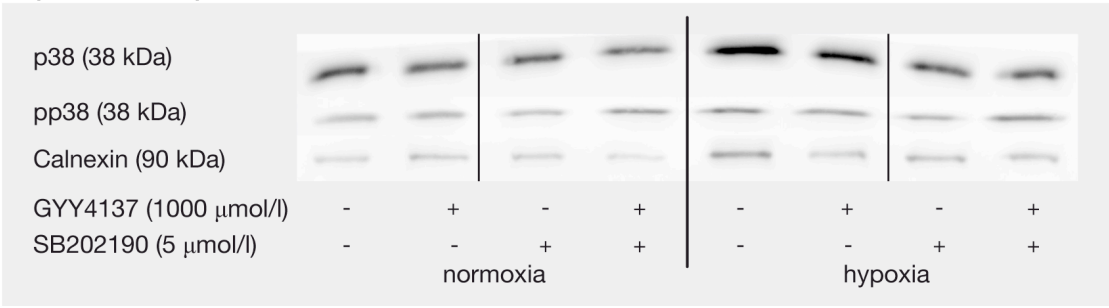

C (24h cytosol)

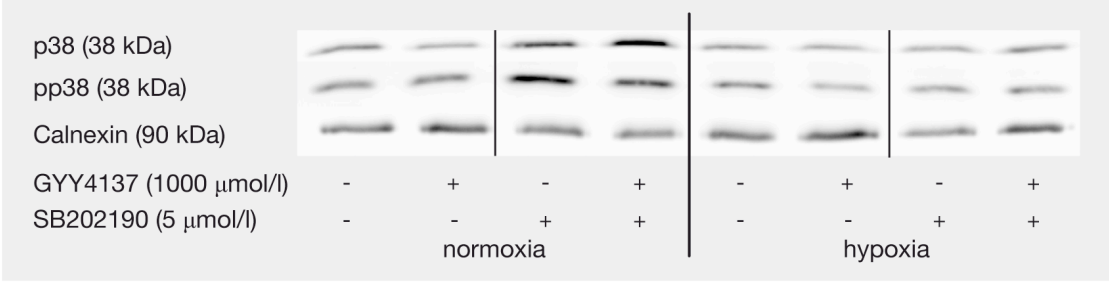

D (24h nucleus)

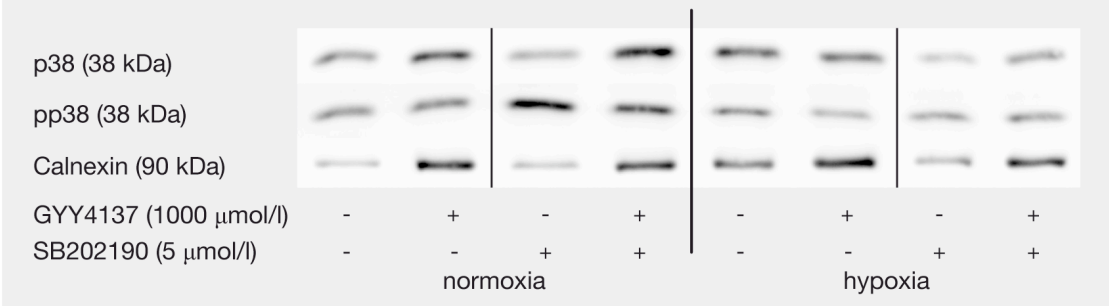

Figure 32: Effect of SB202190 on the protein expression of p38 and pp38 in the cytosol and in the nucleus after 6 and 24 hours. THP-1 cells were differentiated towards macrophages with 160 nmol/l PMA for 72 hours. The cytosolic and the nuclear cell lysates were used to perform Western blot analyses. Protein expression of p38 and pp38 after treatment without or with 5 μmol/l SB202190 in combination without or with 1 mmol/l GYY4137 were detected after 6 and 24 hours normoxia or hypoxia. One representative Western blot of 3 independent experiments is shown. Calnexin was used as loading control.

SB202190 is thought to be highly specific for the isoform p38α and p38β of p38. But it has been reported that the inhibitor also inhibits isoforms of the c-jun kinase N-terminal kinase (JNK) at higher concentrations [MONTERO et al. 2002]. The specificity of SB202190 is the gate keeper threonin (T) 106 in the ATP-binding groove of p38α [MANOJ et al. 2011]. Manthey et al. found that the catalytic activity of p38 was blocked half maximally at 30 nM *in vitro* and at 41 nM *in vivo* by immunoprecipitation of LPS-induced monocyte lysates. They assumed that SB202190 acts specific on p38 [MANTHEY et al. 1998]. Hamanoue et al. observed that SB202190 inhibits p38 with IC_{50} (half maximal inhibitory concentration) values of 50-100 nM in mature oligodendrocytes. Beside they detected morphologic changes after incubation of CG-4 cells and mature oligodendrocytes with 1-30 μM SB202190. These changes were not necessarily due to the inhibition of p38, because SB202190 inhibits also other proteins in concentrations above 50 μM, for example LCK, GSK-3β and PKBα, c-Raf, cyclooxygenase-1, cyclooxygenase-2 and c-src [HAMANOUE et al. 2007].

For us, it was not possible to predict a general decrease of the p38 protein expression after SB202190 incubation. This underlines that SB202190 has a functional effect on the p38 MAPK pathway by disturbing the p38 activity during the forwarding of signals in the MAPK signal cascade. We suggest that SB202190 binds p38 on a specific site, important for its function, and the used antibody for western blotting binds another specific protein site. For binding of the p38 antibody it does not matter if the p38-inhibitor has also already bind the protein or not.

An increase of HIF-1α due to GYY4137 and hypoxia was already shown several times and was also observed in those experiments after 6 and 24 hours. Inhibition of p38, leading to the inactivation of the MAPK pathway, resulted in a decrease of HIF-1α after

6 hours hypoxia in the cytosol and in the nucleus. For the detection of an eventually decrease of HIF-1α due to SB202190 under normoxic conditions, the signal was to weak after 6 hours. After a longer incubation time of 24 hours, an attenuated signal of HIF-1α in the cytosol under hypoxic conditions could be found. In the nucleus, 24 hours SB202190 caused a decrease of HIF-1α during normoxia and hypoxia (Fig. 33). The decrease of HIF-1α, particularly in the nucleus, where it is active, due to 5 μmol/l SB202190 leads to the assumption that HIF-1α is regulated at least in part by the p38 MAPK pathway. This confirms the assumption of Fähling et al., who found that suppression of p38 MAPK pathway with the inhibitor SB220025 led to a decrease of HIF-1α, but not to a complete inhibition [FÄHLING et al. 2012].

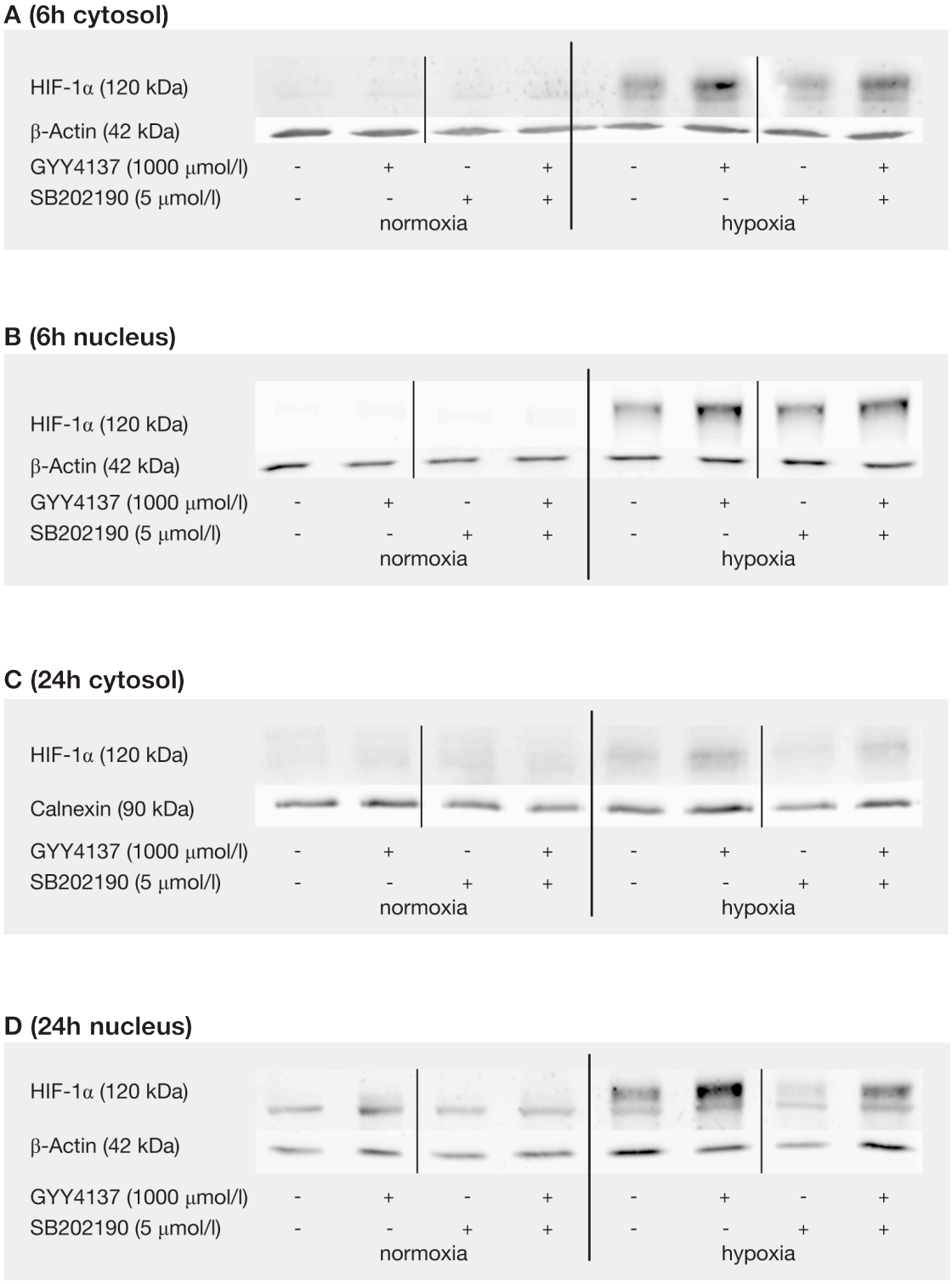

Figure 33: Effect of SB202190 on the protein expression of HIF-1α in the cytosol and in the nucleus after 6 and 24 hours. THP-1 cells were differentiated towards macrophages with 160

nmol/l PMA for 72 hours. The cytosolic and the nuclear cell lysates were used to perform Western blot analyses. Protein expression of HIF-1α after treatment without or with 5 μmol/l SB202190 in combination with or without 1 mmol/l GYY4137 was detected after 6 and 24 hours normoxia or hypoxia. One representative Western blot of 3 independent experiments is shown. β-actin or calnexin was used as loading control.

The results we achieved for the HIF-1α target protein GLUT1 were not explicit. Therefore they are not shown in this evaluations. The experiments working with the p38-inhibitor have to be repeated, especially with the focus on GLUT1.

Next, the effects of SB202190 on the NF-κB subunits were investigated. NF-κB can be activated by inflammatory and cell stress stimuli by which the p38 MAPK pathway can also be induced [reviewed in PERKINS 2007]. So, inhibition of p38 by SB202190 should lead to a decrease of the NF-κB subunits.

The protein expression of NF-κB subunit p105 was found to be decreased after 6 and 24 hours incubation with 5 μmol/l SB202190 in the cytosol and in the nucleus under hypoxia (Fig. 40 and 41). For the processed, active form of p105, p50, no effect could be observed due to SB202190 after 6 hours, neither in the cytosol nor in the nucleus. A longer incubation with SB202190 of 24 hours led to a slight decrease of p50 in the cytosol under hypoxic conditions and in the nucleus under normoxic and hypoxic conditions (Fig. 34 and 35).

The influence of SB202190 on the NF-κB subunit p65 was again very difficult to evaluate. After 6 hours, no or little effect was observed. After 24 hours, a decrease of p65 was detectable due to the inhibition of p38 in the cytosol and in the nucleus, but only under hypoxic conditions (Fig. 34 and 35). An attenuated expression of the activated, phosphorylated form of p65, pp65, caused by SB202190, was measured already after 6 hours in the cytosol and in the nucleus, but again only when hypoxic conditions were chosen. A longer incubation time of 24 hours led to a stronger development of this abetment due to SB202190 treatment. pp65 was clearly decreased in the cytosol and in the nucleus under hypoxic conditions (Fig. 34 and 35).

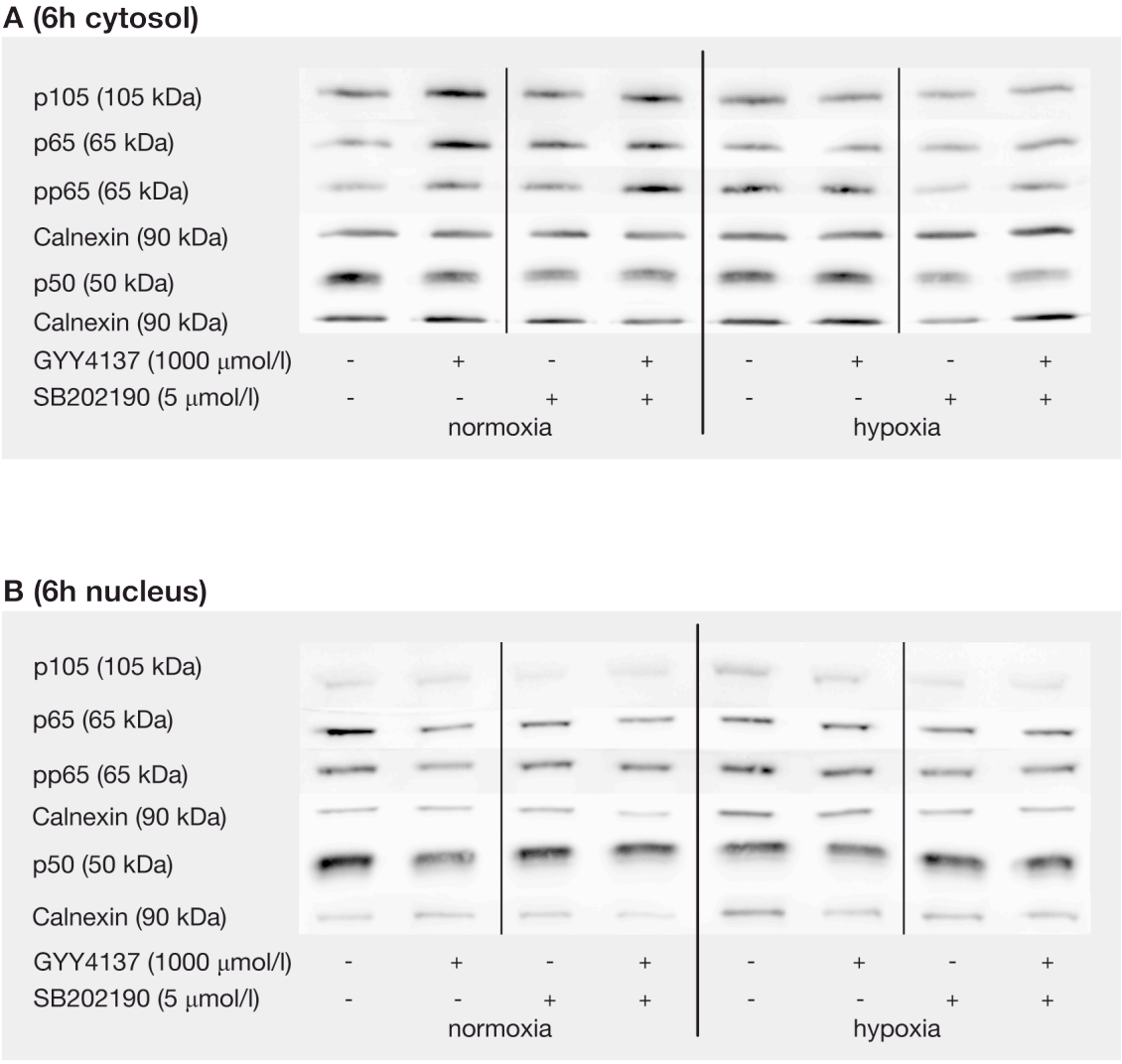

Figure 34: Effect of SB202190 on the protein expression of p105, p50, p65 and pp65 in the cytosol and in the nucleus after 6 hours incubation. THP-1 cells were differentiated towards macrophages with 160 nmol/l PMA for 72 hours. The cytosolic and the nuclear cell lysates were used to perform Western blot analyses. Protein expression of p105, p50, p65 and pp65 after treatment without or with 5 µmol/l SB202190 in combination with or without 1 mmol/l GYY4137 was detected after 6 hours normoxia or hypoxia. One representative Western blot of 3 independent experiments is shown. Calnexin was used as loading control.

C (24h cytosol)

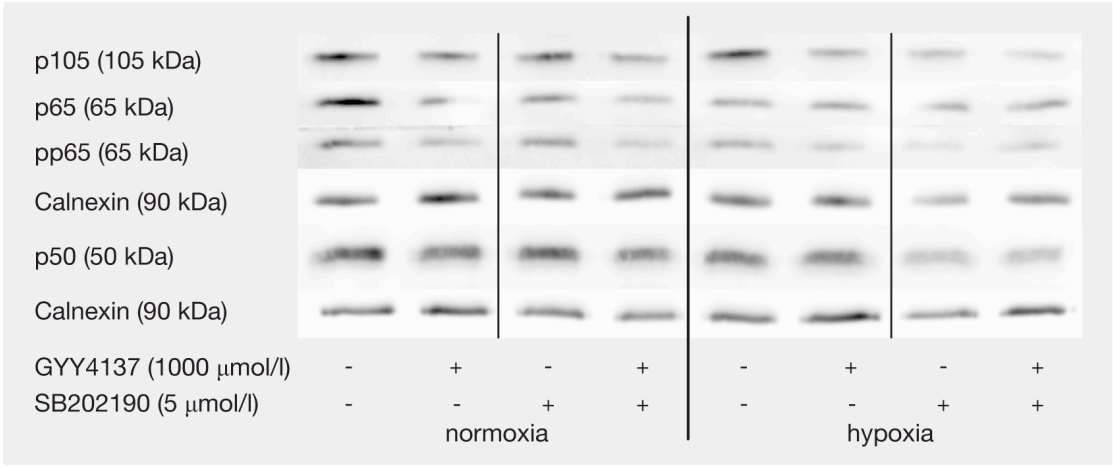

D (24h nucleus)

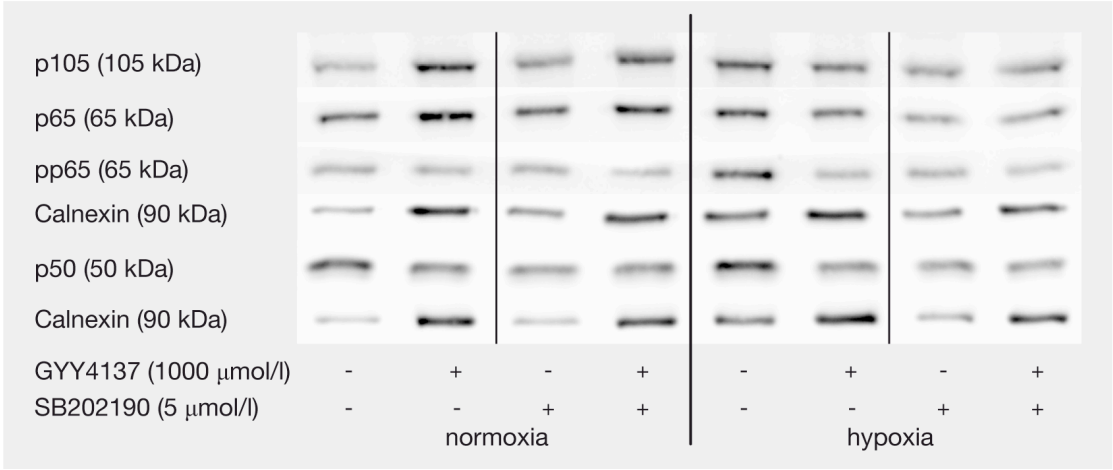

Figure 35: Effect of SB202190 on the protein expression of p105, p50, p65 and pp65 in the cytosol and in the nucleus after 24 hours incubation. THP-1 cells were differentiated towards macrophages with 160 nmol/l PMA for 72 hours. The cytosolic and the nuclear cell lysates were used to perform Western blot analyses. Protein expression of p105, p50, p65 and pp65 after treatment without or with 5 µmol/l SB202190 in combination with or without 1 mmol/l GYY4137 was detected after 24 hours normoxia or hypoxia. One representative Western blot of 3 independent experiments is shown. Calnexin was used as loading control.

Our next focus was to check the influence of SB202190 on the inhibitor of NF-κB, IκB. The increase due to GYY4137 was again observed, but an effect of 5 µmol/l SB202190 after 6 hours incubation could not be observed, neither in the cytosol nor in the nucleus. After 24 hours there was a strong effect of SB202190. IκB decreased due to SB202190

during normoxia and hypoxia in the cytosol and in the nucleus. So, a decrease of IκB by the p38-inhibitor and subsequent activation of the NF-κB pathway is possible, but not confirmed (Fig. 42). The deactivated, phosphorylated form of IκB, pIκB, could only be detected by Western blot analysis after 6 hours. Analysis of pIκB was very hard throughout the experiments. An impact of SB202190 could not be monitored (Fig. 36).

A (6h cytosol)

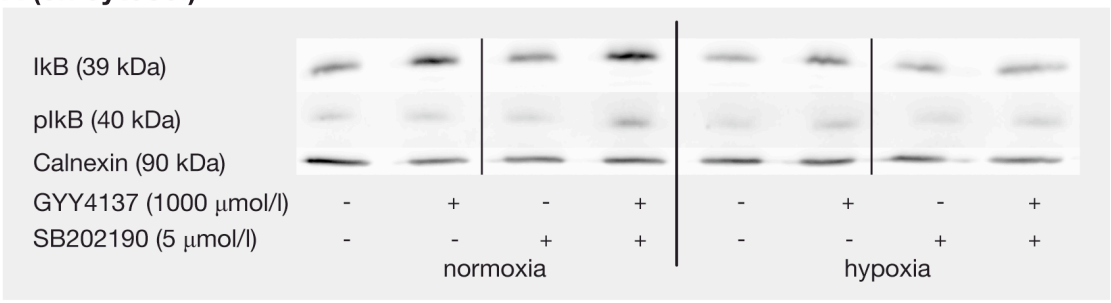

B (6h nucleus)

C (24h cytosol)

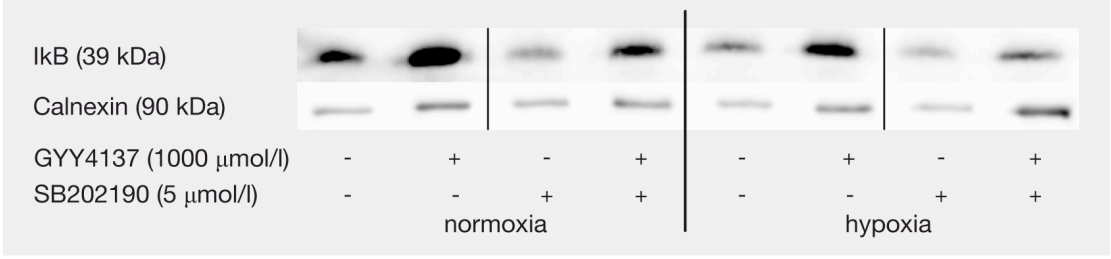

D (24h nucleus)

Figure 36: **Effect of SB202190 on the protein expression of IκB and pIκB in the cytosol and in the nucleus after a and 24 hours incubation.** THP-1 cells were differentiated towards macrophages with 160 nmol/l PMA for 72 hours. The cytosolic and the nuclear cell lysates were used to perform Western blot analyses. Protein expression of IκB and pIκB after treatment without or 5 μmol/l SB202190 in combination with or without 1 mmol/l GYY4137 was detected after 6 hours for IκB and pIκB under normoxia or hypoxia and after 24 hours under normoxia or hypoxia only for IκB. One representative Western blot of 3 independent experiments is shown. Calnexin was used as loading control.

Hypoxia was shown to initiate the activation of the p38 MAPK pathway [KHANDRIKA et al. 2009], which is also the main activator of HIF-1α. In our experiments, we monitored the effect of blocked p38 with the inhibitor SB202190 on the HIF-1α protein expression. Acting on the assumption that the NF-κB and as well the MAPK p38 pathway can be induced by the same stimuli, such as stress and inflammatory stimuli [SACCANI et al. 2002], we tried to examine the effect of inhibited MAPK p38 pathway on NF-κB by using the p38 inhibitor SB202190.
The question in this chain of thoughts was if H_2S could affect HIF-1α or NF-κB activation via the p38 MAPK pathway.

As an early response to hypoxia, the activation of the p38 MAP kinase pathway was observed. Khandrika et al. suggested that activation of the p38 MAPK pathway results in the stabilization of HIF-1α [KHANDRIKA et al. 2009]. The decrease of HIF-1α due to p38-inhibition, found in our experiments, underlines this suggestion. The decline of HIF-1α was visible particularly in the nucleus, where it was found to be present in higher concentrations already in previous experiments. These findings lead us to the assumption that HIF-1α is regulated in part by the p38 MAPK pathway. In 2003, Chun et al. showed that the inhibition of the p38 MAPK pathway, using the inhibitor SB203580, reduced the HIF-1α protein expression under hypoxia in different cell models [CHUN et al. 2003]. An involvement of the p38 MAPK in the activation mechanism of HIF-1α was also suggested in pulmonary artery fibroblasts [Mortimer et al. 2007] and in pancreatic cancer cells [Kwon et al. 2005]. Fähling et al. found that the suppression of the p38 MAPK pathway with the inhibitor SB220025 during PMA-mediated differentiation of THP-1 cells led to a decrease of HIF-1α, due to suppression of the phosphorylation of

TPP, whereas phosphorylated TPP enhances HIF-1α protein expression [FÄHLING et al. 2012]. The observations of Fähling et al. additionally confirmed our suggestion that HIF-1α can be regulated by the p38 MAPK pathway. As we did, this group also monitored no complete inhibition of HIF-1α, pointing out that there are alternative routes to activate HIF-1α. It exists the possibility that SB202190 reverses the stimulation of HIF-1α by GYY4137.

HOFER et al. showed that p42/p44 mitogen-activated protein kinases phosphorylate HIF-1α. After usage of a MAPK inhibitor, called PD98059, which inhibits phosphorylation of HIF-1α, they observed an attenuated HIF-1α protein modification and abolished transactivation ability, but no effect on protein level and DNA-binding ability. This indicates that phosphorylation by the MEK/Erk pathway regulates trans-activation but not HIF-1α stabilization and DNA-binding. They suggest that phosphorylation of HIF-1α by mitogen-activated protein kinase is necessary for full HIF-1α activation [HOFER et al. 2001]. If p42/p44 is involved in the effects we monitored is unclear so far.

The MAPK kinase p38 can be induced by inflammatory and cell stress stimuli, which also induce the NF-κB pathway [SACCANI et al. 2002]. In our experiments we found the inhibitor of NF-κB, IκB, to be decreased due to SB202190 during normoxia and hypoxia. The inhibition of IκB should lead to enhanced activation of NF-κB, what we could not observe. Moreover, we observed that the NF-κB subunits p150, p50, p65 and pp65 decrease after inhibition of the p38 MAPK pathway under hypoxia. A connection of NF-κB and p38 MAPK is for this reason likely and results in the hypothesis that the NF-κB pathway can be induced by the p38 MAPK pathway. The decrease of NF-κB subunits due to the p38-inhibitor was in some cases rather small and can be explained by the big spectrum in which the NF-κB pathway operates and by the many mechanisms that lead to its activation. It was found that activation of the p38 MAPK pathway leads to the phosphorylation of H3 in the promoter region of NF-κB. This further enhances the accessibility of the NF-κB binding site and leads to an increased recruitment of NF-κB and enhanced transcriptional activity. Saccani et al. showed that the p38 signaling pathway is necessary to induce the NF-κB activity in response to bacterial products and CD40L.

They suppose that p38 does this not by binding of NF-κB binding or influencing the transcription [SACCANI et al. 2002]. These findings strengthen our hypothesis that NF-κB activation can be enhanced by the p38 signaling cascade. Phosphorylation of H3 can also happen independent of the p38 pathway. This was observed for the promoter of IκBα [SACCANI et al. 2002].

There are some questions remaining, for example “Why does GYY4137 increase IκB compared to controls?” and “Why does GYY4137 decrease the NF-κB subunits p50 and pp65?”. To answer this questions further investigations are required.

The question if H_2S can affect HIF-1α or NF-κB activation via the p38 MAPK pathway can not be fully answered by now, but the activation of the p38 MAPK pathway is still an opportunity for the explanation of increased HIF-1α due to H_2S. That the decrease of NF-κB is caused by H_2S, is also not to be excluded. Testing the influence of SB202190 on HIF-1α, its target proteins and the NF-κB subunits, is a work in progress and is not completed so far.

7 References

ABE K. and KIMURA H. (1996). “The possible role of hydrogen sulfide as an endogenous neuromodulator.” J Neurosci 16(3):1066-71.

AUWERX J. (1991). “The human leukaemia cell line, THP-1: a multifaceted model for the study of monocyte-macrophage differentiation.” Experentia 47(1): 22-31.

BEINKE S. and LEY SC. (2004). “Functions of NF-kappaB1 and NF-kappaB2 in immune cell biology.” Biochem J 382(Pt 2):393-409.

BENAVIDES GA., SQUADRITO GL., MILLIS RW., PATEL HD., ISBELL TS., PATEL RP., DARLEY-USMAR VM., DOELLER JE. and KRAUS DW. (2007). “Hydrogen sulfide mediates the vasoactivity of garlic.” Proc Natl Acad Sci U S A 104(46):17977-82.

BEN-SHOSHAN J., AFEK A., MAYSEL-AUSLENDER S., BARZELAY A., RUBENSTEIN A., KEREN G. and GEORGE J. (2009). “HIF-1alpha overexpression and experimental murine atherosclerosis.” Arteroscler Thromb Vasc Biol 29(5):665-70.

BERRA E., RICHARD DE., GHOTHIE E. and POUYSSEGUR J. (2001). “HIF-1-dependent transcriptional activity is required for oxygen-mediated HIF-1alpha degradation.” FEBS Lett 491(1-2):85-90.

BONELLO S., ZÄHRINGER C., BELAIBA RS., DJORDJEVIC T., HESS J. MICHIELS C., KIETZMANN T. and GÖRLACH A. (2007). “Reactive oxygen species activate the HIF-1alpha promoter via a functional NFkappaB site.” Arteroscler Thromb Vasc Biol 27(4):755-61.

BUDDE MW. and ROTH MB. (2009). “Hydrogen sulfide increases hypoxia-inducible factor-1 activity independently of von hippel-lindau tumor suppressor-1 in *C. elegans*.” Mol Bio Cell 21(1):212-7.

CAROLL VA. and ASHCROFT M. (2005). “Targeting the molecular basis for tumour hypoxia.” Expert Rev Mol Med 7(6): 1-16.

CÉBE SUAREZ S., PIEREN M., CARIOLATO L., ARN S., HOFMANN U., BOGUCKI A., MANILIUS C., WOOD J. and BALMER-HOFER K. (2006). “A

VEGF-A splice variant defective for heparan sulfate and neurophilin-1 shows attenuated signaling through VEGFR-2." Cell Mol Life Sci 63(17):2067-77.

CHOI YK., KIM CK., LEE H., JEOUNG D., HA KS., KWON YG., KIM KW. and KIM YM. (2010). "Carbon monoxide promotes VEGF expression by increasing HIF-1alpha protein level via two distinct mechanism, translational activation and stabilization of HIF-1alpha protein." J Biol Chem 285(42):32116-25.

CHUN YS., LEE KH., CHOI E., BAE SY., YEO EJ., HUANG LE., KIM MS. and PARK JW. (2003). "Phorbol ester stimulates the nonhypoxic induction of a novel hypoxia-inducible factor 1α isoform: implications for tumor promotion." Cancer Res 63(24):8700-7.

COOPER CE. and BROWN GC. (2008). "The inhibition of mitochondrial cytochrome oxidase by the gases carbon monoxide, nitric oxide, hydrogen cyanide and hydrogen sulfide: chemical mechanism and physiological significance." J Bioenerg Biomembr 40(5):533-9.

DEHNE N. and BRÜNE B. (2009). "HIF-1 in the inflammatory microenvironment." Exp Cell Res 315(11):1791-7.

DORLAND (corporate author) (2011). „Dorland's illustrated medical dictionary." Saunders, 32nd edition.

ELTZSCHIG HK. and CARMELIET P. (2011). „Hypoxia and inflammation." N Engl J Med 364(7):656-65.

FÄHLING M., PERSSON AB., KLINGER B., BENKO E., STEEGE A., KASIM M., PATZAK A., PERSSON PB., WOLF G., BLÜTHGEN N. and MROWKA R. (2012). "Multilevel regulation of HIF-1 signaling by TPP." Mol Biol Cell 23(20):4129-41.

FU M., ZHANG W., WU L., YANG G., LI H. and WANG R. (2012). "Hydrogen sulfide (H2S) metabolism in mitochondria and its regulatory role in energy production." Proc Natl Acad Sci U S A 109(8):2943-8.

FUKUDA R., HIROTA K., FAN F., JUNG YD., ELLIS LM. and SEMENZA GL. (2002). "Insulin-like growth factor 1 induces hypoxia-inducible factor 1-mediated vascular endothelial growth factor expression, which is dependent on MAP kinase and phosphatidylinositol 3-kinase signaling in colon cancer cells." J Biol Chem 277(42):38205-11.

GANSTER F., BURBAN M. de la BOURDONNAYE M., FIZANNE L., DOUAY O., LOUFRANI L., MECAT A., CALES P., REDERMACHER P., HENRION D., ASFAR P. and MEZIANI F. (2010). “Effects of hydrogen sulfide on hemodynamics, inflammatory response and oxidative stress during resuscitated hemorrhagic shock in rats.” Crit Care 14(5):R165.

GAO C., XU DQ., GAO CJ., DING Q., YAO LN., LI ZC. and CHAI W. (2012). “An exogenous hydrogen sulphide donor, NaHS, inhibits the nuclear factor κB inhibitor kinase/nuclear factor κb inhibitor/nuclear factor-κB signaling pathway and exerts cardioprotective effects in a rat hemorrhagic shock model.” Biol Pharm Bull 35(7):1029-34.

GOROSPE M., TOMINAGA K., WU X. FÄHLING M. and IVAN M. (2011). “Post-transcriptional control of the hypoxic response by RNA-binding proteins and microRNAs.” Front Mol Neurosci 4, 7.

GHOSH G., WANG VY., HUANG DB. and FUCSO A. (2012). “NF-κB regulation: lessons from structures.” Immunol Rev 246(1):36-58.

HAGEMANN T., BISWAS SK., LAWRENCE T., SICA A. and LEWIS CE. (2009). “Regulation of macrophage function in tumors: the multifaceted role of NF-kappaB:” Blood 113(14):3139-46.

HAMANOUE M., SATO K. and TEKAMATSU K. (2007). “Inhibition of p38 mitogen-activated protein kinase-induced apoptosis in cultured mature oligodendrocytes using SB202190 and SB203580.” Neurochem Int 51(1):16-24.

HOEKSTRA M., VAN BERKEL TJ. and VAN ECK M. (2010). “Scavenger receptor BI: A multi-purpose player in cholesterol and steroid metabolism.” World j Gastroenterol 16(47):5916-24.

HOFER T., DESBAILLETS I., HÖPFL G., GASSMANN M. and WENGER RH. (2001). “Dissecting hypoxia-dependent and hypoxia-independent steps in the HIF-1alpha activation cascade: implications for HIF-1alpha gene therapy.” FASB J 15(14):2715-7.

HOLMES K., ROBERTS OL. THOMAS AM. and CROS MJ. (2007). “Vascular endothelial growth factor receptor-2: Structure, function, intracellular signalling and therapeutic inhibition.” Cell Signal 19(10):2003-12.

JAVELAUD D. and BESANCON F. (2001). “NF-kappa B activation results in rapid inactivation of JNK in TNF alpha-treated Ewing sarcoma cells: a mechanism for the anti-apoptotic effect of NF-kappa B.” Oncogene 20(32):4365-72.

KAELIN WG. and RATCLIFF PJ. (2008). “Oxygen sensing by metazoans: the central role of the HIF hydroxylases pathway.” Mol. Cell 30(4):393-402.

KAI S., TANAKA T., DAIJO H., HARADA H., KISHIMOTO S., SUZUKI K., TAKABUCHI S., TAKENAGA K., FUKUDA K. and HIROTA K. (2012). “Hydrogen sulfide inhibits hypoxia- but not anoxia-induced hypoxia-inducible factor 1 activation in a von hippel-lindau- and mitochondria-dependent manner.” Antioxid Redox Signal 16(3):203-16.

KHANDRIKA L., LIEBERMANN R., KOUL S., KUMAR B., MARONI P. CHANDOKE R., MEACHAM RB. and KOUL HK. (2009). “Hypoxia-associated p38 mitogen-activated protein kinase-mediated androgen activation and increased HIF-1alpha levels contribute to emergence of an aggressive phenotype in prostate cancer. “ Oncogene 28(9):1248-60.

KAJDANIUK D., MAREK B. FOLTYN W. and KOS-KUDLA B. (2011). “Vascular endothelial growth factor (VEGF) - part 1: in physiology and pathophysiology.” Endokrynol Pol 62(5)444-55.

KASHFI K. and OLSON KR. (2012). „Biology and therapeutic potential of hydrogen sulfide and hydrogen sulfide releasing chimeras.“ Biochem Pharmacol 85(5):689-703.

KWON SJ., SONG JJ and LEE YJ. (2005). “Signal pathway of hypoxia-inducible factor-1alpha phosphorylation and its interaction with von Hippel-Lindau tumor suppressor protein during ischemia in MiaPaCa-2 pancreatic cancer cells.” Clin Cancer Res 11(21):7607-13.

LEE JW., BAE SH. JEONG JW., KIM SH. and KIM WH. (2004). “Hypoxia-inducible factor (HIF-1)alpha: its protein stability and biological functions.” Exp Mol Med. 29;36(1):1-12.

LEE ZW., ZHOU J., CHEN CS., ZHAO Y., TAN CH., LI L., MOORE PK and DENG LW. (2011). “The slow-releasing hydrogen sulfide donor, GYY4137, exhibits novel anti-cancer effects in vitro and in vivo.” PLoS One 6(6):e21077.

LI L., SALTO-TELLEZ M., TAN CH., WHITEMAN M. and MOORE PK. (2009). "GYY4137, a novel hydrogen sulfide-releasing molecule, protects against endotoxic shock in the rat." Free Radic Biol Med 47(1):103-13.

LI L., WHITEMAN M., GUAN YY., NEO KL., CHENG Y., LEE SW., ZHAO Y., BASKAR R., TAN CH. And MOORE PK. (2008). "Characterization of a novel, water soluble hydrogen sulfide-releasing molecule (GYY4137): new insights into the biology of hydrogen sulfide. " Circulation 117(18):2351-60.

LIU X., PAN L., ZHUO Y., GONG Q. ROSE P. and ZHU Y. (2010). "Hypoxia-inducible factor-1α is involved in the pro-angiogenic effect of hydrogen sulfide under hypoxic stress." Biol Pharm Bull 33(9):1550-4.

MANTHEY CL., WANG SW., KINNEY SD. and YAO Z. (1998). "SB202190, a selective inhibitor of p38 mitogen-activated protein kinase, is a powerful regulator of LPS-induced mRNAs in monocytes." J Leukoc Biol 64(3):409-17.

MENON MB., KOTLYAROV A. and GAESTEL M. (2011). "SB202190-induced cell type-specific vacuole formation and defective autophagy do not depend on p38 MAP kinase inhibition." PloS One 6(8):e23054.

MONTEL-HAGEN A., KINET S. MANEL N., MONGELLAZ C, PROHASKA R., BATTIN JL., DELAUNAY J. SITBON M. and TAYLOR N. (2008). "Erythrocyte Glut1 triggers dehydroascorbic acid uptake in mammals unable to synthesize vitamin C." Cell 132(6):1039-48.

MONTERO M., LOBATON CD., MORENO A. and ALVAREZ J. (2002). "A novel regulatory mechanism of the mitochondrial Ca2+ uniporter revealed by the p38 mitogen-activated protein kinase inhibitor SB202190." FASBJ 16(14):1955-7.

MORTIMER HJ., PEACOCK AJ., KIRK A. and WELSH DJ. (2007). "p38 MAP kinase: essential role in hypoxia-mediated human pulmonary artery fibroblast proliferation." Pulm Pharmacol Ther 20(6):718-25.

OZER A., WU LC. and BRUICK RK. (2005). "The candidate tumor suppressor ING4 represses activation of the hypoxia inducible factor (HIF). Proc Natl Acad Sci U S A 102(21):7481-6.

PALMER LA., GASTON B. and JOHNS RA. (2000). "Normoxic stabilization of hypoxia-inducible factor-a expression and activity: redox-dependent effect of nitrogen oxides." Mol Pharmacol 58(6):1197-203.

PERKINS ND. (2007). “Integrating cell-signaling pathways with NF-κB and IKK function.” Nat Rev Cell Biol 8(1):49-62.

PERNER AF., LANZA D., SEPE I., CAPASSO R., DE SANTO NG. and INGROSSO D. (2011). “Hydrogen sulfide, a toxic gas with cardiovascular properties in uremia. How harmful is it?” Blood Purif 31(1-3):102-6.

REIFFENSTEIN RJ., HULBERT WC. and ROTH SH. (1992). “Toxicology of hydrogen sulfide.” Annu Rev Pharmacol Toxicol 32:109-34.

SACCANI S., PANTANO S. and NATOLI G. (2002). “p38-dependent marking of inflammatory genes for increased NF-kappa B recruitment.” Nat Immunol 3(1):69-75.

SCHOFIELD CJ. and RATCLIFFE PJ. (2005). “Signalling hypoxia by HIF hydroxylases.” Biochem Biophys Res Commun 338(1):617-26.

SEMENZA GL. (2000). “HIF-1 and human disease: one highly involved factor.” Genes Dev. 14(16):1983-91.

SEN N., PAUL BD., GADALLA MM., MUSTAFA AK., SEN T., XU R., KIM S. and SNYDER SH. (2012). “Hydrogen sulfide-linked sulfhydration of NF-κB mediates its antiapoptotic actions.” Mol Cell 45(1):13-24.

STUHLMEIER KM., BRÖLL J. and ILVIE B. (2009). “NF-kappaB independent activation of a series of proinflammatory genes by hydrogen sulfide.” Exp Biol Med 234(11):1327-38.

SUN SC. and LEY SC. (2008). “New insights into NF-kappaB regulation and function.” Trends Immunol 29(10):469-78.

SUN SC. and LIU ZG. (2011). “A special issue on NF-κB signaling and function.” Cell Res 21(1):1-2.

TO KK. and HUANG LE. (2005). “Suppression of hypoxia-inducible factor 1alpha transcriptional activity by the HIF prolyl hydroxylase EGLN1.” J Biol Chem 280(45):38102-7.

TSUCHIYA S., YAMABE M., YAMAGUCHI Y., KOBAYASHI Y., KONNO T. and TADA K. (1980). “Establishment and characterization of a human acute monocytic leukaemia cell line (THP-1)”, Int j Cancer 26(2):171-6.

TSUCHIYA S., KOBAYASHI Y., GOTO Y., OKUMURA H., NAKAE S., KONNO T. and TADA K. (1982). " Induction of maturation in cultured human monocytic leukemia cells by a phorbol diester." Cancer Res 42(4): 1530-6.

UMEMURA K. and KIMURA H. (2007). "Hydrogen sulfide enhances reducing activity in neurons: neurotrophic role of H2S in the brain?" Antioxid Redox Signal 9(11):2035-41.

van UDEN P., KENNETH NS., ROCHA S. (2008). "Regulation of hypoxia-inducible factor-1alpha by NF-kappaB." Biochem J 412(3):477-84.

WANG R. (2002). "Two's company, three's crowd: can H2S be the third endogenous gaseous transmitter?" FASB J 16(13).1792-8.

WANG GL. and SEMENZA GL. (1993). "General involvement of hypoxia-inducible factor 1 in transcriptional response to hypoxia." Proc Natl Acad Sci U S A 90(9):4204-8.

WU B., TENG H., YANG G., WU L. and WANG R. (2012). "Hydrogen sulfide inhibits the translational expression of hypoxia-inducible factor-1α." Br J Pharmacol 167(7):1492-5.

Lilian Lohninger Curriculum vitae

Education

July 2013	Certificate of the master programme Molecular Biology (focus on Molecular Medicine)
June 2012 – April 2013	Master thesis: “Influence of H_2S on the transcription factors HIF-1α and NF-κB in THP-1 macrophages“, supervised by Prof. Hilde Laggner
October 2010 – July 2013	Master programme Molecular Biology, University of Vienna
since October 2012	Bachelor programme of Nutritional Science, University of Vienna
March 2010	Certificate of the bachelor
	Programme for Molecular Biology, Bachelor theses: “Down Syndrome”, “Allergic Cross-Reactivity”
2006 – 2010	Bachelor programme Molecular Biology in Salzburg and Linz
June 2006	Matriculation at the Bundes- und Realgymnasium für Berufstätige in Linz
2001 – 2005	BORG Honauerstraße (focus on sport) in Linz

Practical Experience

February – June 2012	Department of Medical Chemistry and Pathobiochemistry, Medical University of Vienna, supervised by Prof. Hilde Laggner
September 2011	Max F. Perutz Laboratories, supervised by Prof. Erwin Ivessa, “Protein biogenesis and degradation by the ER”

Teaching

since 2012	Biochemical practise for nutritionists

since 2011 Practise to histology and cytology

Computer Skills

MS Office, Prism 3.0, InDesign, Photoshop

Language Skills

German (first language)
English
French (basic knowledge)

Vienna, July 2013